

Identification of alpha-synuclein and ataxin-3 expression modifying compounds

Dissertation

zur
Erlangung des Doktorgrades (Dr. rer. nat.)
der
Mathematisch-Naturwissenschaftlichen Fakultät
der
Rheinischen Friedrich-Wilhelms-Universität Bonn

vorgelegt von

Fabian Stahl

aus

Kirchen (Sieg)

Bonn, September 2023

Angefertigt mit Genehmigung der Mathematisch-Naturwissenschaftlichen Fakultät
der Rheinischen Friedrich-Wilhelms-Universität Bonn

1. Gutachter/Betreuer: Prof. Dr. Ullrich Wüllner
2. Gutachter: Prof. Dr. Jörg Höhfeld

Tag der Promotion: 29.01.2024

Erscheinungsjahr: 2024

Table of contents

1	Abstract.....	1
2	Introduction	3
2.1	Neurodegenerative Diseases	3
2.1.1	Background.....	3
2.2	PD	5
2.2.1	Sporadic PD.....	5
2.2.2	Familial PD.....	6
2.3	Alpha-synuclein	6
2.3.1	Structure and function.....	7
2.3.2	Transcriptional regulation.....	8
2.3.3	Epigenetic regulation	9
2.3.4	Posttranscriptional regulation.....	11
2.4	SCA3	11
2.5	Ataxin-3	12
2.5.1	Structure and function.....	12
2.5.2	Transcriptional and epigenetic regulation	14
2.5.3	Posttranscriptional regulation.....	14
2.6	New targets for treatment approaches in PD and SCA3	15
2.7	Aim and scope of the study	18
3	Report sheet Publication 1	20
4	Report sheet Publication 2	23
5	Discussion.....	26
5.1	LUC reporter cell line-based HTS.....	26
5.1.1	Missing inhibitors	26
5.2	HTS for modulators of alpha-synuclein expression	26
5.3	HTS for modulators of ataxin-3 expression	29

5.4	Conclusion.....	33
6	References.....	34
7	Abbreviations	52
8	Danksagung.....	56
9	Appendix	

1 Abstract

Neurodegenerative diseases (NDDs) are affecting millions of people worldwide. A common feature of all NDDs is the neuronal demise in the brain leading to the clinically observed decline of motor- and cognitive capabilities of patients. Despite enormous scientific efforts, no therapies to halt NDDs have yet proven to be effective. Thus, more research is needed to identify new druggable genomic targets or compounds to reduce the expression of disease proteins at transcriptional level, prevent their aggregation and to induce the clearance of protein deposits.

This work focussed on the identification of transcriptional modulators for endogenous regulation of the Parkinson Disease (PD)- and Spinocerebellar Ataxia 3 (SCA3) causing genes alpha-synuclein (*SNCA*) and ataxin-3 (*ATXN3*) by using a novel luciferase (LUC) reporter cell line-based compound screening approach. The human neuroblastoma screening cell lines (SH-SY5Y, *SNCA* and SK-N-SH, *ATXN3*) were genetically modified by using the clustered regularly interspaced short palindromic repeats (CRISPR)/Cas9- based gene editing to insert a *GFP-T2A-LUC* cassette at the respective genomic locus which resulted in full-length *SNCA-GFP-T2A-LUC* and *ATXN3-Exon4-GFP-T2A-LUC* fusions. For each model-, a second control cell line was established bearing a randomly integrated *GFP-T2A-LUC* cassette to exclude unspecific and toxic compounds. These cell lines were used for the high throughput screening (HTS) of libraries containing 1,649 (alpha-synuclein) and 2,640 (ataxin-3) bioactive- and U.S. Food and Drug Administration (FDA) approved drugs.

While no inhibitors were identified in both HTS, activators of endogenous alpha-synuclein and ataxin-3 expression were found. Three non-related compounds modifying alpha-synuclein expression were revealed. The selective estrogen receptor modulator (SERM) Clomiphene, a vasopressin receptor antagonist Conivaptan and the plant anthraquinone Emodin. A potential mechanism explaining the induction of alpha-synuclein expression levels became evident for Emodin which was shown to have histone deacetylase (HDAC) inhibitory effects. Treatment of SH-SY5Y wild type cells led to increased levels of histone marks for H3K4 trimethylation and H3/H4 acetylation which might facilitate binding of specific transcription factors (TF) to the *SNCA* promotor.

The HTS for modulators of ataxin-3 expression revealed four statins increasing LUC signal in the screening cell line. Simvastatin was used for further validation in SK-N-

SH wild type cells. Statins are potent inhibitors of the 3-hydroxy-3-methylglutaryl coenzyme A reductase (HMGCR), the rate limiting enzyme in cholesterol homeostasis. Inhibition leads to cholesterol deprivation and to the activation of sterol regulatory element binding protein (SREBP) TFs to restore cholesterol levels. The observed increase of ataxin-3 expression was likely mediated by Simvastatin induced binding of SREBP1 TF to the *ATXN3* promotor. Overexpression of human and active SREBP1a in murine Neuro 2a cells (N2a) and co-transfection of SREBP1a with a LUC reporter plasmid containing the promotor sequence of human *ATXN3* confirmed SREBP1 dependent expression of ataxin-3. Finally, Simvastatin treatment increased endogenous *ATXN3* protein levels in a SCA3 patient-derived cell line supporting potential clinical implications. These findings suggest that ataxin-3 is a direct target of SREBP1 and indicate a putative role of *ATXN3* in cholesterol homeostasis.

2 Introduction

2.1 Neurodegenerative Diseases

2.1.1 Background

Neurodegenerative diseases (NDDs) are affecting millions of people worldwide and share the common feature of progressive decay of neuronal cells in the brain. Main risk factors for developing NDDs include aging, environmental exposure and genetic predisposition. Besides these, the onset of pathogenesis in NDDs remains enigmatic and many parameters like individual health, sex, lifestyle, and toxins are subjects of ongoing research (Ascherio & Schwarzschild, 2016; Mayeux & Stern, 2012). The neuropathological processes differ among the plethora of NDDs such as Alzheimer's disease (AD), Parkinson's disease (PD), amyotrophic lateral sclerosis (ALS), synucleinopathies, Huntington's disease (HD), and other polyglutamine diseases like spinocerebellar ataxias (SCAs, including SCA3), however a common finding is the presence of particular intra- and extracellular aggregates (Ross & Poirier, 2004). Based on clinical- and laboratory observations of the above mentioned- and other disorders, eight hallmarks have recently been formulated to define NDDs in general: pathological (protein) aggregation, synaptic and neuronal network dysfunction, aberrant proteostasis, cytoskeletal abnormalities, altered energy metabolism, DNA and RNA defects, inflammation and neuronal cell death (Wilson et al., 2023). Genetic analyses revealed that mutations of disease-causing genes in familial forms of AD, PD, ALS, HD, and SCAs (e.g. SCA3) lead to a higher susceptibility of the resulting proteins to misfold and aggregate (Forman et al., 2004). On the other hand, protein aggregation is also found in sporadic forms of NDDs which might be triggered - apart aging - by yet unknown environmental stress factors (Ross & Poirier, 2004).

Thus, misfolding and aggregation of pathological proteins represent a frequently shared phenomenon in a variety of NDDs and can presumably be considered as the driving factor for the neurodegeneration of specific brain regions in these disorders. Intra-or extracellular protein aggregates are generally termed inclusion bodies (IB) and differ in the subcellular localization in the respective NDDs. Whereas protein aggregation in AD is observed as extracellular senile plaques (amyloid beta) and intracellular neurofibrillary tangles (tau), aggregation in sporadic and familial PD and other synucleinopathies occurs in cytoplasmic inclusions, called Lewy bodies (LBs)

mainly consisting of alpha-synuclein. Intranuclear inclusions have been observed in polyglutamine diseases, including HD and SCAs (Ross & Poirier, 2004, 2005; Wilson et al., 2023).

However, it is still under debate whether inclusion bodies of aggregated proteins cause neurodegeneration or represent a potential cellular defence mechanism against misfolded proteins (Ross & Poirier, 2005). Although inclusions are a hallmark of AD there is only weak correlation between senile plaque density in human *post-mortem* samples and *ante-mortem* cognitive defects (Ross & Poirier, 2004; Terry et al., 1991). Similarly, no correlation between LBs content and clinical measures like duration of PD were found nor did increased LB abundancy correlate with neuronal loss in the *substantia nigra* (Schulz-Schaeffer, 2012). There is some evidence, that LB formation display a protective mechanism to scavenge excess amounts of misfolded and potentially cytotoxic proteins (Olanow et al., 2004). The so-called aggresome-formation was observed for familial ALS with the causative protein superoxide dismutase 1 (SOD1) *in vitro* (Johnston et al., 2000). Aggresomes represent actively formed protein deposits which are collected via dynein dependent retrograde transport as perinuclear inclusions at the microtubule-organizing center (MTOC) (Garcia-Mata et al., 1999; Johnston et al., 1998). On the other hand, several studies found that fibrillar intermediates of amyloid beta, alpha-synuclein and polyglutamine proteins lead to cytotoxicity in different disease models (Ross & Poirier, 2004). Based on these reports, a protective role of inclusion bodies in NDDs cannot be ruled out but further research is needed to proof whether they are actively formed protein deposits or just the result of increasing amounts of misfolded, fibrillar intermediates, which tend to aggregate. Despite tremendous research efforts, no therapies are available to halt the misfolding and aggregation of disease-causing proteins and subsequent neuronal decay across the variety of NDDs. Current pharmacologic treatments merely aim to ameliorate clinical symptoms.

2.2 PD

PD is the second most common NDD (next to AD), named after James Parkinson, who gave a thorough description in his “Essay of the Shaking Palsy” (1817) (Parkinson, 2002). The pathophysiological demise of dopaminergic neurons in the *substantia nigra* leads to clinical motor-symptoms including bradykinesia, resting tremor, rigidity and postural instability. In addition, non-motor symptoms like sleeping disorders, cognitive impairment, and mood disorders were observed in patients (Poewe et al., 2017). PD is a fast-growing neurological disorder with a worldwide increase of 118 % from 1990 to 2015. Population studies showed that incidences of the disease range between 10 to 18 within 100,000 patients per year and that onset rises around the age of 65 (Dorsey et al., 2018). In addition to age, several genetic- and environmental risk factors (including pesticides, prior head injury, rural living and beta blocker use) have been identified, whereas the exact cause of onset remains enigmatic (Hernandez et al., 2016; Kalia & Lang, 2015).

2.2.1 Sporadic PD

About 90 % of PD is sporadic and occurs mainly in the elderly population, aging being a major risk factor. PD is considered as a multifactorial disease without an unequivocal reason for onset (Riederer et al., 2019). It has been reported that incidence of PD in men is higher compared to women in most populations. This observation may suggest a protective effect of female sex hormones or sex specific differences in general homeostasis and exposure to environmental factors (pesticides) (Ascherio & Schwarzschild, 2016; Poewe et al., 2017). Sporadic PD can be unambiguously diagnosed by the neuronal loss in the *substantia nigra* together with the widespread observation of LB pathology (post-mortem). Studies showed that degeneration of dopaminergic neurons in the *substantia nigra* begins years before the actual onset of the disease. Clinical diagnosis of PD includes validation of pronounced motor and non-motor symptoms, levodopa (L-DOPA, a dopamine precursor) responsiveness and diagnostic tests like positron emission tomography (PET) and I-ioflupane single-photon emission CT (SPECT) (DaTscan, GE healthcare) or multimodal magnetic resonance imaging (MRI). These tools are crucial for an unequivocal determination of PD since many other types of neurodegeneration includes parkinsonian syndromes (Poewe et al., 2017).

2.2.2 Familial PD

Only 5 to 10% of all PD cases are familial. Genetic screenings and genome wide association studies (GWAS) revealed several risk genes and gene loci to be associated with inherited PD (Poewe et al., 2017). Monogenic forms of familial PD can lead to autosomal dominant- and recessive PD. The majority of recessive forms are due to mutations in genes including *PARKIN*, an E3 ubiquitin ligase coding gene, the PTEN-induced putative kinase 1 (PINK1)- and DJ-1 encoding genes. Most autosomal dominant PD cases are caused by alterations in genes such as the vacuolar protein sorting 35 (VPS35) gene, the leucine-rich repeat kinase 2 (LRRK2)- and in the alpha-synuclein (SNCA) coding genes, leading to the typical symptoms of PD (Bonifati et al., 2003; Funayama et al., 2002; Kitada et al., 1998; Poewe et al., 2017; Polymeropoulos et al., 1997; Valente et al., 2001; Zimprich et al., 2011).

2.3 Alpha-synuclein

The alpha-synuclein encoding gene (*SNCA*) belongs to a family consisting of three synuclein genes (α -, β -, γ synucleins) (George, 2002). It was the first gene identified to cause autosomal dominant PD (Polymeropoulos et al., 1997). Point mutations and dupli- or triplication of the genomic locus lead to increased protein amounts, misfolding and aggregation of the disease protein (Chartier-Harlin et al., 2004; Farrer et al., 2004; Fuchs et al., 2008; Kruger et al., 1998; Miller et al., 2004; Polymeropoulos et al., 1997; Singleton et al., 2003; Zarranz et al., 2004). Genomic duplications resemble the sporadic forms of PD whereas triplications showed earlier age of onset and more severe symptoms, indicating a gene-dosage effect (Chartier-Harlin et al., 2004; Singleton et al., 2003). In the same year of its genetic linkage to autosomal dominant PD, Spillantini and colleagues (1997) detected SNCA as a major component of LBs (Spillantini et al., 1997). These two independent findings assign alpha-synuclein a key role in the neurodegenerative processes of PD.

2.3.1 Structure and function

SNCA is a small 140 amino acid (AA) long, naturally unfolded protein and was initially described as a synaptic and nuclear protein but was also found at abundant levels in red blood cells (RBCs) (Barbour et al., 2008; Maroteaux et al., 1988; Ueda et al., 1993; Weinreb et al., 1996). Its N-terminal region contains a characteristic lipid binding domain which is followed by a non-amyloid containing aggregation prone region and an intrinsically disordered C-terminus (Eliezer et al., 2001; George et al., 1995).

In 2011 Bartels and colleagues reported that endogenous SNCA, under non-denaturing conditions, occurs as helically folded tetramers of approximately 58 kDa in human cell lines and RBCs. In contrast to these data, Burré et al., (2013) showed that native alpha-synuclein, purified from mouse brain is a largely unstructured monomer that shows no stable tetramer formation which is in line with the original observations (Bartels et al., 2011; Burre et al., 2013; Weinreb et al., 1996). However, the physiological role of SNCA is not yet fully understood but the presynaptic localization and the given brain pathology of SNCA in PD prompted studies to focus on potential synaptic functions like neurotransmitter release and synaptic plasticity (Bendor et al., 2013; Iwai et al., 1995). It was reported that SNCA binds to lipids and shares great sequence homology to fatty acid binding proteins (Sharon et al., 2001). After binding to membranes or charged phospholipids the N-terminal region of SNCA structurally changes from a disordered- to an alpha helical conformation (Davidson et al., 1998; Jao et al., 2004).

Chandra and colleagues (2005) found that the neurodegenerative and lethal phenotype in cysteine string protein alpha (CSP α) knockout mice was rescued by the overexpression of SNCA. Vice versa removing of endogenous SNCA even increased these phenotypes. CSP α is a synaptic vesicle protein which was reported to exhibit co-chaperoning functions which are critical for synaptic transmission and neuronal function by interaction with N-ethylmaleimide-sensitive fusion protein attachment protein receptors (SNARE) complexes. These are crucial in vesicle docking and fusion within neurotransmitter release. Knockout of CSP α abolishes SNARE complex assembly and was partially rescued by transgenic SNCA overexpression, indicating a potential function for SNCA as a cochaperone in the synapse (Chandra et al., 2005). Direct interaction of the SNCA non-membrane binding C-terminal-, and the N-terminal region of synaptobrevin-2, a protein located in the SNARE vesicles, has been elegantly

shown. Furthermore, SNARE complex assembly was promoted by SNCA and a triple knockout of all synucleins in mice led to an age dependent decrease in synaptobrevin-2, SNARE complex formation, neurodegeneration and premature death, suggesting a normal role of synucleins in SNARE complex assembly (Burre et al., 2010). The same group proposed a model that SNCA adopts an alpha helical conformation upon binding to synaptic vesicles and assembles into multimers which promotes SNARE complex assembly (Burre et al., 2014; Ramakrishnan et al., 2012).

2.3.2 Transcriptional regulation

In addition to the observation of gene-dosage effects in familial PD with multiplications of the *SNCA* locus, single nucleotide polymorphisms (SNPs) in the *SNCA* gene are associated with higher risk to develop PD and higher alpha-synuclein expression in blood and brain (Fuchs et al., 2008). Increased *SNCA* messenger RNA (mRNA) levels in post-mortem brain samples from sporadic PD patients have also been found suggesting an aberrant endogenous regulation of alpha-synuclein in PD (Guhathakurta et al., 2017). Clough and Stefanis (2007) reported a potential transcriptional regulatory role of the *SNCA* intron 1 region (Clough & Stefanis, 2007). Indeed, one year later, GATA binding protein 1 and 2 (GATA-1, GATA-2) transcription factor (TF) were observed to bind within conserved GATA motifs in intron 1. In contrast to GATA1 which is not expressed in neurons, GATA-2 is critical for neuronal development and expressed in PD affected brain regions like *substantia nigra* and cortex as shown with real time quantitative PCR (RT-qPCR) analysis in human post-mortem brain tissue. Additionally, small interfering RNA (siRNA) mediated knockdown of GATA-2 led to reduced *SNCA* mRNA levels (Scherzer et al., 2008). Another study proofing the importance in transcriptional regulation of *SNCA* intron 1 found that the zinc finger and SCAN protein containing TF (ZSCAN21) bound to intron 1 and additionally revealed ZSCAN219 to regulate *SNCA* transcription by binding to the 5' promotor region (Clough et al., 2009). Brenner and colleagues confirmed direct binding of ZSCAN21 to *SNCA* intron 1 in human brain cells. In contrast to studies from Scherzer and colleagues, they report GATA-2 binding exclusively to *SNCA* intron 2 (Brenner et al., 2015). However, GATA2 polymorphisms did not correlate with sporadic PD and thus might be excluded as a risk factor (Kurzawski et al., 2010). The tumour suppressor p53 was found to be increased in PD affected brains and was confirmed to be a direct activator of *SNCA*

mRNA expression (Duplan et al., 2016). Empty spiracles homeobox 2 (EMX2) and NK6 Homeobox 1 (NKX6-1) TFs, were found to be repressors of *SNCA* transcription and bind to a specific region in intron 4 (Soldner et al., 2016). Another negative regulator, poly (ADP ribose) polymerase-1 (PARP1), was shown to bind relatively far upstream (9Kb) from the transcriptional start site (TSS) to a nonamyloid component of plaques (NACP)-Rep1 region associated with increased risk for PD (Chiba-Falek et al., 2005). The CCAAT/enhancer binding protein (C/EBP) β TF has been proposed to activate *SNCA* transcription (Gomez-Santos et al., 2005). More recently, the C/EBP δ TF was found to modulate alpha-synuclein mRNA- and protein levels. Knockout of C/EBP δ in mice and primary neuronal cultures showed dramatically increased- and *vice versa* overexpression in neuroblastoma cells and primary neuronal cultures decreased alpha-synuclein levels. Direct interaction with the *SNCA* promotor was proofed in chromatin immunoprecipitation (ChIP) experiments performed in mice and human *post-mortem* PD and control brain samples. The authors found reduced C/EBP δ expression in the *substantia nigra* and induced-pluripotent stem cells (iPSC)-derived dopaminergic neurons from patients. These data indicate that reduced C/EBP δ levels may be a pathogenic factor in PD and other synucleinopathies suggesting C/EBP δ as pharmacological target for these NDDs (Valente et al., 2020).

2.3.3 Epigenetic regulation

Epigenetic modifications like DNA methylation and histone modifications have been emerged as potential modulators of alpha-synuclein levels in a variety of cell models, animal models and in post-mortem brain tissue of healthy controls and PD patients. Especially the DNA methylation status of the genomic locus of the aforementioned *SNCA* intron 1 seems to play a crucial role (Guhathakurta et al., 2017). Studies from our group found decreased methylation in *SNCA* intron 1 region in PD patient brains compared to controls (Jowaed et al., 2010). Similar, significant hypomethylation of *SNCA* intron 1 results were found in the cortex of post-mortem PD and dementia with Lewy body (DLB) (Desplats et al., 2011). However, other studies did not observe changes in methylation levels of *SNCA* or a significant correlation between *SNCA* methylation status and protein levels in Lewy body disease (LBD) or PD *post-mortem* brain samples compared to controls (de Boni et al., 2011). The opposing results might be explained by the availability of different brain regions, the varying quality of DNA

extracted from *post-mortem* brain samples and the use of different methodologies. Several studies investigated the DNA methylation status of *SNCA* intron 1 in peripheral blood mononuclear cells (PBMCs). Most of these findings report hypomethylation of *SNCA* intron 1 in PD patients compared to healthy controls. However, correlation of the methylation status and alpha-synuclein expression levels in patients remains contradictory (Guhathakurta et al., 2017).

In addition to DNA methylation, epigenetic mechanisms like histone modifications were found to alter mRNA and protein expression levels of alpha-synuclein. In general, increased acetylation (ac) of histones H3/H4 and trimethylation of histone H3K4 (H3K4me3) were associated with increased transcriptional activity (Bannister & Kouzarides, 2011).

Three histone deacetylase (HDAC) inhibitors, i.e. valproic acid (VPA), sodium 4-phenylbutyrate and trichostatin A (TSA) increased H3ac and alpha-synuclein expression (Leng & Chuang, 2006). In line with these observations, *SNCA* mRNA expression was attenuated when H3K27ac was reduced (Mittal et al., 2017). According to the Encyclopedia of DNA Elements (ENCODE) database, the *SNCA* promotor contains histone marks for active transcription like H3K4me3 and H3K27ac (Rosenbloom et al., 2013). A recent study from Guhathakurta and colleagues examined histone marks at *SNCA* locus in *post-mortem* control and PD brain samples and found significantly enriched H3K4me3 at the *SNCA* promotor. Furthermore, they developed a clustered regularly interspaced short palindromic repeats (CRISPR)/Cas9- based H3K4me3 demethylating system and showed that decreased methylation correlates with decreased alpha-synuclein expression (Guhathakurta et al., 2021). Another study performed a genome-wide histone acetylation analysis in post-mortem brain samples of 21 healthy controls and 28 sporadic PD. The authors observed globally increased acetylation levels in PD samples compared to controls and found that H3K27ac depicts the most prominent change. Chromatin immunoprecipitation sequencing (ChIP-seq) analysis revealed increased H3K27ac at promoters of genes associated with PD, including *SNCA* (Toker, 2020).

2.3.4 Posttranscriptional regulation

Short non-coding RNA species, i.e. micro RNAs (miRNAs) can modulate gene expression at the posttranscriptional level. Upon miRNA binding, the RNA induced-silencing complex (RISC) is guided to the target mRNA. Protein expression is attenuated via degradation or translational inhibition of the target transcript, dependent on the level of complementary in binding between the miRNA and its target mRNA (Bartel, 2004). Junn and colleagues (2009) were the first who found that mainly neuronal expressed miRNA-7 (miR-7) downregulates alpha-synuclein expression by binding to its 3' untranslated region (UTR). To confirm their findings, the authors showed that treatment of SH-SY5Y cells with specific miRNA-7 inhibitors leads to increased alpha-synuclein levels (Junn et al., 2009). Reduced levels of miR-7 were found in the *substantia nigra* of PD patients and knockdown of miR-7 in the *substantia nigra* of mice resulted in upregulation of SNCA levels and the loss of nigral dopaminergic neurons, implicating a role of miR-7 in PD pathology (McMillan et al., 2017). Other miRNAs including miR-153, miR-34b, c and miR-124 bind to the 3'UTR within the SNCA mRNA and lead to downregulation of its expression (Zhao & Wang, 2019).

2.4 SCA3

SCA3 or Machado Joseph Disease (MJD) is an autosomal dominant inherited ataxia (Coutinho & Andrade, 1978). The prevalence of all SCAs ranges from 0 to 5.6 cases per 100,000 individuals. SCA3 is the most common SCA world-wide and accounts for 20-50% of all SCA families (Klockgether et al., 2019). Clinical symptoms include progressive gait imbalance and speech difficulties in the early stages. Patients in late stages are wheelchair-bound and develop severe dysarthria and dysphagia, beside other symptoms. The mean age of onset is between 30 to 40 years and progressive neurodegeneration over 10 to 15 years leads to premature death. SCA3 is caused by an expansion of the C-terminal polyglutamine (polyQ) tract in the *ATXN3* gene. The length of normal polyQ alleles varies from 12 to 42 repeats whereas pathogenicity is induced by expanded alleles ranging from 60 to 87. The polyQ repeat length of SCA3 inversely correlates with age of onset, misfolding, aggregation, and severity of symptoms (Costa Mdo & Paulson, 2012).

Pathological hallmarks in SCA3 are widespread aggregation of ATXN3 protein and formation of inclusion bodies inside and outside of the cell nuclei leading to general loss of neuronal cells within the brain (Evert et al., 1999; Paulson et al., 1997).

2.5 Ataxin-3

The ataxin-3 gene (*ATXN3*) was first cloned by Kawaguchi and colleagues, who found an expanded polyQ coding CAG repeat in *ATXN3* of clinically diagnosed SCA3 patients (Kawaguchi et al., 1994). The genomic locus of normal *ATXN3* comprises 11 exons which encodes the approximately 42 kDa large disease protein ataxin-3 (ATXN3) (Ichikawa et al., 2001; Schmitt et al., 2003). The CAG repeats were found to reside in exon 10 and confer, when expanded, the neurotoxic properties to ATXN3. As a result of alternative splicing, 20 different ATXN3 protein coding mRNAs have been found (Bettencourt et al., 2010). In the brain, the most frequently expressed isoform consists of 11 exons (Harris et al., 2010; Schmidt et al., 1998).

2.5.1 Structure and function

Structurally, the N-terminal domain of ATXN3 represents an evolutionary conserved Josephine domain (JD) (Scheel et al., 2003). The C-terminus harbours two neighbouring ubiquitin-interacting motifs (UIM) upstream- and a third UIM downstream of the polyglutamine tract, dependent on the respective splice variant (Hofmann & Falquet, 2001; Mao et al., 2005). Additionally, downstream of the JD a nuclear export signal (NES) and two C-terminal nuclear localization signals (NLS) were reported (Albrecht et al., 2004).

ATXN3 is ubiquitously expressed and detected in many different regions within the brain and was found to have a dendritic and axonal localization in most neurons. Intracellularly, ATXN3 has mainly been detected in the cytoplasm but tiny amounts were also found in the nucleus (Trottier et al., 1998).

Despite the involvement of ATXN3 in a variety of cellular processes, including participation in the ubiquitin proteasome system (UPS), aggresome formation, cytoskeletal organization, DNA binding and interaction with TFs it can likely be considered as a non-essential protein since ataxin-3 knockout in mice or *C. elegans*

did not show an obvious phenotype (Costa Mdo & Paulson, 2012; Rodrigues et al., 2007; Schmitt et al., 2007).

According to the sequence homology to JDs and its UIMs, a potential function in the UPS of ATXN3 as a deubiquitinating enzyme (DUB) was assumed (Mao et al., 2005; Nicastro et al., 2005; Scheel et al., 2003).

Indeed, it was shown that ATXN3 binds polyubiquitin chains with four or more ubiquitins, which are required for proteasomal recognition and degradation, with its two UIMs upstream of the polyQ stretch. Mutation of the conserved leucine (L229A) in the first UIM almost totally abolished binding of polyubiquitin and a similar mutation (L249A) in the second UIM inhibits binding to a lesser extent. Furthermore, the authors observed a potential ubiquitin protease activity of ATXN3 which was reduced after applying a ubiquitin protease inhibitor (Burnett et al., 2003).

Extended *in vitro* studies of the DUB properties of ATXN3 revealed a regulatory role of UIMs in the trimming of K48-linked ubiquitin chains. It was shown that ATXN3 cleaves polyubiquitin chains to a length of 5-7 ubiquitin from a given substrate and, at the same time, inhibited its proteasomal degradation (Burnett & Pittman, 2005).

Several ATXN3 regulated targets have been associated to the UPS. The ubiquitin E3 ligase parkin, a risk gene for familial PD, was shown to be deubiquitinated by ATXN3 (Durcan et al., 2011). The C-terminus of Hsc70-interacting protein (CHIP) interacts with chaperones to promote degradation of misfolded proteins and was shown to be associated with ATXN3 (Ballinger et al., 1999; Connell et al., 2001; Jana et al., 2005). Findings from Scaglione and colleagues led to the model that ATXN3, together with ubiquitin-conjugating enzyme E2 W (Ube2w), regulate CHIPs activity within the UPS. Interestingly, mutant polyQ ATXN3 led to a more effective de-ubiquitination and subsequent degradation of parkin and CHIP in mouse models expressing human polyQ ATXN3, compared to the wild type mice (Durcan et al., 2011; Scaglione et al., 2011).

Furthermore, earlier studies observed a direct binding of ATXN3 to the valosin containing protein or AAA ATPase p97 (VCP/p97) and another UPS related protein Rad23 via an arginine/lysine motif (AA 277-291) (Boeddrich et al., 2006; Doss-Pepe et al., 2003; Hirabayashi et al., 2001). VCP/p97 is known to target protein complexes for proteasomal degradation and for facilitating endoplasmic reticulum (ER) associated

degradation (ERAD). Together with specific ER membrane components like ER specific E3 ligases, VCP/p97 controls dislocation and degradation of misfolded proteins from the ER. Interaction of VCP/p97 with ATXN3 was accompanied by reduced retro-translocation of ERAD substrates to the proteasome indicating a regulatory role in ERAD turnover for ATXN3. Furthermore, expansion in the polyQ tract led to an accumulation of ERAD substrates compared to wild type suggesting a dysregulation of ERAD in SCA3 (Zhong & Pittman, 2006).

Another protective mechanism of cells, to overcome the burden of misfolded proteins, is the formation aggresomes. Endogenous ATXN3 was found to interact with the complex forming components like histone deacetylase 6 (HDAC6) or dynein. Also, defective aggresome formation was observed in ataxin-3 siRNA knockdown cells, which was reversed by overexpression of ATXN3 protein (Burnett & Pittman, 2005).

2.5.2 Transcriptional and epigenetic regulation

In contrast to the various identified physiological roles of ATXN3, relatively little is known about its transcriptional regulation. Schmitt et al., 2003 characterized the *ATXN3* promotor and identified specificity protein 1 (SP1) TF and CCAAT motif-binding factor (CBF) to bind the *ATXN3* promotor *in vitro* by using electric mobility shift assays (EMSA) (Schmitt et al., 2003). Data for epigenetic modifications of *ATXN3* are scarce. DNA methylation levels of *ATXN3* promotor were analysed from SCA3 patients and controls. In PBMC derived DNA, a hypermethylation of 7/17 CpG sites in the first CpG island have been found in SCA3 patients compared to controls. However, no correlation of *ATXN3* mRNA levels and hypermethylation was observed (Wang et al., 2017).

2.5.3 Posttranscriptional regulation

It was found that ataxin-3 expression can be regulated post-transcriptionally via miRNAs. Different miRNAs like miR-181 and miR-25 family members but also miR-9 and miR-494 have been shown to directly bind to the 3'UTR of *ATXN3*. LUC assays with co-transfection of miRNA expressing vectors and *LUC* vectors, containing wild type and mutated miRNA binding sites of the *ATXN3* 3'UTR sequence, were performed. The generated data revealed that binding of miRNAs reduce LUC signal

for the plasmids with the wild type sequence but not with the respective mutations. An insertion of the 3'UTR sequence of *ATXN3* in the coding sequence of a mutant *ATXN3* expressing plasmid and subsequent transfection into human embryonic kidney cells (HEK) led to reduced expression of the protein and decreased number of *ATXN3* containing aggregates compared with the normal coding sequence. These observations were confirmed in a lentiviral-based mouse model of MJD. The same study showed that genetic silencing or pharmacological inhibition of Dicer and Drosha, key enzymes in miRNA biogenesis, lead to increased *ATXN3* protein levels in HEK cells (Carmona et al., 2017). Expression levels of miRNAs were found to differ in SCA3 patients compared to controls. Whereas miR-25 and miR-181 family members are upregulated in SCA3 patient derived lymphoblastoid cells, miR-9, miR-181a and miR-494 have been shown to be decreased in human SCA3 brain samples and SCA3 models (Krauss et al., 2019). These differences may be due to different cell lines and samples. The regulatory importance of 3'UTR in *ATXN3* expression is further underscored by associations of new SNPs in the close distance to the conserved miR-25 binding site with early onset SCA3 (Krauss & Evert, 2019; Long et al., 2015).

2.6 New targets for treatment approaches in PD and SCA3

Despite enormous efforts, no disease halting therapeutics for PD and SCA3 have yet been found. In general, only treatments to alleviate symptoms are available for the variety of NDDs. In PD patients, L-DOPA treatment restores dopamine levels in the and ameliorates clinical symptoms (Poewe et al., 2017). In SCA3 and other SCAs, no designated specific treatments are available and patients are left with general supportive management like physiotherapy, occupational- and speech therapy, only (Klockgether et al., 2019), (<https://www.ataxia.org/pipeline/sca3/>). Current approaches to halt NDDs concentrate on restoring neuronal plasticity in the affected brain (stem cells), removal of toxic protein aggregates (antibody therapies) and inhibition of the disease protein expression (gene therapy, siRNA, antisense oligonucleotide (ASO)) (Kingwell, 2021; Poewe et al., 2017; Sullivan et al., 2019; Sun & Roy, 2021; Vijjaratnam et al., 2021). Recently, a CRISPR/Cas9-based mediated methylation and subsequent reduction of the PD risk gene *SNCA* has been reported in cell culture experiments which might turn into a potential method for future therapies in a variety of NDDs (Kantor et al., 2018).

Reducing amounts- or preventing aggregation of disease-causing proteins by compound based pharmacological treatments may reach the clinical phases more easily compared to the more invasive approaches such as stem cell transplantation, gene therapies or antibody treatments. To this end, new genetic targets and compounds or new targets for already clinically used drugs (drug repurposing) must be identified to modulate the expression or aggregation of disease proteins. In the past, several alpha-synuclein and ataxin-3 modifier screenings have been conducted (Ashraf et al., 2020; Bilen & Bonini, 2007; Costa et al., 2016; Fardghassemi et al., 2021; Hollerhage et al., 2019; Hollerhage et al., 2017; Stahl et al., 2021; Vo et al., 2012). Two principal approaches, i.e. genetical- and compound modifier screenings were performed to find modulators of SNCA and ATXN3 overexpression induced toxicity. In these studies, measuring growth or cell viability and the reduction of overexpressed toxic proteins served as a readout for effective modulators. However, these screening approaches did not consider the epigenetic, transcriptional and posttranscriptional regulation of endogenous disease related genes (in *cis*) which represents an important target for modulation or inhibition of the proliferation of mutated and potentially deleterious proteins.

While most of the genetic- and compound modifier screenings for SNCA induced toxicity were performed in yeast, Höllerhage and colleagues used Lund human mesencephalic (LUHMES) neurons as a SNCA toxicity model. Toxicity was induced by adenoviral vector mediated overexpression of wild type SNCA which led to ~50 % cell death after six days. They performed a high throughput screening (HTS) of 1,600 U.S. Food and Drug Administration (FDA) approved drugs and identified dipyridamole, an unspecific phosphodiesterase (PDE) inhibitor, conferring strong neuroprotection. Because dipyridamole does not penetrate the blood-brain barrier (BBB), neuroprotection in PD patients was assumed as unlikely. However, the authors identified potent neuroprotective properties of the PDE1 inhibitor vinpocetine, which did not belong to the initial screening library. siRNA-mediated knockdown of PDE1A and inferior silencing of PDE1C mimics the beneficial effect of vinpocetine in this LUHMES cell line model of SNCA toxicity. Also, dopaminergic midbrain neurons were rescued by vinpocetine in a SNCA overexpressing mouse model suggesting PDE1A and/or PDE1c as druggable targets for the treatment of PD and other synucleinopathies (Hollerhage et al., 2017).

In the same year, the first compound screening for endogenous alpha-synuclein expression in SK-N-MC was performed. In a screening library of 1,126 FDA approved and other compounds, β 2 adrenoreceptor (β 2AR) agonists were found to reduce endogenous alpha-synuclein mRNA and protein levels. Metaproterenol was identified in the primary screening and after expansion with other β 2AR agonists, Clenbuterol showed the most prominent effect and was used for further experiments. Treatment of mice revealed that clenbuterol was able to cross the BBB and led to reduced alpha-synuclein mRNA and protein levels in the *substantia nigra*. Overexpression and genetic silencing of β 2AR in SK-N-MC cells reduced or increased alpha-synuclein expression, respectively. Also, clenbuterol showed neuroprotective effects in human iPSC-derived neuronal precursor cells with genomic triplication of *SNCA* (Mittal et al., 2017). These data clearly show that screening for endogenous modulators of disease-causing genes and proteins have great potential for the identification of new drugs and targets in NDDs.

Compared to the large amount of modifier screenings for alpha-synuclein, only a few screenings have been performed in SCA3 models of *Drosophila* and *C. elegans* or human cell lines. All of these models focussed on overexpression induced toxicity of mutated polyQ ATXN3 and its modulation by genetical- or compound modifiers. In the first genetic modifier screening, random overexpression of genes in a SCA3 *Drosophila* model revealed 18 genes showing beneficial effects on toxicity. The majority were found to be part of chaperone and ubiquitin pathways (Bilen & Bonini, 2007). An extensive druggable genome screen has been performed in a human polyQ ATXN3-firefly LUC reporter cell line. SiRNA knockdown of 2,742 druggable genes revealed 15 genes as modifiers for ATXN3 induced toxicity which were further validated in a SCA3 *Drosophila* model. Among the 15 genes, FBXL3, which encodes for a F-box protein that is part of the S-phase Kinase-Associated Protein 1 (SKP1)-Cullin-F-box (SCF) ubiquitin ligase complex was identified to effectively reduce toxicity. Overexpression of FBXL3 in neuronal progenitor control- and SCA3 cells (NPCs) led to reduction of endogenous wild type and pathogenic ATXN3 levels (Ashraf et al., 2020).

So far, two compound modifier screenings to modulate ATXN3 induced toxicity have been performed in human reporter cell lines and *C. elegans* respectively. Aripiprazole, an antipsychotic drug was identified in an unbiased primary screening of 1,250 FDA approved drugs in a SCA3 model cell line. Further validation in *Drosophila* and mouse

SCA3 models revealed increased longevity in flies and reduction of aggregated ATXN3 species in flies and mice brains after Aripiprazole treatment (Costa et al., 2016). Recently, a screening of 3,942 compounds including many FDA approved substances has been performed in a polyQ ATXN3 overexpressing *C. elegans* model. Five compounds were identified to rescue the motor-deficient phenotype, protecting against neurodegeneration and increasing the live span in transgenic worms. When investigating a potential mechanism behind the beneficial effects of these molecules, the authors found that three out of five molecules, namely chenodiol (CHEN), fenbufen (FEN), and sulfaphenazole (SULFA) act as modulators for the transcription factor EB (TFEB/HLH-30) a key factor in autophagy pathways. In TFEB/HLH-30 knockout worms the beneficial effects were not observed indicating a critical role of this TF in rescuing polyQ ATXN3 induced phenotype. On the other hand, overexpression of TFEB/HLH-30 alleviates the motility defect in SCA3 worms. From the three compounds modulating TFEB/HLH-30, FEN is already clinically used as a non-steroidal and anti-inflammatory drug in AD to prevent inflammatory processes observed in patients and thus may have the potential as new treatment option for SCA3 patients (Fardghassesemi et al., 2021).

2.7 Aim and scope of the study

Finding novel druggable genomic targets and compounds modifying the expression levels of disease-causing proteins in NDDs is the prerequisite for the development of new therapies. High throughput screenings (HTS) are suitable approaches to identify yet unknown genetic- or compound modifier candidates for therapies of NDDs. Almost all of the studies consider the pathologically observed hallmark of protein aggregation and used disease protein overexpression induced toxicity models for genetic- or compound modifier libraries. Thus, any potential gene or compound candidates modulating the epigenetic-, transcriptional- and posttranscriptional regulation of misfolding proteins might be missed.

This work presents a novel HTS approach for the identification of endogenous and transcriptional modulators of *SNCA* and *ATXN3* expression via human LUC reporter cell lines. The aim of the studies was to find compounds which significantly modulate expression levels of endogenous alpha-synuclein and ataxin-3 and to identify new epigenetic, transcriptional or posttranscriptional mechanisms for these changes. These

are the first endogenous LUC reporter human cell line-based screenings for the two disease associated genes.

To generate the screening cell lines, the CRISPR/Cas9-based gene editing was used to modify the endogenous *SNCA*- and *ATXN3* gene in an SH-SY5Y and SK-N-SH wild type cell line by insertion of a *GFP-T2A-LUC* cassette, respectively. The gene editing resulted in a genomic full length *SNCA-GFP-T2A-LUC* and an *ATXN3-Exon4-GFP-T2A-LUC* reporter cell line. For each model-, a control cell line with a randomly integrated reporter cassette was established to exclude toxic or unspecific modulators from subsequent experiments. These reporter cell lines allow for the LUC assay-based HTS of compound libraries comprising 1,649 (alpha-synuclein modifier screening) and 2,640 (ataxin-3 modifier screening) bioactive- and FDA approved drugs to identify substances modulating expression levels of alpha-synuclein and ataxin-3 which might be used in future clinical trials to slow down or halt PD and SCA3.

3 Report sheet Publication 1

Activators of alpha-synuclein expression identified by reporter cell line-based high throughput drug screen

Fabian Stahl ^{1,2}, Philip Denner ¹, Dominik Piston ¹, Bernd O. Evert ², Laura de Boni ², Ina Schmitt ², Peter Breuer ²✉ & Ullrich Wüllner ^{1,2}✉

¹DZNE, German Center for Neurodegenerative Diseases, Venusberg-Campus 1/99, 53127 Bonn, Germany.

²Department of Neurology, University Hospital Bonn, 53127 Bonn, Germany

Stahl, F., Denner, P., Piston, D. *et al.* Activators of alpha synuclein expression identified by reporter cell line-based high throughput drug screen. *Sci Rep* **11**, 19857 (2021). <https://doi.org/10.1038/s41598-021-98841-9>

Summary

Alpha-synuclein is a key component in Parkinson's disease (PD) pathophysiology. Mutations and also duplication or triplication of the *SNCA* gene cause familial parkinsonian syndromes and the overall *SNCA* levels correlate with the severity of symptoms (Chartier-Harlin et al., 2004; Polymeropoulos et al., 1997; Singleton et al., 2003; Spillantini et al., 1997). Thus, regulation of alpha-synuclein expression might be an appropriate target for pharmacological treatment. In the past, several modifier screenings for alpha-synuclein based on *SNCA* overexpression induced toxicity have been performed in different transgenic disease models (Hollerhage et al., 2019). In fact, these screenings did not consider the endogenous regulation of *SNCA* and likely missed compounds which affect the epigenetic and transcriptional landscape. Mittal and colleagues (2017) performed the first study addressing endogenous messenger RNA (mRNA) levels of *SNCA* and found that β 2 adrenoreceptor (β 2AR) agonists lead to reduced alpha synuclein mRNA and protein levels in a human cell line (Mittal et al., 2017).

In our study, we have chosen an alternative approach to identify modifiers of *SNCA* expression and designed a luciferase (LUC) reporter cell line-based high throughput screening (HTS). An SH-SY5Y neuroblastoma cell line was used to generate a CRISPR/Cas9 mediated endogenous *SNCA-GFP-T2A-LUC* genomic fusion- and a control cell line with a random integration of the LUC reporter cassette. The established

cell lines allowed us to screen a library of 1,649 bioactive compounds, including the FDA approved drugs (Stahl et al., 2021).

We found no inhibitors but identified three activators of *LUC* mRNA in the *SNCA-GFP-T2A-LUC* screening cell line. We finally determined *SNCA* mRNA expression in non-modified SH-SY5Y wild type cells and verified Clomiphene, Conivaptan and Emodin to increase *SNCA* mRNA levels 1.4 to 2-fold compared to DMSO controls. We confirmed that treatment with these activators also increase *SNCA* protein levels in the wild type cell line by using two independent protein assays: in-cell Western (ICW) and conventional Western blot. Both approaches revealed a 1.3 to 2-fold increase of *SNCA* compared to DMSO control.

The three selective activators comprised hormone receptor interacting drugs, i.e. the selective estrogen receptor modulator (SERM) Clomiphene (<https://go.drugbank.com/drugs/DB00882>) and the vasopressin receptor antagonist Conivaptan (<https://go.drugbank.com/drugs/DB00872>) on the one hand and the plant anthraquinone Emodin on the other (Matsuda et al., 2001).

Clomiphene is a mixture of the two isomers Zuclomiphene (cis-) and Enclomiphene (trans-isomer) which show estrogen agonistic and antagonistic effects (<https://drugs.ncats.io/drug/1HRS458QU2>). To test a potential stereo-selectivity, we treated our cell lines with both isomers and observed a similar increase of *SNCA* mRNA, respectively. The screening library contained other SERMS and drugs affecting estrogen/progesterone receptor pathway which showed no effect in the HTS. We thus considered canonical estrogenic effects as unlikely for the observed increase of alpha-synuclein expression. Similarly, three vaptanes were tested in the HTS but only Conivaptan the vasopressin V1A and V2 receptor antagonist modulated *SNCA* mRNA and *SNCA* protein levels. Treatment with vasopressin alone did not show any effect to *SNCA* mRNA levels suggesting that the observed increase was not related to a vasopressin receptor (V1A, V2) mediated effect (Stahl et al., 2021).

To further explore a potential mechanism behind the observed increase of *SNCA* expression, we analysed global histone modifications and the DNA methylation status of the *SNCA* intron 1 region. We found increased acetylation of histone H3 and H4, and increased histone H3K4 trimethylation after treatment with Emodin in comparable amounts to the positive control valproic acid (VPA). Clomiphene and Conivaptan

showed no significant association with histone acetylation or methylation levels. Neither of the activators led to differential DNA methylation in *SNCA* intron 1 (Stahl et al., 2021).

The absence of a clear-cut inhibitor in our unbiased reporter cell line-based HTS is in contrast to the work of Mittal and colleagues, who quantified mRNA levels of endogenous *SNCA* in SK-N-MC neuroblastoma cells (Mittal et al., 2017). We did not reveal a substance with an immediate translational value for the modulation of alpha-synuclein expression. Because we found no specific mode of action for the identified activators (except global histone modifications for Emodin) future studies will be needed to uncover potential mechanisms leading to the observed increased *SNCA* levels (Stahl et al., 2021).

Contribution of the PhD student

Fabian Stahl established, performed and validated the real time quantitative PCR (RT-qPCR) assay to confirm potential modulators of *LUC*- and *SNCA* mRNA in the *SNCA-GFP-LUC* screening and control cell line after the initial HTS and in the non-modified SH-SY5Y, respectively. Furthermore, he conducted the two independent protein assays: in-cell Western and conventional Western blot to proof increased *SNCA* protein levels. Fabian Stahl designed and conceptualized further experiments together with his supervisor (Prof. Ullrich Wüllner) to elucidate potential mechanisms leading to increased *SNCA* expression levels. Mr. Stahl planned and performed the discussed experiments, including Western blot for histone modifications, DNA methylation assay of *SNCA* intron 1 and additional RT-qPCR for Zu- and Enclomiphene, independently. He conducted a LUC assay and RT-qPCR to determine LUC signal changes in the *SNCA-GFP-LUC* screening cell line and determine *SNCA* mRNA levels after vasopressin treatment, respectively.

Beside the experimental work, Fabian Stahl was responsible for the validation of the generated data and preparation of the figures. Additionally, he was substantially involved in the writing process of this manuscript.

4 Report sheet Publication 2

High Throughput Compound Screening in Neuronal Cells Identifies Statins as Activators of Ataxin-3 Expression

Fabian Stahl^{1,2}, **Ina Schmitt**², **Philip Denner**¹, **Laura de Boni**^{2,3}, **Ullrich Wüllner**^{1,2,4}✉ & **Peter Breuer**^{1,2,4}

¹German Center for Neurodegenerative Diseases, DZNE, Venusberg-Campus 1, 53127 Bonn, NRW, Germany.

²Department of Neurology, University Hospital Bonn, Venusberg-Campus 1, 53127 Bonn, NRW, Germany.

³Institute of Aerospace Medicine, German Aerospace Center, Cologne, Germany.

Stahl, F., Schmitt, I., Denner, P. *et al.* High throughput compound screening in neuronal cells identifies statins as activators of ataxin 3 expression. *Sci Rep* **13**, 14911 (2023). <https://doi.org/10.1038/s41598-023-41192-4>

Summary

The spinocerebellar ataxias (SCAs) comprise a group of inherited neurodegenerative diseases. Machado Joseph Disease (MJD) or Spinocerebellar Ataxia 3 (SCA3) is the most common form, caused by the expansion of CAG repeats within the ataxin-3 (ATXN3) gene (Coutinho & Andrade, 1978; Kawaguchi et al., 1994; Klockgether et al., 2019). The mutation results in the expression of an abnormal ATXN3 protein, containing long polyglutamine (polyQ) stretches that confers a toxic gain of function and leads to misfolding and aggregation of the disease protein in neurons. As a result of the neurodegenerative process, SCA3 patients are severely disabled and die prematurely (Costa Mdo & Paulson, 2012). Thus, reducing the amount of the disease-causing ATXN3 protein could ameliorate the pathology in SCA3 patients. In the past, several screening approaches e.g. druggable genome-wide- and drug library screenings have been performed (Ashraf et al., 2020; Bilen & Bonini, 2007; Costa et al., 2016; Fardghassesemi et al., 2021; Vo et al., 2012). These studies mainly concentrated on the reduction of stably overexpressed polyQ ATXN3 protein, and improvement of the resultant toxicity. However, by considering transgenic overexpression models of toxic ATXN3 alone, potential modulators of endogenous ATXN3 regulation might be missed. Here, we performed, to our knowledge, the first

reporter cell line-based high throughput compound screening (HTS) to identify modulators of endogenous *ATXN3* expression.

We used the CRISPR/Cas9-based gene editing to modify the endogenous *ATXN3* gene in a SK-N-SH wild type cell line and inserted a *GFP-T2A-luciferase (LUC)* cassette in exon 4 (*ATXN3-LUC*). Additionally, a second SK-N-SH cell line with a random integration of the reporter cassette (Rand-*LUC*) was established serving as a control for unspecific modulators and toxicity. We screened a library comprising 2,640 bioactive compounds, including FDA approved drugs. Whereas no unequivocal inhibitor was found, we identified four statins as potential activators. The compound library contained eight different statins but only Mevastatin, Atorvastatin, Fluvastatin and Simvastatin increased LUC signal in the *ATXN3-LUC* screening cell line. Statins are potential inhibitors of 3-hydroxy-3-methylglutaryl coenzyme A reductase (HMGCR) the rate-limiting enzyme in the mevalonate/cholesterol pathway (Endo et al., 1976). The inhibition of HMGCR leads to reduced sterol levels in the cell and activates sterol regulatory element binding proteins (SREBPs) to initiate transcription of genes involved in cholesterol and fatty acid homeostasis (Brown & Goldstein, 1997; Horton et al., 2002). Furthermore, statin treatment has been shown to increase the stability of the HMGCR protein by stopping its ubiquitination and inducing its SREBP dependent transcription (DeBose-Boyd, 2008; Jiang et al., 2018).

Simvastatin showed the most consistent effect in the primary high throughput screening (HTS) and was used for further validation in SK-N-SH wild type cells. We performed time-course experiments and applied Simvastatin for 2, 4 and 8 hours (h). The treatment led to a significant increase of *ATXN3* mRNA (1.4 fold after 2 h) and *ATXN3* protein levels (~1.3 fold after 4 h), compared to DMSO controls. Screening of the MotifMap database (<https://motifmap.ics.uci.edu/>) and the UCSC Genome Browser (<https://genome.ucsc.edu/>) revealed predictions of the SREBP1 binding site at the human- and mouse *ATXN3* promotor as well as ChIP-seq data for SREBP1 binding at the human *ATXN3* promotor (Kent et al., 2002; Mathelier et al., 2014; Rosenbloom et al., 2013; Xie et al., 2009). To test whether Simvastatin induces the pathway for cholesterol restoration in our cell line, the activation of SREBP1 and the accumulation of HMGCR was investigated. We observed significantly increased activation of the SREBP1 transcription factor (TF) after 4 h- and increased HMGCR level after 2 h of Simvastatin treatment. Furthermore, we demonstrated direct binding of SREBP1 to the

human *ATXN3* promotor via ChIP-qPCR experiments, suggesting that the induction of ataxin-3 expression in SK-N-SH wild type cells is likely regulated via SREBP1. We confirmed our findings by time-controlled overexpression of the active human SREBP1a in a tetracycline-controlled trans-activator (tTA) containing (pTet-Off)- and doxycycline (Dox)-responsive murine Neuro 2a (N2a) cell line. Overexpression of SREBP1a significantly increased the protein levels of endogenous *ATXN3*. The same model system was used to confirm SREBP1a binding to human *ATXN3* promotor by co-transfection of a LUC reporter plasmid containing human *ATXN3* promotor sequence, the SREBP1a- and the *Renilla* LUC plasmid for normalization. These data suggest a similar SREBP1 dependent regulation of murine- and human ataxin-3 levels. Finally, we observed increased *ATXN3* and HMGCR protein levels in a SCA3 patient-derived neuronal cell line, underlining the potential clinical relevance of the findings in this study. Based on our data, we postulate a putative new role of *ATXN3* in the regulation of cholesterol homeostasis (Stahl et al., 2023).

Contribution of the PhD student

Fabian Stahl performed the titration of the appropriate cell number for best signal to noise ratio in the initial LUC reporter cell line-based HTS. He was the responsible scientist for the initial HTS, organizing cell preparation, compound treatment, LUC assay and data validation in cooperation with the laboratory automation technologies (LAT) at the Deutsches Zentrum für Neurodegenerative Erkrankungen (DZNE). Fabian Stahl confirmed potential modulators of ataxin-3 expression in the SK-N-SH wild type cell line by performing real-time quantitative PCR (RT-qPCR) (mRNA) and Western blot experiments. Together with his supervisor Prof. Ullrich Wüllner and Dr. Peter Breuer, he formulates ideas to find a potential mechanism behind the statin induced increase of ataxin-3. Fabian Stahl performed the ChIP-qPCR assays, conducted transient transfections and time-controlled overexpression experiments in murine N2a cells. He cloned the *ATXN3* promotor containing LUC plasmid and performed the co-expression experiments. Finally, he was responsible for cultivation of the SCA3 patient-derived cells and experimental implementation.

Beside the experimental work, Fabian Stahl was responsible for the preparation of the figures and for writing of the main body of this manuscript.

5 Discussion

5.1 LUC reporter cell line-based HTS

In this study two independent LUC reporter cell line-based HTS for modulators of alpha-synuclein and ataxin-3 expression were performed. Libraries containing 1,649 and 2,640 bioactive- and FDA approved drugs were screened, respectively. Neither of the HTS revealed unequivocal transcriptional inhibitors for *SNCA* or *ATXN3* but identified potential activators which were further analysed in non-modified wild type cell lines.

5.1.1 Missing inhibitors

The design of such screenings has major impact on their outcome. On the one hand, the selection of a screening cell line is crucial, because the transcriptome- and proteome expression patterns vary among different cell lines which might lead to ambiguous results in different studies. On the other hand, the concentration- and duration of compound treatment certainly affect the results of any screening approach. The HTS for alpha-synuclein and ataxin-3 was performed at a standard concentration of 10 μ M for the respective compounds and cells were treated for 24 h whereas others (see below) have chosen a lower concentration (1 μ M) and prolonged incubation time (48 h) (Mittal et al., 2017). Dependent on the half maximal inhibitory-/effective concentrations (IC₅₀/EC₅₀) of compounds, treatment concentrations above may result in enhanced toxicity to the cells and potentially masks transcriptional inhibitors. In contrast to other studies, control cell lines, bearing a randomly integrated LUC reporter cassette, were used in the performed HTS. This allowed the rigorous selection of rather specific transcriptional effects at the *SNCA* or *ATXN3* promotor in the screening cell lines and the exclusion of potentially non-specific transcriptional inhibitors.

5.2 HTS for modulators of alpha-synuclein expression

The lack of a clear-cut inhibitor for alpha-synuclein expression is in contrast to the findings from Mittal and colleagues. They published the first endogenous HTS for modulators of alpha-synuclein expression levels and identified β 2AR agonists as inhibitors of alpha-synuclein. Our screening library also contained β 2AR modulators but none were active in the primary LUC assay-based HTS. By using the online

database Human Protein Atlas (<https://www.proteinatlas.org/>) it was revealed that SH-SY5Y cells do not express β 2AR which has been confirmed by western blot experiments (Mittal et al., 2017; Stahl et al., 2021). These findings highlight that contradicting results can be obtained and explained by using different cell lines for the respective screening approaches. Thus, the selection of appropriate cell lines used for such screenings is critical and should resemble human neurons most closely. Human derived iPSC-derived neuronal cells could represent a better model system for the respective disease in future HTS approaches despite difficulties of the experimental optimization.

Three activators of alpha-synuclein mRNA and protein levels have been confirmed in SH-SY5Y wild type cells, comprising two hormone receptor interacting drugs Clomiphene and Conivaptan and on the other hand the plant anthraquinone Emodin on the other.

Estrogenic effects are assumed to play a protective role in PD, as women appear to be less susceptible to the disease than men (Taylor et al., 2007). However, epidemiological studies addressing the question of whether endogenous estrogens, including factors like age of menopause and menarche or fertile lifespan and exogenous estrogens such as hormone replacement therapy (HRT) and contraceptive (CV) use affecting the development of PD, have found contradicting results. A recent meta-analysis of observational studies did not provide a significant association between these factors and PD in women (Lv et al., 2017). On the other hand, estrogens or estrogenic compounds have been reported to be neuroprotective in cell- and mouse models but no data of potential estrogenic effects on alpha-synuclein levels were reported (Bustamante-Barrientos et al., 2021).

Clomiphene was the only selective estrogen receptor modulator (SERM) in the screening library increasing alpha-synuclein mRNA and protein levels. Clomiphene is a mixture of the two isomers Zuclomiphene (cis-) and Enclomiphene (trans-isomer) which have estrogenic agonistic and antagonistic properties, respectively (<https://drugs.ncats.io/drug/1HRS458QU2>). Further validation in wild type SH-SY5Y revealed that both isomers lead to similar increase of *SNCA* mRNA level and no stereo selectivity was identified (Stahl et al., 2021). Interestingly, the plant-derived compound Emodin was reported to exert estrogenic effects (Matsuda et al., 2001).

Several other compounds affecting the estrogen/progesterone receptor pathway including SERMS, estrogen receptor antagonists, aromatase inhibitors, progestones, estradiol and their derivatives were included in the screening library. Raloxifene decreased the LUC signal in the *SNCA-GFP-T2A-LUC* screening cell line but showed no consistent effect in the RT-qPCR assays. Taken together, these findings suggest that canonical estrogenic effects are unlikely responsible for the observed Clomiphene induced transcriptional modulation of *SNCA*.

Conivaptan represents a vasopressin V1A and V2 receptor antagonist and was the second hormone receptor interacting drug found in the HTS (<https://go.drugbank.com/drugs/DB00872>). Two other vaptans were part of the screening but proved ineffective. The receptor agonist vasopressin was tested in subsequent experiments but did not alter *SNCA* mRNA levels in the wild type cell line, indicating no vasopressin receptor (V1A, V2) mediated effect (Stahl et al., 2021). Interestingly, mean plasma vasopressin levels were observed to be significantly higher in treated- compared to treatment-naïve PD patients. However, no association was found between vasopressin levels and disease severity or L-DOPA dosage (Arai, 2011).

Since no specific mechanisms for the compound induced increase of alpha-synuclein levels were found in this study, more global effects causing transcriptional regulation of *SNCA* have been investigated. Epigenetic alterations like changed DNA methylation of *SNCA* intron 1 and modulations of histone marks, especially increased histone H3K4 trimethylation and increased histone H3 acetylation have been observed in PD patients and reported to affect alpha-synuclein levels (see introduction).

The analysis of the *SNCA* intron 1 promotor methylation levels revealed no alterations after treatment with Clomiphene, Conivaptan and Emodin compared to DMSO controls. However, by investigating changes of histone marks in compound treated SH-SY5Y cells, Emodin treatment was found to significantly increase H3K4me3 and global H3/H4ac levels in comparable amounts to the positive control valproic acid (VPA), a known HDAC and alpha-synuclein expression inducer (Leng & Chuang, 2006; Stahl et al., 2021). These findings are in line with another study which reported HDAC inhibitory effects of Emodin (Godoy et al., 2017).

On the other hand, the screening library included 23 known HDAC inhibitors which showed no- or no consistent effect in the HTS, suggesting that altered histone acetylation alone is unlikely to increase alpha-synuclein expression. Furthermore, Emodin and VPA did not alter LUC signal levels in the control cell line with the random *GFP-T2A-LUC* cassette integration, indicating a more specific downstream regulatory mechanism. The observed changes in open chromatin marks could facilitate the direct binding of TFs to genomic regions of *SNCA* increasing its expression or indirectly via a cascade of interposed regulatory events, since histone modifications occurring as global transcriptional modifications.

VPA is clinically used as an anticonvulsant and mood-stabilizer that can, albeit at low frequency, trigger parkinsonian symptoms in patients that have been shown to be reversible after VPA cessation (Mahmoud & Tampi, 2011). However, the use of Emodin has not been associated with parkinsonism yet.

5.3 HTS for modulators of ataxin-3 expression

Statins were identified as potential activators of ataxin-3 expression in the primary LUC assay-based HTS. The screening library contained eight statins from which Atorvastatin, Mevastatin, Fluvastatin and Simvastatin altered LUC signal in the screening cell line.

Statins represent a potent compound class halting the conversion of 3-hydroxy-3-methylglutaryl coenzyme A to mevalonate by inhibiting 3-hydroxy-3-methylglutaryl coenzyme A reductase (HMGCR), the rate limiting enzyme in cholesterol homeostasis (Endo et al., 1976). Inhibition of HMGCR results in cholesterol deprivation and induce the activation of sterol regulatory element binding proteins (SREBPs). Three SREBPs have been identified and were found to function as classic basic-helix-loop-helix leucine finger (bHLH zip) TFs which are involved in cholesterol (SREBP1a/ SREBP2) and fatty acid (SREBP1a/ SREBP1c) homeostasis (Horton et al., 2002; Horton et al., 2003). SREBP1a/c are transcribed from one gene (*SREBP1*) and differs in the N-terminal transactivation domain whereas SREBP2 is encoded by the *SREBP2* gene (Horton et al., 2002). SREBPs are located in the endoplasmic reticulum (ER) membrane and bind to the SREBP-cleavage activating protein (SCAP) which sense cholesterol levels in the cell. Under low cholesterol levels, SCAP escorts SREBP via

COPII vesicles to the Golgi where site-1 and site-2 proteases release the active (mSREBP) TF for nuclear translocation and transcriptional activation. At normal or high cholesterol levels, SCAP retains SREBP in the ER membrane by direct interaction with the insulin-induced genes 1 and 2 (INSIG1, INSIG2) (Brown & Goldstein, 1997; Espenshade & Hughes, 2007). INSIGs are oxysterol sensing proteins which are also bound to HMGCR and mediate its ubiquitination and proteasomal degradation under normal or high sterol levels. Statin-induced sterol deprivation mediates the dissociation of INSIG and HMGCR and leads to subsequent accumulation of the enzyme which is further enhanced through its SREBP dependent increased transcriptional expression (DeBose-Boyd, 2008; Jiang et al., 2018).

In the HTS, Simvastatin showed the most consistent effect and was confirmed to raise ataxin-3 expression. By screening the MotifMap database (<https://motifmap.ics.uci.edu/>) and the UCSC Genome Browser (<https://genome.ucsc.edu/>), SREBP1 binding site predictions at the human and mouse *ATXN3* promotor, and ChIP-seq data for SREBP1 binding at the human *ATXN3* promotor were obtained (Kent et al., 2002; Mathelier et al., 2014; Rosenbloom et al., 2013; Xie et al., 2009). To proof whether Simvastatin treatment lead to the induction of the cellular mechanisms for cholesterol restoration, the HMGCR expression level and SREBP1 activation were analysed. Western blot data revealed a significant increase of HMGCR and SREBP1 activation in the SK-N-SH wild type cell line. Increased *ATXN3* expression was likely mediated through direct binding of the SREBP1 TF to the *ATXN3* promotor as shown in ChIP-qPCR assays. To confirm these results, time-controlled overexpression of active human SREBP1a in murine pTet-Off N2a was performed and increased levels of endogenous *ATXN3* protein were observed. To verify SREBP1a binding to the human *ATXN3* promotor sequence, the same model system was used to co-express a LUC plasmid containing the human *ATXN3* promotor sequence, the SREBP1a- and a *Renilla* LUC plasmid for normalization. Co-expression resulted in an increased LUC signal, suggesting a similar SREBP1 dependent regulation of murine and human ataxin-3. Finally, we found that Simvastatin treatment of SCA3 patient-derived neuronal cells led to increased expression of endogenous *ATXN3* and HMGCR protein levels, indicating a potential clinical relevance (Stahl et al., 2023).

In the brain, cholesterol is the main component of myelin sheaths of axons and crucial for synapse formation and proper function (Mauch et al., 2001; Pfrieger, 2003). The brain accounts only 2 % of total body weight but consists of 23 % of whole-body cholesterol (Dietschy & Turley, 2004). All of the required cholesterol must be synthesized *de novo* since the BBB restrict cholesterol crossing from the peripheral blood stream. In perinatal and adolescent years high levels of cholesterol are required for formation of myelin sheaths around the axons in the developing brain. In the mature brain, cholesterol synthesis is reduced by 90 % and mainly takes place in glia cells but also slightly in neurons (Edmond et al., 1991; Jurevics & Morell, 1995; Nieweg et al., 2009; Quan et al., 2003). Astroglia produces two to three times more cholesterol than neurons and provide it to the latter. In the brain cholesterol mainly associates with apolipoprotein E (APOE) which is synthesized in astroglia, exported via ATP-binding cassette (ABC) transporters, and taken up by neurons through low-density lipoprotein family receptors (LDLR) (Fracassi et al., 2019).

Dysregulation of cholesterol homeostasis has been discussed for a variety of NDDs, especially AD. The cholesterol transporter APOE gene exists in three polymorphic alleles $\epsilon 2$, $\epsilon 3$ and $\epsilon 4$. APOE $\epsilon 4$ is highly associated with late onset AD (LOAD) where the allelic frequency of $\epsilon 4$ increased to ~40 % in AD patients. Studies found that APOE $\epsilon 4$ has the lowest efficiency in transporting cholesterol compared to $\epsilon 2$ and $\epsilon 3$, which might affect the transmission of cholesterol from astroglia to neurons and thus may lead to reduced neuronal health provoking neurodegeneration (Liu et al., 2013). However, contradicting results have been found in the levels of total cholesterol in AD and it is still under debate whether high or low cholesterol levels increase the risk for AD. Similarly, studies investigating total cholesterol levels in PD and HD revealed no conclusive results. Motor symptoms of PD patients have been associated with low levels of apolipoprotein A-I (ApoA1) which is part of the transporter complex of high-density lipoprotein (HDL), suggesting a critical role of cholesterol metabolism in PD. Furthermore, several reports found that cholesterol interacts- and potentially leads to aggregation of SNCA (Dai et al., 2021).

Statins are traditionally used to treat hypercholesteremia and are mainly metabolized in the liver. There is increasing evidence that statins may be useful for the treatment of NDDs (Fracassi et al., 2019). It was shown that statin treatment can alter gene expression and affect cholesterol synthesis in in the brain of mice (Johnson-Anuna et

al., 2005; Lutjohann et al., 2004). The ability to cross the BBB is dependent on their lipophilicity. Simvastatin and Lovastatin are thought to pass the BBB via passive diffusion, less lipophilic statins like Fluvastatin and Pravastatin might be actively transported via organic anion transporter polypeptide 2 (OATP2) or monocarboxylic acid transporter (MCT) (Fracassi et al., 2019; Hamelin & Turgeon, 1998). Besides the cholesterol lowering properties, statins were shown to have beneficial anti-inflammatory effects, the ability to improve long term potential (LTP) and to induce neurite and axonal outgrowth which might be considerable aspects for the treatment of NDDs (Li et al., 2016; Mans et al., 2012; Pahan et al., 1997; Roy et al., 2015). Cell culture experiments, animal models, retrospective studies and randomized control trials revealed mainly positive effects of statin treatment in AD and PD (Dai et al., 2021). On the other hand, a huge meta study including mental disorders and NDDs like AD, PD, and HD concluded that further research is needed, despite many reports describing beneficial effects of statin treatments, since some studies did not confirm the initially observed effects (Fracassi et al., 2019).

Only a few studies linked altered cholesterol homeostasis to SCA3. Toonen and colleagues (2018) found transcriptional changes in genes related to cholesterol biosynthesis pathways in brains of a SCA3 mouse model (Toonen et al., 2018). Another study reported that cholesterol 24-hydroxylase (CYP46A1), which converts cholesterol into 24-hydroxycholesterol (24-OHC) enabling cholesterol turnover and efflux via the BBB into circulation, was reduced in cerebellar extracts of SCA3 patients and in a SCA3 mouse model. The authors showed, that overexpression CYP46A1 in SCA3 mice led to reduced accumulation of polyQ ATXN3 and neuroprotection whereas knockout of CYP46A1 impairs cholesterol metabolism and led to severe neurodegeneration (Nobrega et al., 2019).

CYP46A1 expression was found to be reduced in other NDDs including AD and HD in patient derived *post-mortem* brain samples and mouse models suggesting a more general role of this enzyme in brain plasticity and protection against neurodegeneration. Overexpression of CYP46A1 was shown to have beneficial effects in neuroprotection, implementing that probably cholesterol turnover and efflux rate of 24-OHC is critical in NDDs (Boussicault et al., 2016; Maioli et al., 2013; Pikuleva & Cartier, 2021; Testa et al., 2016).

Despite the above-mentioned implications of cholesterol synthesis or turnover in SCA3, none of the studies described a potential function of *ATXN3* in cholesterol homeostasis. Based on the results from this study, *ATXN3* is likely a SREBP1 regulated gene and may play a (yet) unknown role in the SREBP dependent regulation of cholesterol homeostasis. HMGCR, the key enzyme in cholesterol homeostasis, is an ERAD dependent substrate and degraded under high cholesterol conditions. Ubiquitination of HMGCR is initiated via binding of INSIG which in turn is associated with VCP/p97, the ubiquitin-conjugating enzyme E2 (Ubc7) and glycoprotein 78 E3 ubiquitin ligase (gp78) (DeBose-Boyd, 2008).

Earlier studies reported that *ATXN3* directly interacts with VCP/p97 and plays a potential role in regulating the flow and turnover within the ERAD pathway (see introduction). Thus, it is tempting to hypothesize that *ATXN3* could also be involved in HMGCR stability. Since the expansion of the polyQ tract of *ATXN3* affects the binding to its substrates, HMGCR turnover might be altered and lead to impaired cholesterol homeostasis and to subsequent neurodegeneration.

5.4 Conclusion

In summary, this work has proven that LUC reporter cell line-based HTS are viable approaches enabling fast and cost-effective screening of compound libraries to identify modulators of endogenous alpha-synuclein and ataxin-3 expression. Furthermore, new genetic targets for FDA-approved compounds and drugs which are already in clinical use (Clomiphen, Conivaptan and Simvastatin) can be found within such screenings allowing drug repurposing. Despite the lack of any inhibitors, transcriptional activators for both genes were identified and potential mechanisms behind the expression change were investigated. Whereas no specific mechanism for altered alpha-synuclein expression (except histone modifications) was found, the ataxin-3 screening provides evidence for a transcriptional regulation of *ATXN3* expression by the SREBP1 TF and suggests a potential new role of *ATXN3* in cholesterol homeostasis.

6 References

- Albrecht, M., Golatta, M., Wullner, U., & Lengauer, T. (2004, Aug). Structural and functional analysis of ataxin-2 and ataxin-3. *Eur J Biochem*, 271(15), 3155-3170. <https://doi.org/10.1111/j.1432-1033.2004.04245.x>
- Arai, M. (2011). Increased plasma arginine vasopressin levels in dopamine agonist-treated Parkinson's disease patients. *Neuro Endocrinol Lett*, 32(1), 39-43. <https://www.ncbi.nlm.nih.gov/pubmed/21407160>
- Ascherio, A., & Schwarzschild, M. A. (2016, Nov). The epidemiology of Parkinson's disease: risk factors and prevention. *Lancet Neurol*, 15(12), 1257-1272. [https://doi.org/10.1016/S1474-4422\(16\)30230-7](https://doi.org/10.1016/S1474-4422(16)30230-7)
- Ashraf, N. S., Sutton, J. R., Yang, Y., Ranxhi, B., Libohova, K., Shaw, E. D., Barget, A. J., Todi, S. V., Paulson, H. L., & Costa, M. D. C. (2020, Apr). Druggable genome screen identifies new regulators of the abundance and toxicity of ATXN3, the Spinocerebellar Ataxia type 3 disease protein. *Neurobiol Dis*, 137, 104697. <https://doi.org/10.1016/j.nbd.2019.104697>
- Ballinger, C. A., Connell, P., Wu, Y., Hu, Z., Thompson, L. J., Yin, L. Y., & Patterson, C. (1999, Jun). Identification of CHIP, a novel tetratricopeptide repeat-containing protein that interacts with heat shock proteins and negatively regulates chaperone functions. *Mol Cell Biol*, 19(6), 4535-4545. <https://doi.org/10.1128/MCB.19.6.4535>
- Bannister, A. J., & Kouzarides, T. (2011, Mar). Regulation of chromatin by histone modifications. *Cell Res*, 21(3), 381-395. <https://doi.org/10.1038/cr.2011.22>
- Barbour, R., Kling, K., Anderson, J. P., Banducci, K., Cole, T., Diep, L., Fox, M., Goldstein, J. M., Soriano, F., Seubert, P., & Chilcote, T. J. (2008). Red blood cells are the major source of alpha-synuclein in blood. *Neurodegener Dis*, 5(2), 55-59. <https://doi.org/10.1159/000112832>
- Bartel, D. P. (2004, Jan 23). MicroRNAs: genomics, biogenesis, mechanism, and function. *Cell*, 116(2), 281-297. [https://doi.org/10.1016/s0092-8674\(04\)00045-5](https://doi.org/10.1016/s0092-8674(04)00045-5)
- Bartels, T., Choi, J. G., & Selkoe, D. J. (2011, Aug 14). alpha-Synuclein occurs physiologically as a helically folded tetramer that resists aggregation. *Nature*, 477(7362), 107-110. <https://doi.org/10.1038/nature10324>
- Bendor, J. T., Logan, T. P., & Edwards, R. H. (2013, Sep 18). The function of alpha-synuclein. *Neuron*, 79(6), 1044-1066. <https://doi.org/10.1016/j.neuron.2013.09.004>

- Bettencourt, C., Santos, C., Montiel, R., Costa Mdo, C., Cruz-Morales, P., Santos, L. R., Simoes, N., Kay, T., Vasconcelos, J., Maciel, P., & Lima, M. (2010, May). Increased transcript diversity: novel splicing variants of Machado-Joseph disease gene (ATXN3). *Neurogenetics*, 11(2), 193-202. <https://doi.org/10.1007/s10048-009-0216-y>
- Bilen, J., & Bonini, N. M. (2007, Oct). Genome-wide screen for modifiers of ataxin-3 neurodegeneration in *Drosophila*. *PLoS Genet*, 3(10), 1950-1964. <https://doi.org/10.1371/journal.pgen.0030177>
- Boeddrich, A., Gaumer, S., Haacke, A., Tzvetkov, N., Albrecht, M., Evert, B. O., Muller, E. C., Lurz, R., Breuer, P., Schugardt, N., Plassmann, S., Xu, K., Warrick, J. M., Suopanki, J., Wullner, U., Frank, R., Hartl, U. F., Bonini, N. M., & Wanker, E. E. (2006, Apr 5). An arginine/lysine-rich motif is crucial for VCP/p97-mediated modulation of ataxin-3 fibrillogenesis. *EMBO J*, 25(7), 1547-1558. <https://doi.org/10.1038/sj.emboj.7601043>
- Bonifati, V., Rizzu, P., Squitieri, F., Krieger, E., Vanacore, N., van Swieten, J. C., Brice, A., van Duijn, C. M., Oostra, B., Meco, G., & Heutink, P. (2003, Oct). DJ-1 (PARK7), a novel gene for autosomal recessive, early onset parkinsonism. *Neurol Sci*, 24(3), 159-160. <https://doi.org/10.1007/s10072-003-0108-0>
- Boussicault, L., Alves, S., Lamaziere, A., Planques, A., Heck, N., Moumne, L., Despres, G., Bolte, S., Hu, A., Pages, C., Galvan, L., Piguët, F., Aubourg, P., Cartier, N., Caboche, J., & Betuing, S. (2016, Mar). CYP46A1, the rate-limiting enzyme for cholesterol degradation, is neuroprotective in Huntington's disease. *Brain*, 139(Pt 3), 953-970. <https://doi.org/10.1093/brain/awv384>
- Brenner, S., Wersinger, C., & Gasser, T. (2015, Jul 10). Transcriptional regulation of the alpha-synuclein gene in human brain tissue. *Neurosci Lett*, 599, 140-145. <https://doi.org/10.1016/j.neulet.2015.05.029>
- Brown, M. S., & Goldstein, J. L. (1997, May 2). The SREBP pathway: regulation of cholesterol metabolism by proteolysis of a membrane-bound transcription factor. *Cell*, 89(3), 331-340. [https://doi.org/10.1016/s0092-8674\(00\)80213-5](https://doi.org/10.1016/s0092-8674(00)80213-5)
- Burnett, B., Li, F., & Pittman, R. N. (2003, Dec 1). The polyglutamine neurodegenerative protein ataxin-3 binds polyubiquitylated proteins and has ubiquitin protease activity. *Hum Mol Genet*, 12(23), 3195-3205. <https://doi.org/10.1093/hmg/ddg344>
- Burnett, B. G., & Pittman, R. N. (2005, Mar 22). The polyglutamine neurodegenerative protein ataxin 3 regulates aggresome formation. *Proc Natl Acad Sci U S A*, 102(12), 4330-4335. <https://doi.org/10.1073/pnas.0407252102>

- Burre, J., Sharma, M., & Sudhof, T. C. (2014, Oct 7). alpha-Synuclein assembles into higher-order multimers upon membrane binding to promote SNARE complex formation. *Proc Natl Acad Sci U S A*, 111(40), E4274-4283. <https://doi.org/10.1073/pnas.1416598111>
- Burre, J., Sharma, M., Tsetsenis, T., Buchman, V., Etherton, M. R., & Sudhof, T. C. (2010, Sep 24). Alpha-synuclein promotes SNARE-complex assembly in vivo and in vitro. *Science*, 329(5999), 1663-1667. <https://doi.org/10.1126/science.1195227>
- Burre, J., Vivona, S., Diao, J., Sharma, M., Brunger, A. T., & Sudhof, T. C. (2013, Jun 13). Properties of native brain alpha-synuclein. *Nature*, 498(7453), E4-6; discussion E6-7. <https://doi.org/10.1038/nature12125>
- Bustamante-Barrientos, F. A., Mendez-Ruette, M., Ortloff, A., Luz-Crawford, P., Rivera, F. J., Figueroa, C. D., Molina, L., & Batiz, L. F. (2021). The Impact of Estrogen and Estrogen-Like Molecules in Neurogenesis and Neurodegeneration: Beneficial or Harmful? *Front Cell Neurosci*, 15, 636176. <https://doi.org/10.3389/fncel.2021.636176>
- Carmona, V., Cunha-Santos, J., Onofre, I., Simoes, A. T., Vijayakumar, U., Davidson, B. L., & Pereira de Almeida, L. (2017, Apr 5). Unravelling Endogenous MicroRNA System Dysfunction as a New Pathophysiological Mechanism in Machado-Joseph Disease. *Mol Ther*, 25(4), 1038-1055. <https://doi.org/10.1016/j.ymthe.2017.01.021>
- Chandra, S., Gallardo, G., Fernandez-Chacon, R., Schluter, O. M., & Sudhof, T. C. (2005, Nov 4). Alpha-synuclein cooperates with CSPalpha in preventing neurodegeneration. *Cell*, 123(3), 383-396. <https://doi.org/10.1016/j.cell.2005.09.028>
- Chartier-Harlin, M. C., Kachergus, J., Roumier, C., Mouroux, V., Douay, X., Lincoln, S., Levecque, C., Larvor, L., Andrieux, J., Hulihan, M., Waucquier, N., Defebvre, L., Amouyel, P., Farrer, M., & Destee, A. (2004, Sep 25-Oct 1). Alpha-synuclein locus duplication as a cause of familial Parkinson's disease. *Lancet*, 364(9440), 1167-1169. [https://doi.org/10.1016/S0140-6736\(04\)17103-1](https://doi.org/10.1016/S0140-6736(04)17103-1)
- Chiba-Falek, O., Kowalak, J. A., Smulson, M. E., & Nussbaum, R. L. (2005, Mar). Regulation of alpha-synuclein expression by poly (ADP ribose) polymerase-1 (PARP-1) binding to the NACP-Rep1 polymorphic site upstream of the SNCA gene. *Am J Hum Genet*, 76(3), 478-492. <https://doi.org/10.1086/428655>
- Clough, R. L., Dermentzaki, G., & Stefanis, L. (2009, Sep). Functional dissection of the alpha-synuclein promoter: transcriptional regulation by ZSCAN21 and ZNF219. *J Neurochem*, 110(5), 1479-1490. <https://doi.org/10.1111/j.1471-4159.2009.06250.x>

- Clough, R. L., & Stefanis, L. (2007, Feb). A novel pathway for transcriptional regulation of alpha-synuclein. *FASEB J*, 21(2), 596-607. <https://doi.org/10.1096/fj.06-7111com>
- Connell, P., Ballinger, C. A., Jiang, J., Wu, Y., Thompson, L. J., Hohfeld, J., & Patterson, C. (2001, Jan). The co-chaperone CHIP regulates protein triage decisions mediated by heat-shock proteins. *Nat Cell Biol*, 3(1), 93-96. <https://doi.org/10.1038/35050618>
- Costa, M. D. C., Ashraf, N. S., Fischer, S., Yang, Y., Schapka, E., Joshi, G., McQuade, T. J., Dharia, R. M., Dulchavsky, M., Ouyang, M., Cook, D., Sun, D., Larsen, M. J., Gestwicki, J. E., Todi, S. V., Ivanova, M. I., & Paulson, H. L. (2016, Nov 1). Unbiased screen identifies aripiprazole as a modulator of abundance of the polyglutamine disease protein, ataxin-3. *Brain*, 139(11), 2891-2908. <https://doi.org/10.1093/brain/aww228>
- Costa Mdo, C., & Paulson, H. L. (2012, May). Toward understanding Machado-Joseph disease. *Prog Neurobiol*, 97(2), 239-257. <https://doi.org/10.1016/j.pneurobio.2011.11.006>
- Coutinho, P., & Andrade, C. (1978, Jul). Autosomal dominant system degeneration in Portuguese families of the Azores Islands. A new genetic disorder involving cerebellar, pyramidal, extrapyramidal and spinal cord motor functions. *Neurology*, 28(7), 703-709. <https://doi.org/10.1212/wnl.28.7.703>
- Dai, L., Zou, L., Meng, L., Qiang, G., Yan, M., & Zhang, Z. (2021, May). Cholesterol Metabolism in Neurodegenerative Diseases: Molecular Mechanisms and Therapeutic Targets. *Mol Neurobiol*, 58(5), 2183-2201. <https://doi.org/10.1007/s12035-020-02232-6>
- Davidson, W. S., Jonas, A., Clayton, D. F., & George, J. M. (1998, Apr 17). Stabilization of alpha-synuclein secondary structure upon binding to synthetic membranes. *J Biol Chem*, 273(16), 9443-9449. <https://doi.org/10.1074/jbc.273.16.9443>
- de Boni, L., Tierling, S., Roeber, S., Walter, J., Giese, A., & Kretschmar, H. A. (2011, Dec). Next-generation sequencing reveals regional differences of the alpha-synuclein methylation state independent of Lewy body disease. *Neuromolecular Med*, 13(4), 310-320. <https://doi.org/10.1007/s12017-011-8163-9>
- DeBose-Boyd, R. A. (2008, Jun). Feedback regulation of cholesterol synthesis: sterol-accelerated ubiquitination and degradation of HMG CoA reductase. *Cell Res*, 18(6), 609-621. <https://doi.org/10.1038/cr.2008.61>
- Desplats, P., Spencer, B., Coffee, E., Patel, P., Michael, S., Patrick, C., Adame, A., Rockenstein, E., & Masliah, E. (2011, Mar 18). Alpha-synuclein sequesters

- Dnmt1 from the nucleus: a novel mechanism for epigenetic alterations in Lewy body diseases. *J Biol Chem*, 286(11), 9031-9037. <https://doi.org/10.1074/jbc.C110.212589>
- Dietschy, J. M., & Turley, S. D. (2004, Aug). Thematic review series: brain Lipids. Cholesterol metabolism in the central nervous system during early development and in the mature animal. *J Lipid Res*, 45(8), 1375-1397. <https://doi.org/10.1194/jlr.R400004-JLR200>
- Dorsey, E. R., Sherer, T., Okun, M. S., & Bloem, B. R. (2018). The Emerging Evidence of the Parkinson Pandemic. *J Parkinsons Dis*, 8(s1), S3-S8. <https://doi.org/10.3233/JPD-181474>
- Doss-Pepe, E. W., Stenroos, E. S., Johnson, W. G., & Madura, K. (2003, Sep). Ataxin-3 interactions with rad23 and valosin-containing protein and its associations with ubiquitin chains and the proteasome are consistent with a role in ubiquitin-mediated proteolysis. *Mol Cell Biol*, 23(18), 6469-6483. <https://doi.org/10.1128/MCB.23.18.6469-6483.2003>
- Duplan, E., Giordano, C., Checler, F., & Alves da Costa, C. (2016, Feb 2). Direct alpha-synuclein promoter transactivation by the tumor suppressor p53. *Mol Neurodegener*, 11, 13. <https://doi.org/10.1186/s13024-016-0079-2>
- Durcan, T. M., Kontogiannia, M., Thorarinsdottir, T., Fallon, L., Williams, A. J., Djarmati, A., Fantaneanu, T., Paulson, H. L., & Fon, E. A. (2011, Jan 1). The Machado-Joseph disease-associated mutant form of ataxin-3 regulates parkin ubiquitination and stability. *Hum Mol Genet*, 20(1), 141-154. <https://doi.org/10.1093/hmg/ddq452>
- Edmond, J., Korsak, R. A., Morrow, J. W., Torok-Both, G., & Catlin, D. H. (1991, Sep). Dietary cholesterol and the origin of cholesterol in the brain of developing rats. *J Nutr*, 121(9), 1323-1330. <https://doi.org/10.1093/jn/121.9.1323>
- Eliezer, D., Kutluay, E., Bussell, R., Jr., & Browne, G. (2001, Apr 6). Conformational properties of alpha-synuclein in its free and lipid-associated states. *J Mol Biol*, 307(4), 1061-1073. <https://doi.org/10.1006/jmbi.2001.4538>
- Endo, A., Kuroda, M., & Tanzawa, K. (1976, Dec 31). Competitive inhibition of 3-hydroxy-3-methylglutaryl coenzyme A reductase by ML-236A and ML-236B fungal metabolites, having hypocholesterolemic activity. *FEBS Lett*, 72(2), 323-326. [https://doi.org/10.1016/0014-5793\(76\)80996-9](https://doi.org/10.1016/0014-5793(76)80996-9)
- Espenshade, P. J., & Hughes, A. L. (2007). Regulation of sterol synthesis in eukaryotes. *Annu Rev Genet*, 41, 401-427. <https://doi.org/10.1146/annurev.genet.41.110306.130315>

- Evert, B. O., Wullner, U., Schulz, J. B., Weller, M., Groscurth, P., Trottier, Y., Brice, A., & Klockgether, T. (1999, Jul). High level expression of expanded full-length ataxin-3 in vitro causes cell death and formation of intranuclear inclusions in neuronal cells. *Hum Mol Genet*, 8(7), 1169-1176. <https://doi.org/10.1093/hmg/8.7.1169>
- Fardghassemi, Y., Maios, C., & Parker, J. A. (2021, Apr). Small Molecule Rescue of ATXN3 Toxicity in *C. elegans* via TFEB/HLH-30. *Neurotherapeutics*, 18(2), 1151-1165. <https://doi.org/10.1007/s13311-020-00993-5>
- Farrer, M., Kachergus, J., Forno, L., Lincoln, S., Wang, D. S., Hulihan, M., Maraganore, D., Gwinn-Hardy, K., Wszolek, Z., Dickson, D., & Langston, J. W. (2004, Feb). Comparison of kindreds with parkinsonism and alpha-synuclein genomic multiplications. *Ann Neurol*, 55(2), 174-179. <https://doi.org/10.1002/ana.10846>
- Forman, M. S., Trojanowski, J. Q., & Lee, V. M. (2004, Oct). Neurodegenerative diseases: a decade of discoveries paves the way for therapeutic breakthroughs. *Nat Med*, 10(10), 1055-1063. <https://doi.org/10.1038/nm1113>
- Fracassi, A., Marangoni, M., Rosso, P., Pallottini, V., Fioramonti, M., Siteni, S., & Segatto, M. (2019). Statins and the Brain: More than Lipid Lowering Agents? *Curr Neuroparmacol*, 17(1), 59-83. <https://doi.org/10.2174/1570159X15666170703101816>
- Fuchs, J., Tichopad, A., Golub, Y., Munz, M., Schweitzer, K. J., Wolf, B., Berg, D., Mueller, J. C., & Gasser, T. (2008, May). Genetic variability in the SNCA gene influences alpha-synuclein levels in the blood and brain. *FASEB J*, 22(5), 1327-1334. <https://doi.org/10.1096/fj.07-9348com>
- Funayama, M., Hasegawa, K., Kowa, H., Saito, M., Tsuji, S., & Obata, F. (2002, Mar). A new locus for Parkinson's disease (PARK8) maps to chromosome 12p11.2-q13.1. *Ann Neurol*, 51(3), 296-301. <https://doi.org/10.1002/ana.10113>
- Garcia-Mata, R., Bebok, Z., Sorscher, E. J., & Sztul, E. S. (1999, Sep 20). Characterization and dynamics of aggresome formation by a cytosolic GFP-chimera. *J Cell Biol*, 146(6), 1239-1254. <https://doi.org/10.1083/jcb.146.6.1239>
- George, J. M. (2002). The synucleins. *Genome Biol*, 3(1), REVIEWS3002. <https://doi.org/10.1186/gb-2001-3-1-reviews3002>
- George, J. M., Jin, H., Woods, W. S., & Clayton, D. F. (1995, Aug). Characterization of a novel protein regulated during the critical period for song learning in the zebra finch. *Neuron*, 15(2), 361-372. [https://doi.org/10.1016/0896-6273\(95\)90040-3](https://doi.org/10.1016/0896-6273(95)90040-3)

- Godoy, L. D., Lucas, J. E., Bender, A. J., Romanick, S. S., & Ferguson, B. S. (2017, Apr). Targeting the epigenome: Screening bioactive compounds that regulate histone deacetylase activity. *Mol Nutr Food Res*, 61(4). <https://doi.org/10.1002/mnfr.201600744>
- Gomez-Santos, C., Barrachina, M., Gimenez-Xavier, P., Dalfo, E., Ferrer, I., & Ambrosio, S. (2005, Feb 15). Induction of C/EBP beta and GADD153 expression by dopamine in human neuroblastoma cells. Relationship with alpha-synuclein increase and cell damage. *Brain Res Bull*, 65(1), 87-95. <https://doi.org/10.1016/j.brainresbull.2004.11.008>
- Guhathakurta, S., Bok, E., Evangelista, B. A., & Kim, Y. S. (2017, Jul). Deregulation of alpha-synuclein in Parkinson's disease: Insight from epigenetic structure and transcriptional regulation of SNCA. *Prog Neurobiol*, 154, 21-36. <https://doi.org/10.1016/j.pneurobio.2017.04.004>
- Guhathakurta, S., Kim, J., Adams, L., Basu, S., Song, M. K., Adler, E., Je, G., Fiadeiro, M. B., & Kim, Y. S. (2021, Feb 5). Targeted attenuation of elevated histone marks at SNCA alleviates alpha-synuclein in Parkinson's disease. *EMBO Mol Med*, 13(2), e12188. <https://doi.org/10.15252/emmm.202012188>
- Hamelin, B. A., & Turgeon, J. (1998, Jan). Hydrophilicity/lipophilicity: relevance for the pharmacology and clinical effects of HMG-CoA reductase inhibitors. *Trends Pharmacol Sci*, 19(1), 26-37. [https://doi.org/10.1016/s0165-6147\(97\)01147-4](https://doi.org/10.1016/s0165-6147(97)01147-4)
- Harris, G. M., Dodelzon, K., Gong, L., Gonzalez-Alegre, P., & Paulson, H. L. (2010, Oct 27). Splice isoforms of the polyglutamine disease protein ataxin-3 exhibit similar enzymatic yet different aggregation properties. *PLoS One*, 5(10), e13695. <https://doi.org/10.1371/journal.pone.0013695>
- Hernandez, D. G., Reed, X., & Singleton, A. B. (2016, Oct). Genetics in Parkinson disease: Mendelian versus non-Mendelian inheritance. *J Neurochem*, 139 Suppl 1(Suppl 1), 59-74. <https://doi.org/10.1111/jnc.13593>
- Hirabayashi, M., Inoue, K., Tanaka, K., Nakadate, K., Ohsawa, Y., Kamei, Y., Popiel, A. H., Sinohara, A., Iwamatsu, A., Kimura, Y., Uchiyama, Y., Hori, S., & Kakizuka, A. (2001, Oct). VCP/p97 in abnormal protein aggregates, cytoplasmic vacuoles, and cell death, phenotypes relevant to neurodegeneration. *Cell Death Differ*, 8(10), 977-984. <https://doi.org/10.1038/sj.cdd.4400907>
- Hofmann, K., & Falquet, L. (2001, Jun). A ubiquitin-interacting motif conserved in components of the proteasomal and lysosomal protein degradation systems. *Trends Biochem Sci*, 26(6), 347-350. [https://doi.org/10.1016/s0968-0004\(01\)01835-7](https://doi.org/10.1016/s0968-0004(01)01835-7)

- Hollerhage, M., Bickle, M., & Hoglinger, G. U. (2019, Feb 9). Unbiased Screens for Modifiers of Alpha-Synuclein Toxicity. *Curr Neurol Neurosci Rep*, 19(2), 8. <https://doi.org/10.1007/s11910-019-0925-z>
- Hollerhage, M., Moebius, C., Melms, J., Chiu, W. H., Goebel, J. N., Chakraborty, T., Koeglsperger, T., Oertel, W. H., Rosler, T. W., Bickle, M., & Hoglinger, G. U. (2017, Sep 13). Protective efficacy of phosphodiesterase-1 inhibition against alpha-synuclein toxicity revealed by compound screening in LUHMES cells. *Sci Rep*, 7(1), 11469. <https://doi.org/10.1038/s41598-017-11664-5>
- Horton, J. D., Goldstein, J. L., & Brown, M. S. (2002, May). SREBPs: activators of the complete program of cholesterol and fatty acid synthesis in the liver. *J Clin Invest*, 109(9), 1125-1131. <https://doi.org/10.1172/JCI15593>
- Horton, J. D., Shah, N. A., Warrington, J. A., Anderson, N. N., Park, S. W., Brown, M. S., & Goldstein, J. L. (2003, Oct 14). Combined analysis of oligonucleotide microarray data from transgenic and knockout mice identifies direct SREBP target genes. *Proc Natl Acad Sci U S A*, 100(21), 12027-12032. <https://doi.org/10.1073/pnas.1534923100>
- Ichikawa, Y., Goto, J., Hattori, M., Toyoda, A., Ishii, K., Jeong, S. Y., Hashida, H., Masuda, N., Ogata, K., Kasai, F., Hirai, M., Maciel, P., Rouleau, G. A., Sakaki, Y., & Kanazawa, I. (2001). The genomic structure and expression of MJD, the Machado-Joseph disease gene. *J Hum Genet*, 46(7), 413-422. <https://doi.org/10.1007/s100380170060>
- Iwai, A., Masliah, E., Yoshimoto, M., Ge, N., Flanagan, L., de Silva, H. A., Kittel, A., & Saitoh, T. (1995, Feb). The precursor protein of non-A beta component of Alzheimer's disease amyloid is a presynaptic protein of the central nervous system. *Neuron*, 14(2), 467-475. [https://doi.org/10.1016/0896-6273\(95\)90302-X](https://doi.org/10.1016/0896-6273(95)90302-X)
- Jana, N. R., Dikshit, P., Goswami, A., Kotliarova, S., Murata, S., Tanaka, K., & Nukina, N. (2005, Mar 25). Co-chaperone CHIP associates with expanded polyglutamine protein and promotes their degradation by proteasomes. *J Biol Chem*, 280(12), 11635-11640. <https://doi.org/10.1074/jbc.M412042200>
- Jao, C. C., Der-Sarkissian, A., Chen, J., & Langen, R. (2004, Jun 1). Structure of membrane-bound alpha-synuclein studied by site-directed spin labeling. *Proc Natl Acad Sci U S A*, 101(22), 8331-8336. <https://doi.org/10.1073/pnas.0400553101>
- Jiang, S. Y., Li, H., Tang, J. J., Wang, J., Luo, J., Liu, B., Wang, J. K., Shi, X. J., Cui, H. W., Tang, J., Yang, F., Qi, W., Qiu, W. W., & Song, B. L. (2018, Dec 3). Discovery of a potent HMG-CoA reductase degrader that eliminates statin-

- induced reductase accumulation and lowers cholesterol. *Nat Commun*, 9(1), 5138. <https://doi.org/10.1038/s41467-018-07590-3>
- Johnson-Anuna, L. N., Eckert, G. P., Keller, J. H., Igbavboa, U., Franke, C., Fechner, T., Schubert-Zsilavecz, M., Karas, M., Muller, W. E., & Wood, W. G. (2005, Feb). Chronic administration of statins alters multiple gene expression patterns in mouse cerebral cortex. *J Pharmacol Exp Ther*, 312(2), 786-793. <https://doi.org/10.1124/jpet.104.075028>
- Johnston, J. A., Dalton, M. J., Gurney, M. E., & Kopito, R. R. (2000, Nov 7). Formation of high molecular weight complexes of mutant Cu, Zn-superoxide dismutase in a mouse model for familial amyotrophic lateral sclerosis. *Proc Natl Acad Sci U S A*, 97(23), 12571-12576. <https://doi.org/10.1073/pnas.220417997>
- Johnston, J. A., Ward, C. L., & Kopito, R. R. (1998, Dec 28). Aggresomes: a cellular response to misfolded proteins. *J Cell Biol*, 143(7), 1883-1898. <https://doi.org/10.1083/jcb.143.7.1883>
- Jowaed, A., Schmitt, I., Kaut, O., & Wullner, U. (2010, May 5). Methylation regulates alpha-synuclein expression and is decreased in Parkinson's disease patients' brains. *J Neurosci*, 30(18), 6355-6359. <https://doi.org/10.1523/JNEUROSCI.6119-09.2010>
- Junn, E., Lee, K. W., Jeong, B. S., Chan, T. W., Im, J. Y., & Mouradian, M. M. (2009, Aug 4). Repression of alpha-synuclein expression and toxicity by microRNA-7. *Proc Natl Acad Sci U S A*, 106(31), 13052-13057. <https://doi.org/10.1073/pnas.0906277106>
- Jurevics, H., & Morell, P. (1995, Feb). Cholesterol for synthesis of myelin is made locally, not imported into brain. *J Neurochem*, 64(2), 895-901. <https://doi.org/10.1046/j.1471-4159.1995.64020895.x>
- Kalia, L. V., & Lang, A. E. (2015, Aug 29). Parkinson's disease. *Lancet*, 386(9996), 896-912. [https://doi.org/10.1016/S0140-6736\(14\)61393-3](https://doi.org/10.1016/S0140-6736(14)61393-3)
- Kantor, B., Tagliafierro, L., Gu, J., Zamora, M. E., Ilich, E., Grenier, C., Huang, Z. Y., Murphy, S., & Chiba-Falek, O. (2018, Nov 7). Downregulation of SNCA Expression by Targeted Editing of DNA Methylation: A Potential Strategy for Precision Therapy in PD. *Mol Ther*, 26(11), 2638-2649. <https://doi.org/10.1016/j.ymthe.2018.08.019>
- Kawaguchi, Y., Okamoto, T., Taniwaki, M., Aizawa, M., Inoue, M., Katayama, S., Kawakami, H., Nakamura, S., Nishimura, M., Akiguchi, I., & et al. (1994, Nov). CAG expansions in a novel gene for Machado-Joseph disease at chromosome 14q32.1. *Nat Genet*, 8(3), 221-228. <https://doi.org/10.1038/ng1194-221>

- Kent, W. J., Sugnet, C. W., Furey, T. S., Roskin, K. M., Pringle, T. H., Zahler, A. M., & Haussler, D. (2002, Jun). The human genome browser at UCSC. *Genome Res*, 12(6), 996-1006. <https://doi.org/10.1101/gr.229102>
- Kingwell, K. (2021, Jun). Double setback for ASO trials in Huntington disease. *Nat Rev Drug Discov*, 20(6), 412-413. <https://doi.org/10.1038/d41573-021-00088-6>
- Kitada, T., Asakawa, S., Hattori, N., Matsumine, H., Yamamura, Y., Minoshima, S., Yokochi, M., Mizuno, Y., & Shimizu, N. (1998, Apr 9). Mutations in the parkin gene cause autosomal recessive juvenile parkinsonism. *Nature*, 392(6676), 605-608. <https://doi.org/10.1038/33416>
- Klockgether, T., Mariotti, C., & Paulson, H. L. (2019, Apr 11). Spinocerebellar ataxia. *Nat Rev Dis Primers*, 5(1), 24. <https://doi.org/10.1038/s41572-019-0074-3>
- Krauss, S., & Evert, B. O. (2019, Apr 19). The Role of MicroRNAs in Spinocerebellar Ataxia Type 3. *J Mol Biol*, 431(9), 1729-1742. <https://doi.org/10.1016/j.jmb.2019.01.019>
- Krauss, S., Nalavade, R., Weber, S., Carter, K., & Evert, B. O. (2019). Upregulation of miR-25 and miR-181 Family Members Correlates with Reduced Expression of ATXN3 in Lymphocytes from SCA3 Patients. *Microna*, 8(1), 76-85. <https://doi.org/10.2174/2211536607666180821162403>
- Kruger, R., Kuhn, W., Muller, T., Woitalla, D., Graeber, M., Kosel, S., Przuntek, H., Epplen, J. T., Schols, L., & Riess, O. (1998, Feb). Ala30Pro mutation in the gene encoding alpha-synuclein in Parkinson's disease. *Nat Genet*, 18(2), 106-108. <https://doi.org/10.1038/ng0298-106>
- Kurzwaski, M., Bialecka, M., Slawek, J., Klodowska-Duda, G., & Drozdziak, M. (2010, May). Association study of GATA-2 transcription factor gene (GATA2) polymorphism and Parkinson's disease. *Parkinsonism Relat Disord*, 16(4), 284-287. <https://doi.org/10.1016/j.parkreldis.2009.10.006>
- Leng, Y., & Chuang, D. M. (2006, Jul 12). Endogenous alpha-synuclein is induced by valproic acid through histone deacetylase inhibition and participates in neuroprotection against glutamate-induced excitotoxicity. *J Neurosci*, 26(28), 7502-7512. <https://doi.org/10.1523/JNEUROSCI.0096-06.2006>
- Li, H., Kuwajima, T., Oakley, D., Nikulina, E., Hou, J., Yang, W. S., Lowry, E. R., Lamas, N. J., Amoroso, M. W., Croft, G. F., Hosur, R., Wichterle, H., Sefti, S., Filbin, M. T., Stockwell, B., & Henderson, C. E. (2016, Jul 12). Protein Prenylation Constitutes an Endogenous Brake on Axonal Growth. *Cell Rep*, 16(2), 545-558. <https://doi.org/10.1016/j.celrep.2016.06.013>

- Liu, C. C., Liu, C. C., Kanekiyo, T., Xu, H., & Bu, G. (2013, Feb). Apolipoprotein E and Alzheimer disease: risk, mechanisms and therapy. *Nat Rev Neurol*, 9(2), 106-118. <https://doi.org/10.1038/nrneurol.2012.263>
- Long, Z., Chen, Z., Wang, C., Huang, F., Peng, H., Hou, X., Ding, D., Ye, W., Wang, J., Pan, Q., Li, J., Xia, K., Tang, B., Ashizawa, T., & Jiang, H. (2015). Two novel SNPs in ATXN3 3' UTR may decrease age at onset of SCA3/MJD in Chinese patients. *PLoS One*, 10(2), e0117488. <https://doi.org/10.1371/journal.pone.0117488>
- Lutjohann, D., Stroick, M., Bertsch, T., Kuhl, S., Lindenthal, B., Thelen, K., Andersson, U., Bjorkhem, I., Bergmann Kv, K., & Fassbender, K. (2004, Jun). High doses of simvastatin, pravastatin, and cholesterol reduce brain cholesterol synthesis in guinea pigs. *Steroids*, 69(6), 431-438. <https://doi.org/10.1016/j.steroids.2004.03.012>
- Lv, M., Zhang, Y., Chen, G. C., Li, G., Rui, Y., Qin, L., & Wan, Z. (2017, Sep 29). Reproductive factors and risk of Parkinson's disease in women: A meta-analysis of observational studies. *Behav Brain Res*, 335, 103-110. <https://doi.org/10.1016/j.bbr.2017.07.025>
- Mahmoud, F., & Tampi, R. R. (2011, Dec). Valproic acid-induced parkinsonism in the elderly: a comprehensive review of the literature. *Am J Geriatr Pharmacother*, 9(6), 405-412. <https://doi.org/10.1016/j.amjopharm.2011.09.002>
- Maioli, S., Bavner, A., Ali, Z., Heverin, M., Ismail, M. A., Puerta, E., Olin, M., Saeed, A., Shafaati, M., Parini, P., Cedazo-Minguez, A., & Bjorkhem, I. (2013). Is it possible to improve memory function by upregulation of the cholesterol 24S-hydroxylase (CYP46A1) in the brain? *PLoS One*, 8(7), e68534. <https://doi.org/10.1371/journal.pone.0068534>
- Mans, R. A., McMahon, L. L., & Li, L. (2012, Jan 27). Simvastatin-mediated enhancement of long-term potentiation is driven by farnesyl-pyrophosphate depletion and inhibition of farnesylation. *Neuroscience*, 202, 1-9. <https://doi.org/10.1016/j.neuroscience.2011.12.007>
- Mao, Y., Senic-Matuglia, F., Di Fiore, P. P., Polo, S., Hodsdon, M. E., & De Camilli, P. (2005, Sep 6). Deubiquitinating function of ataxin-3: insights from the solution structure of the Josephin domain. *Proc Natl Acad Sci U S A*, 102(36), 12700-12705. <https://doi.org/10.1073/pnas.0506344102>
- Maroteaux, L., Campanelli, J. T., & Scheller, R. H. (1988, Aug). Synuclein: a neuron-specific protein localized to the nucleus and presynaptic nerve terminal. *J Neurosci*, 8(8), 2804-2815. <https://doi.org/10.1523/JNEUROSCI.08-08-02804.1988>

- Mathelier, A., Zhao, X., Zhang, A. W., Parcy, F., Worsley-Hunt, R., Arenillas, D. J., Buchman, S., Chen, C. Y., Chou, A., Ienasescu, H., Lim, J., Shyr, C., Tan, G., Zhou, M., Lenhard, B., Sandelin, A., & Wasserman, W. W. (2014, Jan). JASPAR 2014: an extensively expanded and updated open-access database of transcription factor binding profiles. *Nucleic Acids Res*, 42(Database issue), D142-147. <https://doi.org/10.1093/nar/gkt997>
- Matsuda, H., Shimoda, H., Morikawa, T., & Yoshikawa, M. (2001, Jul 23). Phytoestrogens from the roots of *Polygonum cuspidatum* (Polygonaceae): structure-requirement of hydroxyanthraquinones for estrogenic activity. *Bioorg Med Chem Lett*, 11(14), 1839-1842. [https://doi.org/10.1016/s0960-894x\(01\)00318-3](https://doi.org/10.1016/s0960-894x(01)00318-3)
- Mauch, D. H., Nagler, K., Schumacher, S., Goritz, C., Muller, E. C., Otto, A., & Pfrieder, F. W. (2001, Nov 9). CNS synaptogenesis promoted by glia-derived cholesterol. *Science*, 294(5545), 1354-1357. <https://doi.org/10.1126/science.294.5545.1354>
- Mayeux, R., & Stern, Y. (2012, Aug 1). Epidemiology of Alzheimer disease. *Cold Spring Harb Perspect Med*, 2(8). <https://doi.org/10.1101/cshperspect.a006239>
- McMillan, K. J., Murray, T. K., Bengoa-Vergniory, N., Cordero-Llana, O., Cooper, J., Buckley, A., Wade-Martins, R., Uney, J. B., O'Neill, M. J., Wong, L. F., & Caldwell, M. A. (2017, Oct 4). Loss of MicroRNA-7 Regulation Leads to alpha-Synuclein Accumulation and Dopaminergic Neuronal Loss In Vivo. *Mol Ther*, 25(10), 2404-2414. <https://doi.org/10.1016/j.ymthe.2017.08.017>
- Miller, D. W., Hague, S. M., Clarimon, J., Baptista, M., Gwinn-Hardy, K., Cookson, M. R., & Singleton, A. B. (2004, May 25). Alpha-synuclein in blood and brain from familial Parkinson disease with SNCA locus triplication. *Neurology*, 62(10), 1835-1838. <https://doi.org/10.1212/01.wnl.0000127517.33208.f4>
- Mittal, S., Bjornevik, K., Im, D. S., Flierl, A., Dong, X., Locascio, J. J., Abo, K. M., Long, E., Jin, M., Xu, B., Xiang, Y. K., Rochet, J. C., Engeland, A., Rizzu, P., Heutink, P., Bartels, T., Selkoe, D. J., Caldarone, B. J., Glicksman, M. A., Khurana, V., Schule, B., Park, D. S., Riise, T., & Scherzer, C. R. (2017, Sep 1). beta2-Adrenoreceptor is a regulator of the alpha-synuclein gene driving risk of Parkinson's disease. *Science*, 357(6354), 891-898. <https://doi.org/10.1126/science.aaf3934>
- Nicastro, G., Menon, R. P., Masino, L., Knowles, P. P., McDonald, N. Q., & Pastore, A. (2005, Jul 26). The solution structure of the Josephin domain of ataxin-3: structural determinants for molecular recognition. *Proc Natl Acad Sci U S A*, 102(30), 10493-10498. <https://doi.org/10.1073/pnas.0501732102>

- Nieweg, K., Schaller, H., & Pfrieder, F. W. (2009, Apr). Marked differences in cholesterol synthesis between neurons and glial cells from postnatal rats. *J Neurochem*, 109(1), 125-134. <https://doi.org/10.1111/j.1471-4159.2009.05917.x>
- Nobrega, C., Mendonca, L., Marcelo, A., Lamaziere, A., Tome, S., Despres, G., Matos, C. A., Mehmet, F., Langui, D., den Dunnen, W., de Almeida, L. P., Cartier, N., & Alves, S. (2019, Nov). Restoring brain cholesterol turnover improves autophagy and has therapeutic potential in mouse models of spinocerebellar ataxia. *Acta Neuropathol*, 138(5), 837-858. <https://doi.org/10.1007/s00401-019-02019-7>
- Olanow, C. W., Perl, D. P., DeMartino, G. N., & McNaught, K. S. (2004, Aug). Lewy-body formation is an aggresome-related process: a hypothesis. *Lancet Neurol*, 3(8), 496-503. [https://doi.org/10.1016/S1474-4422\(04\)00827-0](https://doi.org/10.1016/S1474-4422(04)00827-0)
- Pahan, K., Sheikh, F. G., Namboodiri, A. M., & Singh, I. (1997, Dec 1). Lovastatin and phenylacetate inhibit the induction of nitric oxide synthase and cytokines in rat primary astrocytes, microglia, and macrophages. *J Clin Invest*, 100(11), 2671-2679. <https://doi.org/10.1172/JCI119812>
- Parkinson, J. (2002, Spring). An essay on the shaking palsy. 1817. *J Neuropsychiatry Clin Neurosci*, 14(2), 223-236; discussion 222. <https://doi.org/10.1176/jnp.14.2.223>
- Paulson, H. L., Perez, M. K., Trottier, Y., Trojanowski, J. Q., Subramony, S. H., Das, S. S., Vig, P., Mandel, J. L., Fischbeck, K. H., & Pittman, R. N. (1997, Aug). Intranuclear inclusions of expanded polyglutamine protein in spinocerebellar ataxia type 3. *Neuron*, 19(2), 333-344. [https://doi.org/10.1016/s0896-6273\(00\)80943-5](https://doi.org/10.1016/s0896-6273(00)80943-5)
- Pfrieder, F. W. (2003, Mar 10). Role of cholesterol in synapse formation and function. *Biochim Biophys Acta*, 1610(2), 271-280. [https://doi.org/10.1016/s0005-2736\(03\)00024-5](https://doi.org/10.1016/s0005-2736(03)00024-5)
- Pikuleva, I. A., & Cartier, N. (2021). Cholesterol Hydroxylating Cytochrome P450 46A1: From Mechanisms of Action to Clinical Applications. *Front Aging Neurosci*, 13, 696778. <https://doi.org/10.3389/fnagi.2021.696778>
- Poewe, W., Seppi, K., Tanner, C. M., Halliday, G. M., Brundin, P., Volkman, J., Schrag, A. E., & Lang, A. E. (2017, Mar 23). Parkinson disease. *Nat Rev Dis Primers*, 3, 17013. <https://doi.org/10.1038/nrdp.2017.13>
- Polymeropoulos, M. H., Lavedan, C., Leroy, E., Ide, S. E., Dehejia, A., Dutra, A., Pike, B., Root, H., Rubenstein, J., Boyer, R., Stenroos, E. S., Chandrasekharappa, S., Athanassiadou, A., Papapetropoulos, T., Johnson, W. G., Lazzarini, A. M.,

- Duvoisin, R. C., Di Iorio, G., Golbe, L. I., & Nussbaum, R. L. (1997, Jun 27). Mutation in the alpha-synuclein gene identified in families with Parkinson's disease. *Science*, 276(5321), 2045-2047. <https://doi.org/10.1126/science.276.5321.2045>
- Quan, G., Xie, C., Dietschy, J. M., & Turley, S. D. (2003, Dec 19). Ontogenesis and regulation of cholesterol metabolism in the central nervous system of the mouse. *Brain Res Dev Brain Res*, 146(1-2), 87-98. <https://doi.org/10.1016/j.devbrainres.2003.09.015>
- Ramakrishnan, N. A., Drescher, M. J., & Drescher, D. G. (2012, May). The SNARE complex in neuronal and sensory cells. *Mol Cell Neurosci*, 50(1), 58-69. <https://doi.org/10.1016/j.mcn.2012.03.009>
- Riederer, P., Berg, D., Casadei, N., Cheng, F., Classen, J., Dresel, C., Jost, W., Kruger, R., Muller, T., Reichmann, H., Riess, O., Storch, A., Strobel, S., van Eimeren, T., Volker, H. U., Winkler, J., Winklhofer, K. F., Wullner, U., Zunke, F., & Monoranu, C. M. (2019, Jul). alpha-Synuclein in Parkinson's disease: causal or bystander? *J Neural Transm (Vienna)*, 126(7), 815-840. <https://doi.org/10.1007/s00702-019-02025-9>
- Rodrigues, A. J., Coppola, G., Santos, C., Costa Mdo, C., Ailion, M., Sequeiros, J., Geschwind, D. H., & Maciel, P. (2007, Apr). Functional genomics and biochemical characterization of the C. elegans orthologue of the Machado-Joseph disease protein ataxin-3. *FASEB J*, 21(4), 1126-1136. <https://doi.org/10.1096/fj.06-7002com>
- Rosenbloom, K. R., Sloan, C. A., Malladi, V. S., Dreszer, T. R., Learned, K., Kirkup, V. M., Wong, M. C., Maddren, M., Fang, R., Heitner, S. G., Lee, B. T., Barber, G. P., Harte, R. A., Diekhans, M., Long, J. C., Wilder, S. P., Zweig, A. S., Karolchik, D., Kuhn, R. M., Haussler, D., & Kent, W. J. (2013, Jan). ENCODE data in the UCSC Genome Browser: year 5 update. *Nucleic Acids Res*, 41(Database issue), D56-63. <https://doi.org/10.1093/nar/gks1172>
- Ross, C. A., & Poirier, M. A. (2004, Jul). Protein aggregation and neurodegenerative disease. *Nat Med*, 10 Suppl, S10-17. <https://doi.org/10.1038/nm1066>
- Ross, C. A., & Poirier, M. A. (2005, Nov). Opinion: What is the role of protein aggregation in neurodegeneration? *Nat Rev Mol Cell Biol*, 6(11), 891-898. <https://doi.org/10.1038/nrm1742>
- Roy, A., Jana, M., Kundu, M., Corbett, G. T., Rangaswamy, S. B., Mishra, R. K., Luan, C. H., Gonzalez, F. J., & Pahan, K. (2015, Aug 4). HMG-CoA Reductase Inhibitors Bind to PPARalpha to Upregulate Neurotrophin Expression in the Brain and Improve Memory in Mice. *Cell Metab*, 22(2), 253-265. <https://doi.org/10.1016/j.cmet.2015.05.022>

- Scaglione, K. M., Zavodszky, E., Todi, S. V., Patury, S., Xu, P., Rodriguez-Lebron, E., Fischer, S., Konen, J., Djarmati, A., Peng, J., Gestwicki, J. E., & Paulson, H. L. (2011, Aug 19). Ube2w and ataxin-3 coordinately regulate the ubiquitin ligase CHIP. *Mol Cell*, 43(4), 599-612. <https://doi.org/10.1016/j.molcel.2011.05.036>
- Scheel, H., Tomiuk, S., & Hofmann, K. (2003, Nov 1). Elucidation of ataxin-3 and ataxin-7 function by integrative bioinformatics. *Hum Mol Genet*, 12(21), 2845-2852. <https://doi.org/10.1093/hmg/ddg297>
- Scherzer, C. R., Grass, J. A., Liao, Z., Pepivani, I., Zheng, B., Eklund, A. C., Ney, P. A., Ng, J., McGoldrick, M., Mollenhauer, B., Bresnick, E. H., & Schlossmacher, M. G. (2008, Aug 5). GATA transcription factors directly regulate the Parkinson's disease-linked gene alpha-synuclein. *Proc Natl Acad Sci U S A*, 105(31), 10907-10912. <https://doi.org/10.1073/pnas.0802437105>
- Schmidt, T., Landwehrmeyer, G. B., Schmitt, I., Trottier, Y., Auburger, G., Laccone, F., Klockgether, T., Volpel, M., Epplen, J. T., Schols, L., & Riess, O. (1998, Oct). An isoform of ataxin-3 accumulates in the nucleus of neuronal cells in affected brain regions of SCA3 patients. *Brain Pathol*, 8(4), 669-679. <https://doi.org/10.1111/j.1750-3639.1998.tb00193.x>
- Schmitt, I., Evert, B. O., Khazneh, H., Klockgether, T., & Wuellner, U. (2003, Sep 18). The human MJD gene: genomic structure and functional characterization of the promoter region. *Gene*, 314, 81-88. [https://doi.org/10.1016/s0378-1119\(03\)00706-6](https://doi.org/10.1016/s0378-1119(03)00706-6)
- Schmitt, I., Linden, M., Khazneh, H., Evert, B. O., Breuer, P., Klockgether, T., & Wuellner, U. (2007, Oct 26). Inactivation of the mouse Atxn3 (ataxin-3) gene increases protein ubiquitination. *Biochem Biophys Res Commun*, 362(3), 734-739. <https://doi.org/10.1016/j.bbrc.2007.08.062>
- Schulz-Schaeffer, W. J. (2012, Dec 11). Neurodegeneration in Parkinson disease: moving Lewy bodies out of focus. *Neurology*, 79(24), 2298-2299. <https://doi.org/10.1212/WNL.0b013e318278b6a7>
- Sharon, R., Goldberg, M. S., Bar-Josef, I., Betensky, R. A., Shen, J., & Selkoe, D. J. (2001, Jul 31). alpha-Synuclein occurs in lipid-rich high molecular weight complexes, binds fatty acids, and shows homology to the fatty acid-binding proteins. *Proc Natl Acad Sci U S A*, 98(16), 9110-9115. <https://doi.org/10.1073/pnas.171300598>
- Singleton, A. B., Farrer, M., Johnson, J., Singleton, A., Hague, S., Kachergus, J., Hulihan, M., Peuralinna, T., Dutra, A., Nussbaum, R., Lincoln, S., Crawley, A., Hanson, M., Maraganore, D., Adler, C., Cookson, M. R., Muentner, M., Baptista, M., Miller, D., Blancato, J., Hardy, J., & Gwinn-Hardy, K. (2003, Oct 31). alpha-

- Synuclein locus triplication causes Parkinson's disease. *Science*, 302(5646), 841. <https://doi.org/10.1126/science.1090278>
- Soldner, F., Stelzer, Y., Shivalila, C. S., Abraham, B. J., Latourelle, J. C., Barrasa, M. I., Goldmann, J., Myers, R. H., Young, R. A., & Jaenisch, R. (2016, May 5). Parkinson-associated risk variant in distal enhancer of alpha-synuclein modulates target gene expression. *Nature*, 533(7601), 95-99. <https://doi.org/10.1038/nature17939>
- Spillantini, M. G., Schmidt, M. L., Lee, V. M., Trojanowski, J. Q., Jakes, R., & Goedert, M. (1997, Aug 28). Alpha-synuclein in Lewy bodies. *Nature*, 388(6645), 839-840. <https://doi.org/10.1038/42166>
- Stahl, F., Denner, P., Piston, D., Evert, B. O., de Boni, L., Schmitt, I., Breuer, P., & Wullner, U. (2021, Oct 6). Activators of alpha synuclein expression identified by reporter cell line-based high throughput drug screen. *Sci Rep*, 11(1), 19857. <https://doi.org/10.1038/s41598-021-98841-9>
- Stahl, F., Schmitt, I., Denner, P., de Boni, L., Wullner, U., & Breuer, P. (2023, Sep 9). High throughput compound screening in neuronal cells identifies statins as activators of ataxin 3 expression. *Sci Rep*, 13(1), 14911. <https://doi.org/10.1038/s41598-023-41192-4>
- Sullivan, R., Yau, W. Y., O'Connor, E., & Houlden, H. (2019, Feb). Spinocerebellar ataxia: an update. *J Neurol*, 266(2), 533-544. <https://doi.org/10.1007/s00415-018-9076-4>
- Sun, J., & Roy, S. (2021, Mar). Gene-based therapies for neurodegenerative diseases. *Nat Neurosci*, 24(3), 297-311. <https://doi.org/10.1038/s41593-020-00778-1>
- Taylor, K. S., Cook, J. A., & Counsell, C. E. (2007, Aug). Heterogeneity in male to female risk for Parkinson's disease. *J Neurol Neurosurg Psychiatry*, 78(8), 905-906. <https://doi.org/10.1136/jnnp.2006.104695>
- Terry, R. D., Masliah, E., Salmon, D. P., Butters, N., DeTeresa, R., Hill, R., Hansen, L. A., & Katzman, R. (1991, Oct). Physical basis of cognitive alterations in Alzheimer's disease: synapse loss is the major correlate of cognitive impairment. *Ann Neurol*, 30(4), 572-580. <https://doi.org/10.1002/ana.410300410>
- Testa, G., Staurengi, E., Zerbinati, C., Gargiulo, S., Iuliano, L., Giaccone, G., Fanto, F., Poli, G., Leonarduzzi, G., & Gamba, P. (2016, Dec). Changes in brain oxysterols at different stages of Alzheimer's disease: Their involvement in neuroinflammation. *Redox Biol*, 10, 24-33. <https://doi.org/10.1016/j.redox.2016.09.001>

- Toker, L., Tran, T. G., Sundaresan, J., Tysnes, B.O., Alves, G., Haugarvoll, K., Nido, S.G., Dölle, C., Tzoulis, C. . (2020). Genome-wide dysregulation of histone acetylation in the Parkinson's disease brain. *Preprint at <https://www.biorxiv.org/content/10.1101/785550v3>*
- Toonen, L. J. A., Overzier, M., Evers, M. M., Leon, L. G., van der Zeeuw, S. A. J., Mei, H., Kielbasa, S. M., Goeman, J. J., Hettne, K. M., Magnusson, O. T., Poirel, M., Seyer, A., t Hoen, P. A. C., & van Roon-Mom, W. M. C. (2018, Jun 22). Transcriptional profiling and biomarker identification reveal tissue specific effects of expanded ataxin-3 in a spinocerebellar ataxia type 3 mouse model. *Mol Neurodegener*, 13(1), 31. <https://doi.org/10.1186/s13024-018-0261-9>
- Trottier, Y., Cancel, G., An-Gourfinkel, I., Lutz, Y., Weber, C., Brice, A., Hirsch, E., & Mandel, J. L. (1998, Nov). Heterogeneous intracellular localization and expression of ataxin-3. *Neurobiol Dis*, 5(5), 335-347. <https://doi.org/10.1006/nbdi.1998.0208>
- Ueda, K., Fukushima, H., Masliah, E., Xia, Y., Iwai, A., Yoshimoto, M., Otero, D. A., Kondo, J., Ihara, Y., & Saitoh, T. (1993, Dec 1). Molecular cloning of cDNA encoding an unrecognized component of amyloid in Alzheimer disease. *Proc Natl Acad Sci U S A*, 90(23), 11282-11286. <https://doi.org/10.1073/pnas.90.23.11282>
- Valente, E. M., Bentivoglio, A. R., Dixon, P. H., Ferraris, A., Ialongo, T., Frontali, M., Albanese, A., & Wood, N. W. (2001, Apr). Localization of a novel locus for autosomal recessive early-onset parkinsonism, PARK6, on human chromosome 1p35-p36. *Am J Hum Genet*, 68(4), 895-900. <https://doi.org/10.1086/319522>
- Valente, T., Dentesano, G., Ezquerra, M., Fernandez-Santiago, R., Martinez-Martin, J., Gallastegui, E., Domuro, C., Compta, Y., Marti, M. J., Bachs, O., Marquez-Kisinousky, L., Straccia, M., Sola, C., & Saura, J. (2020, Feb). CCAAT/enhancer binding protein delta is a transcriptional repressor of alpha-synuclein. *Cell Death Differ*, 27(2), 509-524. <https://doi.org/10.1038/s41418-019-0368-8>
- Vijjaratnam, N., Simuni, T., Bandmann, O., Morris, H. R., & Foltynie, T. (2021, Jul). Progress towards therapies for disease modification in Parkinson's disease. *Lancet Neurol*, 20(7), 559-572. [https://doi.org/10.1016/S1474-4422\(21\)00061-2](https://doi.org/10.1016/S1474-4422(21)00061-2)
- Vo, S. H., Butzlaff, M., Pru, S. K., Ni Charthaigh, R. A., Karsten, P., Lankes, A., Hamm, S., Simons, M., Adryan, B., Schulz, J. B., & Voigt, A. (2012). Large-scale screen for modifiers of ataxin-3-derived polyglutamine-induced toxicity in Drosophila. *PLoS One*, 7(11), e47452. <https://doi.org/10.1371/journal.pone.0047452>

- Wang, C., Peng, H., Li, J., Ding, D., Chen, Z., Long, Z., Peng, Y., Zhou, X., Ye, W., Li, K., Xu, Q., Ai, S., Song, C., Weng, L., Qiu, R., Xia, K., Tang, B., & Jiang, H. (2017, May). Alteration of methylation status in the ATXN3 gene promoter region is linked to the SCA3/MJD. *Neurobiol Aging*, 53, 192 e195-192 e110. <https://doi.org/10.1016/j.neurobiolaging.2016.12.014>
- Weinreb, P. H., Zhen, W., Poon, A. W., Conway, K. A., & Lansbury, P. T., Jr. (1996, Oct 29). NACP, a protein implicated in Alzheimer's disease and learning, is natively unfolded. *Biochemistry*, 35(43), 13709-13715. <https://doi.org/10.1021/bi961799n>
- Wilson, D. M., 3rd, Cookson, M. R., Van Den Bosch, L., Zetterberg, H., Holtzman, D. M., & Dewachter, I. (2023, Feb 16). Hallmarks of neurodegenerative diseases. *Cell*, 186(4), 693-714. <https://doi.org/10.1016/j.cell.2022.12.032>
- Xie, X., Rigor, P., & Baldi, P. (2009, Jan 15). MotifMap: a human genome-wide map of candidate regulatory motif sites. *Bioinformatics*, 25(2), 167-174. <https://doi.org/10.1093/bioinformatics/btn605>
- Zarranz, J. J., Alegre, J., Gomez-Esteban, J. C., Lezcano, E., Ros, R., Ampuero, I., Vidal, L., Hoenicka, J., Rodriguez, O., Atares, B., Llorens, V., Gomez Tortosa, E., del Ser, T., Munoz, D. G., & de Yébenes, J. G. (2004, Feb). The new mutation, E46K, of alpha-synuclein causes Parkinson and Lewy body dementia. *Ann Neurol*, 55(2), 164-173. <https://doi.org/10.1002/ana.10795>
- Zhao, L., & Wang, Z. (2019). MicroRNAs: Game Changers in the Regulation of alpha-Synuclein in Parkinson's Disease. *Parkinsons Dis*, 2019, 1743183. <https://doi.org/10.1155/2019/1743183>
- Zhong, X., & Pittman, R. N. (2006, Aug 15). Ataxin-3 binds VCP/p97 and regulates retrotranslocation of ERAD substrates. *Hum Mol Genet*, 15(16), 2409-2420. <https://doi.org/10.1093/hmg/ddl164>
- Zimprich, A., Benet-Pages, A., Struhal, W., Graf, E., Eck, S. H., Offman, M. N., Haubenberger, D., Spielberger, S., Schulte, E. C., Lichtner, P., Rossle, S. C., Klopp, N., Wolf, E., Seppi, K., Pirker, W., Presslauer, S., Mollenhauer, B., Katzenschlager, R., Foki, T., Hotzy, C., Reinthaler, E., Harutyunyan, A., Kralovics, R., Peters, A., Zimprich, F., Brucke, T., Poewe, W., Auff, E., Trenkwalder, C., Rost, B., Ransmayr, G., Winkelmann, J., Meitinger, T., & Strom, T. M. (2011, Jul 15). A mutation in VPS35, encoding a subunit of the retromer complex, causes late-onset Parkinson disease. *Am J Hum Genet*, 89(1), 168-175. <https://doi.org/10.1016/j.ajhg.2011.06.008>

7 Abbreviations

Abbreviation	Full name
24-OHC	24-hydroxylcholesterol
AA	Amino acid
ABC	ATP-binding cassette
Ac	Acetylation
AD	Alzheimer's disease
ALS	Amyotrophic lateral sclerosis
ApoA1	Apolipoprotein A-I
APOE	Apolipoprotein E
ASO	Allele-specific oligonucleotide
ATXN3	Ataxin-3
BBB	Blood-brain barrier
bHLH-zip	Basic-helix-loop-helix leucine finger zipper
C/EBP	CCAAT/enhancer binding protein
CBF	CCAAT motif-binding factor
CHEN	Chenodiol
ChIP	Chromatin immunoprecipitation
CHIP	C-terminus of Hsc70-interacting protein
ChIP-seq	Chromatin immunoprecipitation sequencing
CRISPR	Clustered regularly interspaced short palindromic repeats
CSP α	Cysteine string protein alpha
CV	Contraceptive
CYP46A1	Cholesterol 24-hydroxylase
DLB	Dementia with Lewy body
DUB	Deubiquitinating enzyme
DZNE	Deutsches Zentrum Neurodegenerativer Erkrankungen
EC50	Half maximal effective concentrations
EMSA	Electric mobility shift assays
EMX2	Empty spiracles homeobox 2
ENCODE	Encyclopedia of DNA Elements
ER	Endoplasmic reticulum
ERAD	Endoplasmic reticulum associated degradation

Abbreviations

Abbreviation	Full name
FDA	U.S. Food and Drug Administration
FEN	Fenbufen
GATA-1, GATA-2	GATA binding protein 1 and 2
gp78	Glycoprotein 78 E3 ubiquitin ligase
GWAS	Genome wide association studies
H3K4me3	Trimethylation of histone H3K4
HD	Huntington's disease
HDAC	Histone deacetylases
HDL	High-density lipoprotein
HEK	Human embryonic kidney cells
HMGCR	3-hydroxy-3-methylglutaryl coenzyme A reductase
HRT	Hormone replacement therapy
HTS	High throughput screening
HTS	High throughput screenings
IB	Inclusion bodies
IC50	Half maximal inhibitory concentration
ICW	In-cell Western
i.e.	Id est
INSIG1	Insulin-induced genes 1 and 2
iPSC	Induced-pluripotent stem cells
JD	Josephine domain
Kb	Kilo bases
LAT	Laboratory automation technologies
LBD	Lewy body disease
LBs	Lewy bodies
LDLR	Low-density lipoprotein family receptors
L-DOPA	Levodopa
LOAD	Late onset AD
LRRK2-	Leucine-rich repeat kinase 2
LTP	Long term potential
LUC	Luciferase
LUHMES	Lund human mesencephalic

Abbreviations

Abbreviation	Full name
MCT	Monocarboxylic acid transporter
MiRNAs	Micro RNAs
MJD	Machado-Joseph Disease
MRI	Magnetic resonance imaging
mRNA	Messenger RNA
MTOC	Microtubule-organizing center
N2a	Neuro 2a cells
NACP-Rep1	Nonamyloid component of plaques
NDDs	Neurodegenerative diseases
NES	Nuclear export signal
NKX6-1	NK6 Homeobox 1
NLS	Nuclear localization signals
NPCs	Neuronal progenitor cells
OATP2	Organic anion transporter polypeptide 2
p53	Tumour suppressor p53
PARP1	Poly (ADP ribose) polymerase-1
PBMC	Peripheral blood mononuclear cell
PD	Parkinson Disease
PDE	Phosphodiesterase
PET	Positron emission tomography
PINK1	PTEN-induced putative kinase 1
polyQ	Polyglutamine
Rand-LUC	Random integration of the reporter cassette
RISC	RNA induced-silencing complex
RT-qPCR	Real time quantitative PCR
SCA	Spinocerebellar Ataxia
SCA3	Spinocerebellar Ataxia 3
SCAP	SREBP-cleavage activating protein
SCF	SKP1-Cullin-F-box
SERM	Selective estrogen receptor modulator
siRNA	Small interfering RNA
SKP1	S-phase Kinase-Associated Protein 1

Abbreviations

Abbreviation	Full name
SNARE	N-ethylmaleimide-sensitive fusion protein attachment protein receptors
SNCA	Alpha-synuclein protein
<i>SNCA</i>	Alpha-synuclein gene
SNPs	Single nucleotide polymorphisms
SOD1	Superoxide dismutase 1
SP1	Specificity protein 1
SPECT	Single-photon emission CT
SREBP	Sterol regulatory element binding protein
SULFA	Sulfaphenazole
tTA	Tetracycline-controlled trans-activator
TF	Transcription factor
TFEB/HLH-30	Transcription factor EB
TSA	Trichostatin A
TSS	Transcriptional start site
Ubc7	Ubiquitin-conjugating enzyme E2 7
Ube2w	Ubiquitin-conjugating enzyme E2 W
UIM	Ubiquitin-interacting motifs
UPS	Ubiquitin proteasome system
UTR	3' untranslated region
VCP/p97	Valosin containing proteins or AAA ATPase p97
VPA	Valproic acid
VPS35	Vacuolar protein sorting 35
ZSCAN21	Zinc finger and SCAN protein containing TF
β2AR	β2 adrenoreceptor

8 Danksagung

Zuerst möchte ich mich bei Prof. Ullrich Wüllner und Prof. Jörg Höhfeld für die Begleitung meiner Promotion und für die Begutachtung meiner Arbeit bedanken. Darüber hinaus danke ich Prof. Ullrich Wüllner für die Möglichkeit zur Promotion in diesem Labor.

Prof. Dieter Lütjohann und Prof. Christa Müller danke ich für die freundliche Bereiterklärung mein weiteres Prüfungskomitee zu bilden.

Dr. Peter Breuer danke ich für die wissenschaftlichen Diskussionen und Anregungen aber auch für alle außerfachlichen und erheiternde Gespräche.

Dr. Bernd Evert danke ich ebenfalls für die wissenschaftlichen Diskussionen, die stets unterstützenden Ratschläge und die gute Zeit im Labor.

Hassan Khazneh und Sabine Proske-Schmitz danke ich für die exzellente technische Hilfe und Unterstützung im Labor. Gleiches gilt für die ehemaligen Kolleginnen Dr. Ina Schmitt und Katrin Haustein.

Dr. Philip Denner und Brigit Kurkowsky danke ich für die Hilfe bei den initialen Screening Experimenten und Auswertungen der Ergebnisse am DZNE.

Meinen wissenschaftlichen Mitstreitern Yousuf Bakhit und Xin-yu Han danke ich zum einen für die schöne Zeit im Labor und zum anderen für die wöchentlichen abendlichen Sitzungen in einschlägigen Bonner Lokalen.

Für die schöne Zeit in Bonn möchte ich mich auch bei Tim bedanken, der mich erstens nach Bonn vermittelt hat und zweitens die damit verbundene Aufgabe übernehmen durfte mein Gemecker zu ertragen, wenn es mal nicht so lief.

Meiner Familie möchte ich für die Unterstützung in allen möglichen Situationen und für die schönen Kurztrips danken, bei denen ich ab und zu auch abschalten konnte.

Chiara, dir gebührt der größte Dank, da du einfach ein wunderbarer Mensch bist, der in allen Situationen an meiner Seite stand, mich ausgehalten und motiviert hat.

Am Erfolg eines Projektes sind oftmals viele Personen auf verschiedenen Ebenen beteiligt, daher ein abschließendes Dankeschön an alle namentlich genannten-, nicht genannten- und eventuell vergessenen Menschen!

9 Appendix



OPEN

Activators of alpha synuclein expression identified by reporter cell line-based high throughput drug screen

Fabian Stahl^{1,2}, Philip Denner¹, Dominik Piston¹, Bernd O. Evert², Laura de Boni², Ina Schmitt², Peter Breuer²✉ & Ullrich Wüllner^{1,2}✉

Multiplications, mutations and dysregulation of the alpha synuclein gene (*SNCA*) are associated with the demise of dopaminergic neurons and are considered to play important roles in the pathogenesis of familial and sporadic forms of Parkinson's disease. Regulation of *SNCA* expression might thus be an appropriate target for treatment. We aimed to identify specific modulators of *SNCA* transcription, generated CRISPR/Cas9 modified *SNCA-GFP-luciferase (LUC)* genomic fusion- and control cell lines and screened a library of 1649 bioactive compounds, including the FDA approved drugs. We found no inhibitors but three selective activators which increased *SNCA* mRNA and protein levels.

α -Synuclein (α -syn) is a key component in familial and sporadic Parkinson's disease (PD) pathophysiology. Point mutations in the *SNCA* gene and multiplication of wildtype *SNCA* cause familial parkinsonian syndromes. Increased α -syn protein levels correlate with the severity of symptoms¹. These gene-dosage effects suggest that *SNCA* mRNA levels are a relevant target to be addressed. Several modifier screens (genetically or compound modifiers) for α -syn induced toxicity based on α -syn overexpression-models have been performed in different organisms like yeast, *E. coli*, *C. elegans*, in rodent- and human cell lines. In these approaches, measuring cell growth and/or cell viability served as readout for presumed α -syn protein toxicity. Despite the large number of studies, unbiased screens in human derived cell lines had been scarce². α -Syn overexpression screens do not account for a regulation of endogenous *SNCA*. Thus, genes or compounds which modulate the epigenetic and transcriptional landscape might have been missed. Mittal and colleagues³ performed the first study addressing endogenous *SNCA* mRNA expression by screening a library of FDA approved compounds and found that β 2 adrenoreceptor (β 2AR) agonists reduced *SNCA* mRNA and α -syn protein levels. We had chosen an alternative approach to identify modifiers of *SNCA* expression and designed a luciferase (*LUC*) reporter-based high throughput screening of 1649 bioactive drugs including 845 FDA approved compounds in CRISPR/Cas9 modified human SH-SY5Y neuroblastoma cell lines. We identified three selective activators of *SNCA* mRNA and α -syn protein levels.

Results

Reporter cell line-based screening of 1649 bioactive compounds. A CRISPR/Cas9 *SNCA-GFP-T2A-LUC* fusion cell line (A1) expressing α -syn-GFP and LUC under the control of the endogenous human *SNCA* promoter was generated to identify modulators of *SNCA* expression (Fig. 1A). Cell lines with random integration of the reporter construct (A6) were selected as control for unspecific modulators of gene expression (example of unspecific modulators see Supplementary Fig. S1). Proper integration of the constructs was analyzed by PCR (Fig. 1B, upper panel) and Western blot (Fig. 1B, lower panel).

Three independent experimental repetitions revealed 153 potentially inhibiting and 164 activating compounds; 1322 compounds were within the four-fold SD cut off or without any effect (Figs. 1C and 2B).

To exclude cytotoxic effects of potential inhibitors, a cell viability test comprising a homogenous resazurin- and an image based high content screen (HCS) on single cell level were performed in a dose range from 250 nM to 40 μ M. We tested the 94 most potent inhibitors while all activators were considered as non-toxic. Sixty-nine

¹DZNE, German Center for Neurodegenerative Diseases, Venusberg-Campus 1/99, 53127 Bonn, Germany.

²Department of Neurology, University Hospital Bonn, 53127 Bonn, Germany. ✉email: peter.breuer@ukbonn.de; ullrich.wuellner@dzne.de

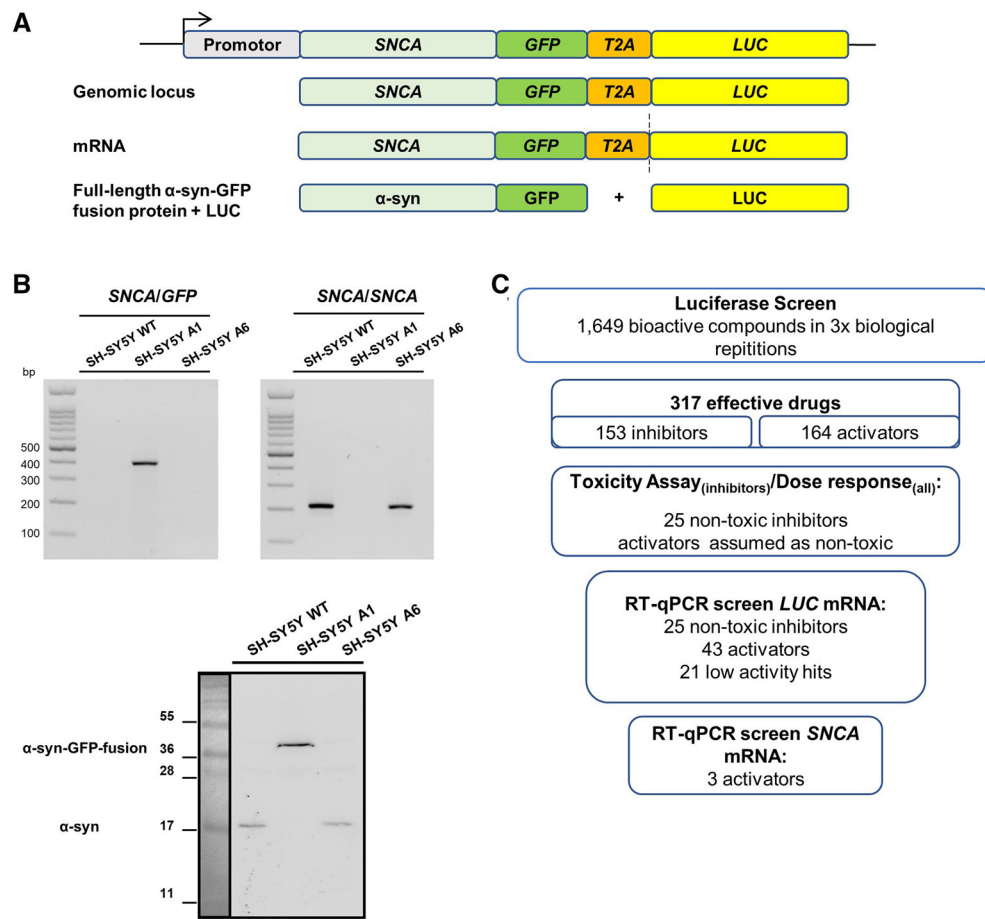


Figure 1. SNCA-GFP-LUC reporter cell line-based high throughput screening assay of 1649 FDA approved drugs identifies modulators of α-syn mRNA and protein levels. **(A)** Schematic overview of CRISPR/Cas9 generated, genomic SNCA-GFP-LUC fusion under control of the endogenous SNCA promoter in the SH-SY5Y cell line. Translation of its mRNA results in both, α-syn-GFP fusion protein and a functional LUC protein, separated by a ribosome skipping event due to the T2A sequence. **(B)** Agarose gel-electrophoresis of PCR from cDNA (top) and Western blot (bottom) of the reporter cell line confirming in-frame SNCA-GFP-LUC fusion at mRNA- and α-syn-GFP at protein level, respectively. **(C)** Workflow of the screening and validation procedure of α-syn modulating drugs. Several exposure images of full-size WB in **(B)** (lower panel) see Supplementary Fig. S2.

potential inhibitors were identified as toxic for our cells and were omitted from subsequent experiments (workflow see Fig. 1C).

Compounds modulating LUC and SNCA mRNA and α-syn protein expression levels. To corroborate that the observed changes in LUC derived chemiluminescence were indeed due to altered LUC gene expression, we performed additional RT-qPCR analysis. Quantifying the LUC mRNA in an intermediate step allowed the direct comparison between the A1 screening- and A6 counter-screening cell line to exclude compounds inducing rather unspecific gene expression changes (Fig. 3).

Thus, the 25 non-toxic inhibitors, 43 activators and 21 low activity hits were investigated by RT-qPCR. None of the putative non-toxic inhibitors reduced LUC mRNA levels at the SNCA locus, whereas three compounds increased LUC mRNA specifically in the A1 cell line. These compounds were also tested for pleiotropic modulation of transcription in the A6 control cell line and found to be sufficiently specific for SNCA (Fig. 3).

We finally determined SNCA mRNA expression levels in native non-modified SH-SY5Y wildtype cells and verified three compounds increasing SNCA mRNA levels 1.4 to twofold compared to DMSO control (Fig. 4A): clomiphene-citrate (Clo), a selective estrogen receptor modulator (SERM), conivaptan-HCL (Coni) a vasopressin receptor antagonist and the anthraquinone emodin (Emo).

To assess whether increased SNCA mRNA transcripts result in potentially relevant increases in α-syn protein amount, we performed two independent protein assays: in-cell Western (ICW) (example ICW see Supplementary Fig. S3) and conventional Western blot (WB). Both approaches revealed that treatment with the SNCA activators resulted in a 1.3 to 2-fold increase of α-syn protein levels compared to DMSO control samples (Fig. 4B,C).

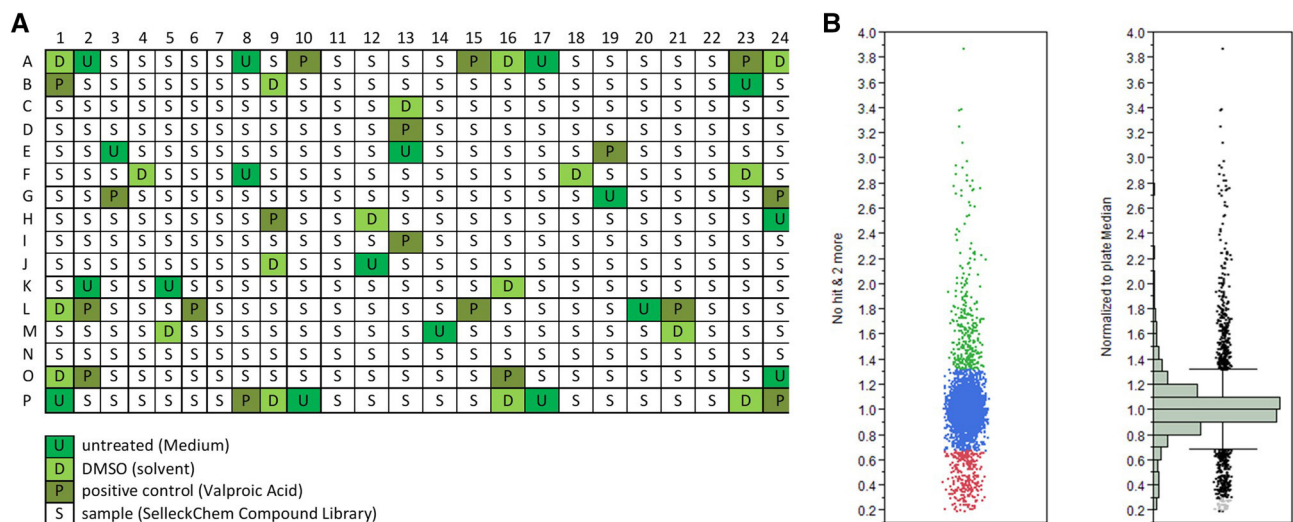


Figure 2. Plate layout and quality control of the luciferase reporter drug screening assay. **(A)** Plate layout of randomly distributed drugs and controls. **(B)** Threshold for hit definition: compounds were considered as effective when showing a difference beyond the four-fold standard deviation ($4 \times SD = 0.33$) compared to untreated control.

The relative changes in protein level of ICW and WB, corresponded to the observed SNCA mRNA changes in the previous RT-qPCR assay.

Effects on histone modification and DNA methylation in SH-SY5Y wild type cells. To investigate, whether chromatin alterations were involved in the observed SNCA mRNA increases, we analyzed global acetylation at histone H3 and H4 (H3/H4ac) and H3K4 tri-methylation (H3K4me3). We found that Emo consistently increased H3/H4ac and H3K4me3 marks (Fig. 5, lower). Clo and Coni showed no significant association with histone methylation or acetylation levels (see Supplementary Fig. S5F). Also, no differences in SNCA intron 1 DNA methylation⁴ were observed after treatment with either compound (see Supplementary Fig. S6).

Discussion

We performed a *LUC* reporter-based high throughput screen (HTS) and subsequent RT-qPCR assays to screen a library of 1649 bioactive compounds for transcriptional modifiers of SNCA expression. Initially, 163 potential activators and 153 potential inhibitors were identified. After cell viability assessment, we selected 25 inhibitors, 43 activators and 21 low activity hits for further characterization (Fig. 1C). To exclude non-transcriptional modulators and compounds confounding the *LUC* readout, RT-qPCR assays were performed^{5,6}. Indeed, among the 25 potential inhibitors we found none which reduced SNCA mRNA levels, but identified three compounds which specifically increased SNCA mRNA and α -syn protein levels (Figs. 3, 4).

The absence of a clear-cut inhibitor is in contrast to the work of Mittal and colleagues, who quantified mRNA levels of endogenous SNCA in SK-N-MC neuroblastoma cells. They discovered the selective β 2 adrenoreceptor (β 2AR) agonist metaproterenol to reduce SNCA mRNA and α -syn protein levels^{3,6}. Our screening approach included 47 adrenergic receptor modulators but none of the tested modulators (agonists and antagonists, including metaproterenol) were active in the primary *LUC* assay. A literature search and the online database “Human Protein Atlas” (data available from: <https://www.proteinatlas.org/ENSG00000169252-ADRB2/cell>)⁷ revealed that β 2AR are not expressed in SH-SY5Y cells. Indeed, WB did not detect β 2AR expression in our SH-SY5Y cells (see Supplementary Figs. S7, S8). We had selected the SH-SY5Y neuroblastoma lineage, which is frequently chosen to model PD, because of human origin, catecholaminergic neuronal properties and the ease of genetic engineering—very similar to SK-N-MC⁸. Clearly, the diverging results call for an even more conscientious selection of the screening cells. Induced human pluripotent stem cells (iPSC) or thereof derived cells are closer to the actual neurons in human brain and may offer an alternative, although these cells are difficult to standardize on the other hand.

The three selective activators comprised hormone receptor interacting drugs, i.e. the selective estrogen receptor modulator (SERM) clomiphene-citrate (Clo) and the vasopressin receptor antagonist conivaptan-HCL on the one hand and the plant anthraquinone emodin (Emo) on the other.

Clo was the only SERM in the library which activated SNCA mRNA expression. Depending on the target tissue, Clo acts as an estrogenic agonist or antagonist but its precise mechanism is still unknown (<https://go.drugbank.com/drugs/DB00882>)⁹. Clo is a mixture of the two isomers zuclomiphene (cis-) and enclomiphene (trans-isomer) which show estrogen agonistic and antagonistic effects, respectively (<https://drugs.ncats.io/drug/1HRS458QU2>). We therefore investigated the effect of zuclomiphene and enclomiphene in our cell lines. Both isomers lead to similar increases of SNCA mRNA and no stereo-selectivity was identified (see Supplementary Fig. S9).

Interestingly, estrogenic effects have been reported for the plant derived compound Emo¹⁰.

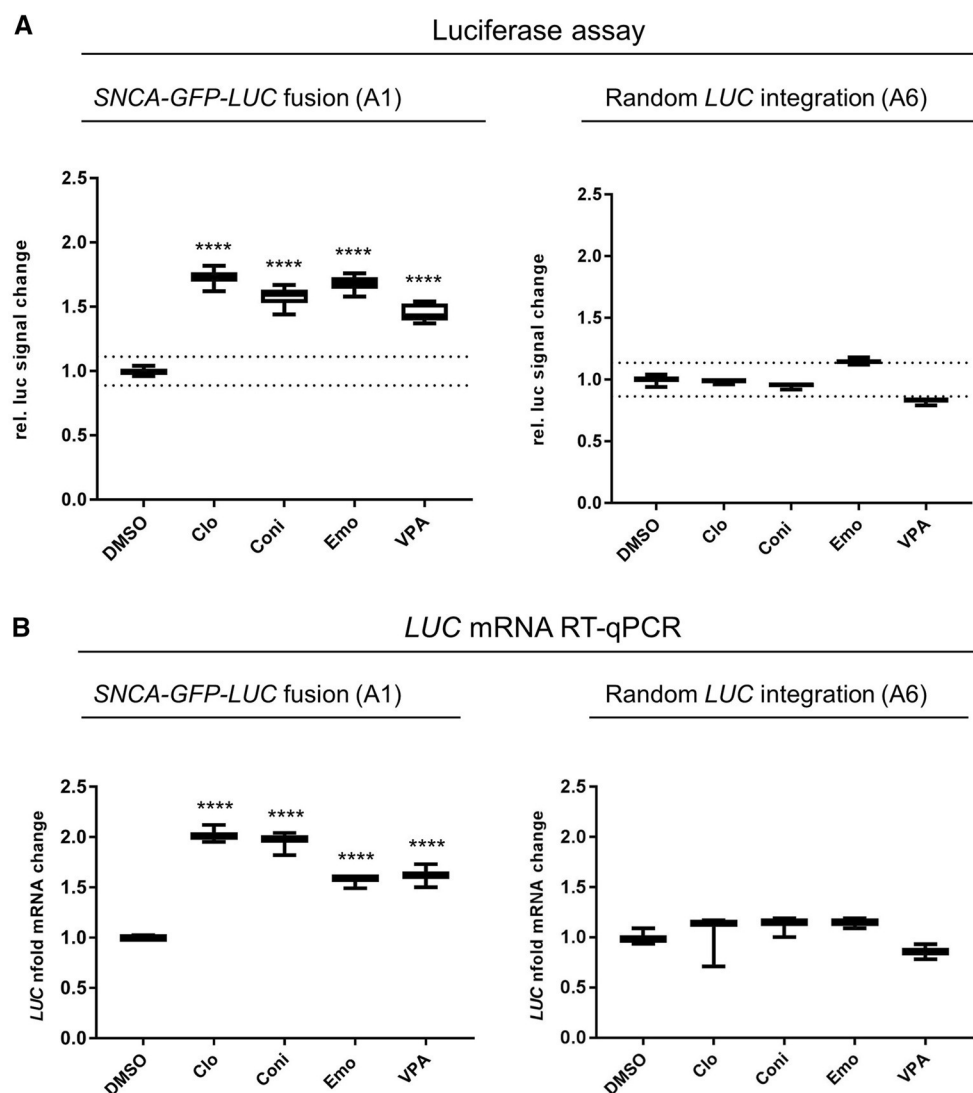


Figure 3. LUC assay and *LUC* RT-qPCR in the screening (A1) and control cell line (A6) for activators of α -syn. **(A)** Signal fold-change in the LUC assay of A1 and A6 cell lines and **(B)** expression fold changes of *LUC* mRNA measured with RT-qPCR. LUC signal change was determined by normalizing six replicates of treated cells to DMSO. RT-qPCR data were normalized to three housekeeping genes and DMSO control, in triplicates, respectively. Boxplot diagrams represent 5–95 percentile. Dotted lines in **(A)** depicts threshold of four-fold standard deviation of DMSO control. Compounds were applied at a final concentration of 25 μ M (Clo 12.5 μ M) for 24 h. VPA was used as a positive control at a concentration of 600 μ M. **** p = 0.0001.

The screening library contains a wide spectrum of other SERMS (like bazedoxifene-HCl and toremifene-citrate), ER antagonists (like fulvestrant and raloxifene) and several drugs affecting the estrogen/progesterone receptor pathway (among others aromatase inhibitors, progesterones, progestins, estradiol and its derivatives). Raloxifene was among the inhibitors identified in the *LUC* reporter assay but showed no consistent effect in the RT-qPCR assay. Thus, canonical estrogenic effects were considered unlikely for the observed transcriptional modulation of *SNCA*.

Similarly, three vaptans were tested in the HTS but only Coni the vasopressin V_{1A} and V_2 receptor antagonist (<https://go.drugbank.com/drugs/DB00872>)⁹ modulated *SNCA* mRNA and α -syn protein levels. Likely, the observed increase was not related to a vasopressin receptor (V_{1A} , V_2) mediated effect, as vasopressin (10 μ M) alone did not show any effect to *SNCA* mRNA levels (see Supplementary Fig. S10).

Epigenetic modifications, i.e. DNA methylation and histone modifications have emerged as important regulators of (*SNCA*) gene expression in PD^{11,12}. To date, several findings revealed that posttranslational histone modifications can lead to altered expression levels of *SNCA*. Treatment with valproic acid (VPA), a known histone deacetylase inhibitor (HDAC), induces hyperacetylation of global histone H3 at the *SNCA* promoter and leads to an increase of *Snca* in rat cerebral granule cells, cortex and cerebellum¹³. Additionally, VPA was shown to increase *SNCA* mRNA and α -syn protein levels in SH-SY5Y cells¹⁴. Vice versa, reduced H3K27 acetylation marks across the *SNCA* promoter resulted in decreased *SNCA* mRNA levels³.

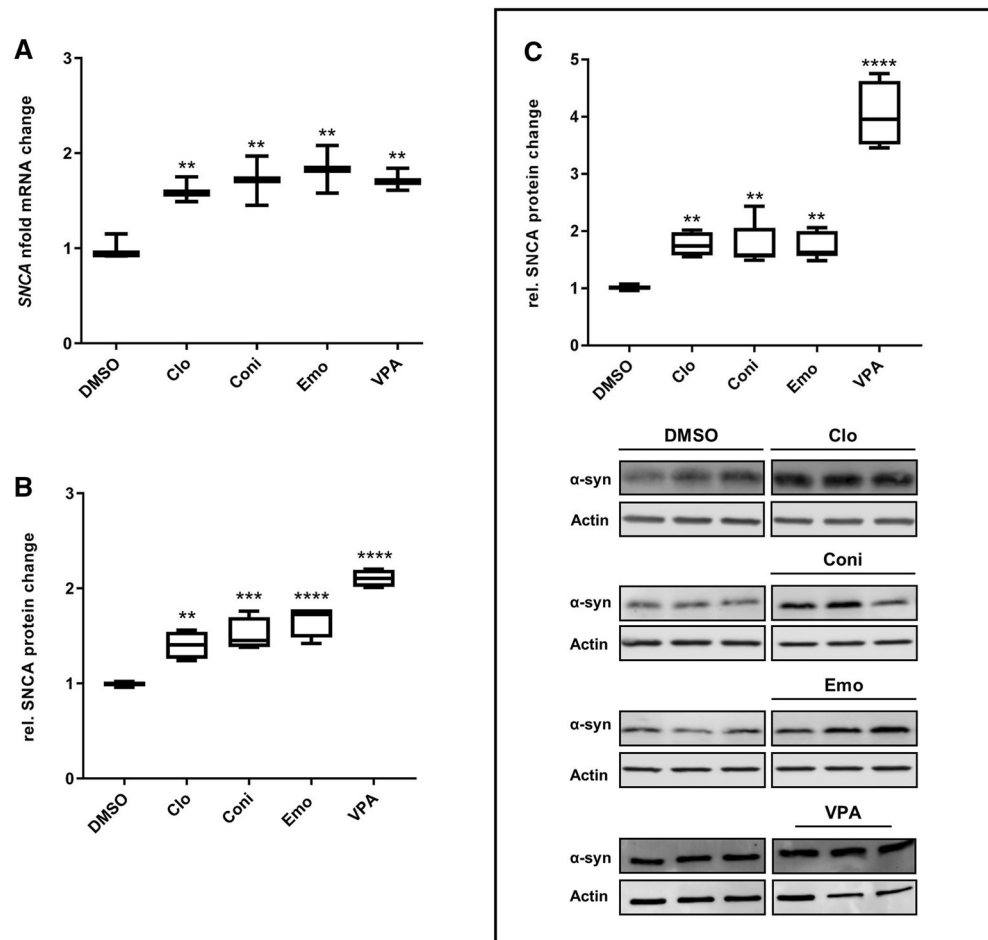


Figure 4. Compound treatment increased α -syn mRNA and protein levels in SH-SY5Y wildtype cells. **(A)** Expression fold change of *SNCA* mRNA measured with RT-qPCR. **(B)** Protein levels were determined by ICW and **(C)** WB in SH-SY5Y wild type cells. RT-qPCR data were normalized to three housekeeping genes and DMSO control, in triplicates, respectively. The Boxplot diagrams for **(B)** ICW represent the normalized mean of four 96-well plates with six to seven repetitions per compound, respectively. **(C)** For WBs six (VPA $n =$ four) repetitions were conducted. Boxplot diagrams represent 5–95 percentile. **(C, lower)** Representative WB. Compounds were applied at a final concentration of 25 μ M (Clo 12.5 μ M) for 24 h. VPA was used as a positive control at a concentration of 600 μ M. * $p < 0.1$, ** $p < 0.01$, *** $p < 0.001$, **** $p = 0.0001$. Full-size WB of DMSO and Clo see Supplementary Fig. S4A, DMSO and Coni see Supplementary Fig. S4B, DMSO and Emo see Supplementary Fig. S4C and DMSO and VPA see Supplementary Fig. S4D. ICWs **(B)** and WB **(C)** membranes were imaged with the LI-COR Odyssey Clx (Model 9140; S/N CLX-0554) and signals were quantified using the Image Studio software 4.0.21.

Guhathakurta and colleagues found the transcription promoting mark H3K4me3 significantly enriched at the *SNCA* promoter and intron1 region of substantia nigra in post-mortem PD brain samples. Furthermore, directed de-methylation of H3K4me3 at the *SNCA* promoter decreased *SNCA* mRNA and protein levels in SH-SY5Y cells and idiopathic PD-iPSC¹⁵.

A recent genome-wide study compared the overall histone acetylation levels in the PD brain and controls. The findings implicated that hyperacetylation of H3K27 is a general phenomenon within PD brains and 24 of the 83 genes bearing hyperacetylated regions of H3K27—including *SNCA*—were marked as risk genes for PD¹⁶.

Among the screened activators of *SNCA* expression and protein level, Emo led to a significant increase of histone marks for open chromatin, i.e. H3K4me3 and global H3/H4ac levels, similar to VPA (Fig. 5). Our findings are in accordance to earlier studies which found Emo to exhibit HDAC inhibitory function in recombinant HDAC activity assay performed in bovine cardiac tissue¹⁷. Interestingly, no increased *LUC* signals or mRNA levels were observed for Emo and VPA in the control cell line (A6), which was to be expected if global histone modifications were effective. Emo and emodin-rich rhubarb, however, have been shown to exert gene expression changes similar to the well-established pan-HDAC inhibitor trichostatin A (also part of the screening library)¹⁸.

Among the 23 known “canonical” HDAC inhibitors in the screening library only Rocilinostat (ACY-1215) was found to increase *LUC* signal but was excluded from further analysis because it did not meet the quality control criteria. Thus, it seems rather unlikely that increased global histone acetylation alone lead to elevated α -syn levels.

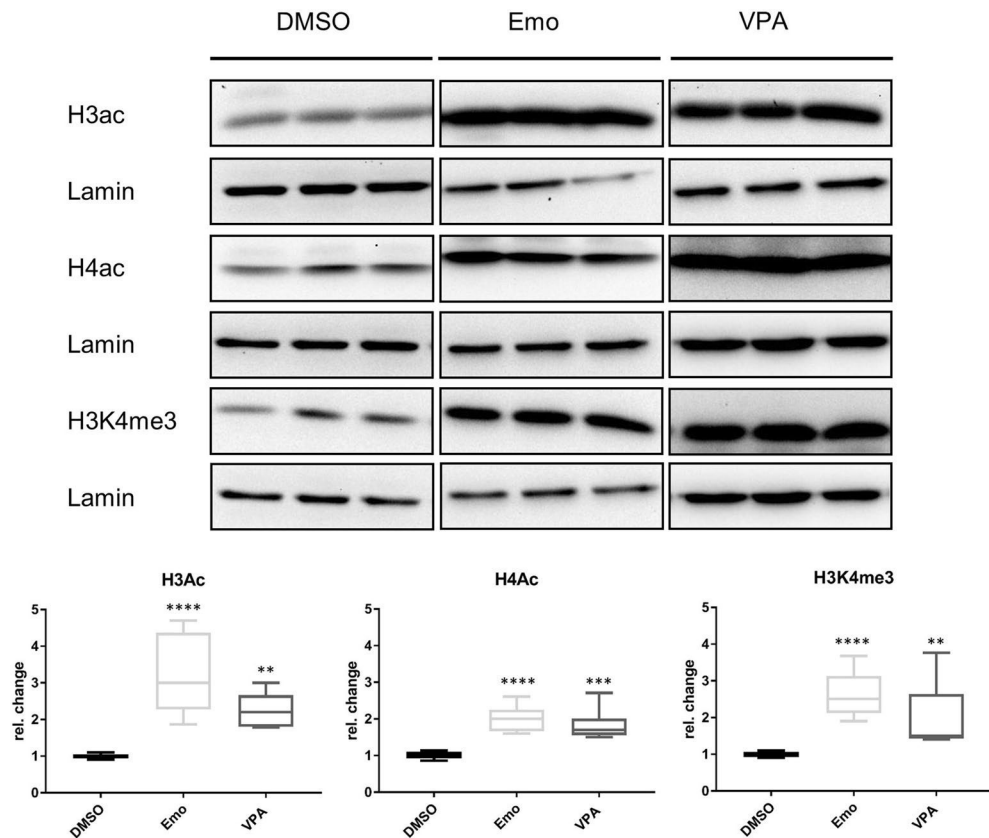


Figure 5. Emo increased histone H3/H4ac and H3K4me3 levels. Representative WB (upper) and boxplot diagrams (lower) represent 5–95 percentile. Three independent experiments with three repetitions were conducted. Protein levels were determined by Western blot and normalized to Lamin B1 and DMSO, respectively. Compounds were applied at a final concentration of 25 μ M for 24 h. VPA was used as a positive control at a concentration of 600 μ M. ** $p < 0.01$, *** $p < 0.001$, **** $p = 0.0001$. Full-size WBs of H3ac for DMSO, Emo and VPA see Supplementary Fig. S5A,B. Full size WBs of H4ac for DMSO, Emo and VPA see Supplementary Fig. S5C,D, and WBs of H3K4me3 see Supplementary Fig. S5D (VPA) and E (DMSO, Emo).

It remains to be determined whether Emo and VPA induced histone modifications might be prerequisites for more specific downstream regulations at the *SNCA* promotor.

Compared to the observed mutations^{19,20} and multiplications^{1,21} of the *SNCA* gene in familial PD, the role of *SNCA* in sporadic PD seems to be more elusive. Previous studies have shown conflicting data regarding the expression levels of *SNCA* mRNA in idiopathic PD (iPD). While studies found no alterations of *SNCA* mRNA expression in laser captured dopaminergic neurons from *postmortem* substantia nigra and blood samples from iPD patients and healthy controls^{22,23} another study reported decreased *SNCA* mRNA levels in the substantia nigra-, frontal- and temporal cortex neurons²⁴. Increased levels of *SNCA* mRNA were observed in UV-laser micro dissected human *postmortem* substantia nigra neurons and mid-brain tissue including the substantia nigra from iPD patients compared to controls^{25,26}.

Our unbiased reporter cell line-based screening of 1649 bioactive and FDA approved compounds did not reveal a substance with an immediate translational value for the modulation of *SNCA* expression. Since we found no specific mode of action for the identified activators (except global histone modifications for Emo) future studies will be needed to uncover potential mechanisms and to evaluate the utility for translational application of these compounds.

Intriguingly, Emo and other anthraquinone-type analogs, like aloë-emodin and emodic acid, have been associated with a variety of neuroprotective effects, i.e. inhibition of NF- κ B activity and prevention of NAD⁺ and ATP depletion²⁷. On the other hand, increased *SNCA* expression is considered to be the culprit in PD pathophysiology. In contrast to VPA which has been used as an anticonvulsant and mood-stabilizer in a great number of patients over the years, no reports have associated the use of Emo with Parkinsonism (yet). Given the relatively low frequency of the incidence of parkinsonian symptoms observed with VPA (which are reversible upon cessation of VPA), one may assume that also Emo carries only a minor risk for parkinsonism and that none of the FDA approve compounds will affect *SNCA* expression to an extent which could increase the risk of PD²⁸.

Methods

Cultivation and cell treatments of human neuroblastoma cell lines. The human SH-SY5Y neuroblastoma cell line was purchased from the European Collection of Authenticated Cell Cultures (ECACC) and used for the generation of our screening cell lines. All cell lines were cultivated in DMEM F12 Glutamax (Gibco) supplemented with 1% penicillin/streptomycin (Gibco) and 10% inactivated FBS (Sigma-Aldrich), respectively. For detachment, cells were treated with 1% Trypsin-EDTA (Gibco) for 10 min at 37 °C. All compounds were purchased from Selleckchem.

Generation of *SNCA-GFP-LUC* fusion cell line via CRISPR/Cas9 gene editing and homologous recombination. CRISPR target sites for *SNCA* exon 6 were selected from the web tool chopchop (<https://chopchop.cbu.uib.no/>)^{29,30} using the genomic sequence of exon 6 of *SNCA* (NG_011851.1) and cloned into GeneArt CRISPR Nuclease Vector Kit (Thermo Fisher Scientific) according to manufacturer's protocol. Primers for *SNCA*_CRISPR target site 1 Exon 6 as follows: forward TGGGAGCAAAGATATTTCTTGTGTTT, reverse AAGAAATATCTTTGCTCCACGGTG.

For cloning of the homologous recombination (HR) vector HR150PA-1 (PrecisionX HR Targeting Vectors, System Bioscience), primers for the HR arms were tagged with 5' palindromic sequences for respective restriction enzymes (bold) and amplified with Herculase II Fusion DNA Polymerase (Agilent) from genomic DNA (gDNA) of SH-SY5Y. Primers were as follows: left HR arms upstream *GFP-LUC* cassette (HR150PA-1), forward **GAATTC**GACATTCTGGCACAAGGGAATATCAG and reverse **GAATTC**GGCTTCAGGTTTCGTAGTCTTGATACC, *EcoRI*; for right HR arm downstream *GFP-LUC* cassette (HR150PA-1), forward **GGATCC**AATATCTTGTCTCCAGTTTCTTGAG and reverse **GTCGAC**GACAGGATTGAAGGGAGAAATAGACC, *BamHI* and *Sall*, respectively. Total length of HR arms were as follows: left HR arm 905 bp and right HR arm 889 bp. PCR products were sub-cloned into pJET1.2 (CloneJET PCR Cloning Kit, Thermo Fisher Scientific) and finally inserted into the HR150PA-1. Vector integrity was confirmed by sequencing. All restriction enzymes were fast digest enzymes and purchased from Fermentas, Thermo Fisher Scientific.

Transfection, selection and screening of the *SNCA-GFP-LUC* knock-in cell line. Transfection of the CRISPR/Cas9- and the HR-plasmids, were performed with the Roti-Fect PLUS (Roth) transfection mix, according to manufacturer's protocol. Selection pressure was applied after 24 h and maintained for 1–2 weeks. Single colonies were picked by using Corning Cloning Cylinders according to manufacturer's protocol. Plates were duplicated when cells reached 80% confluency and protein lysates were generated to screen clones via western blot.

Isolation of nucleic acids. *Genomic DNA (gDNA).* Pelleted cells were incubated with 350 µl TENS buffer (50 mM TrisCl pH 8.0, 100 mM EDTA pH 8.0, 100 mM NaCl, 1% SDS) and 17.5 µl Proteinase K (10 mg/ml) overnight in a water bath at 55 °C. At the next day, 150 µl NaCl solution (saturated in H₂O) were added, samples were incubated on ice for 5 min and centrifuged for 30 min. The supernatant was transferred into a fresh reaction tube, mixed with 500 µl isopropanol and incubated for 10 min at room temperature (RT). Samples were centrifuged for 30 min, supernatant was discarded and gDNA pellets were washed with 70% ethanol followed by 15 min centrifugation. Air-dried DNA was resolved in 10 mM Tris pH 7.5. All centrifugation steps were carried out at 16,000 rcf and 4 °C (adapted from "The Jacks Lab: DNA Isolation from Tail-Proteinase K Method").

Miniprep/Maxiprep. We used Top10F' *E. coli* cells for transformation and mini- and maxi preparation ZR Plasmid Miniprep—Classic (Zymo Research) and the NucleoBond Xtra Maxi kit (Macherey-Nagel) were used, respectively.

PCR. *Standard PCR and gel-electrophoreses.* For the generation of the homologous recombination arms 100–200 ng DNA was amplified in a total volume of 20 µl. Mastermix was prepared at final concentrations of 1 × reaction buffer (BioTherm, Genecraft), 250 µM dNTPs (Thermo Fisher Scientific), 0.2 µM of each primer, 1 unit Taq DNA polymerase (BioTherm, Genecraft) and filled up to 20 µl with H₂O. After initial denaturation at 94 °C for 3 min PCR were run for 30 cycles (denaturation 94 °C for 30 s, annealing for 30 s at respective temperature, extension 68 °C for 1 min). PCR products were amplified in the Biometra TADVANCED thermocycler and separated in 1% TBE agarose gel containing 2.5 × GelRed Nucleic Acid Gel Stain (Biotium) for visualization. For the validation of *SNCA-GFP-LUC*-fusion, mRNA was converted into cDNA and amplified by using *SNCA*qF2 GGACCAGTTGGGCAAGAATG and HR150GFP reverse TGTCACGATCAAAGGACTCTGG primer. As a negative control for the wildtype locus we used *SNCA*qF2 and the corresponding reverse primer *SNCA*qR2 GGCACATTGGAAGTGGAC.

RT-qPCR assays. *LUC mRNA.* Total RNA for initial RT-qPCR assays was isolated with the Qiagen Fast-Lane Cell RT-PCR SYBR Green Kit. Cells were seeded at a density of 8 × 10⁴ in 50 µl/well and 96 well format and treated the next day at effective compound concentration of 25 µM and equivalent DMSO controls. Each plate contained 30 compounds in triplicates and six DMSO controls. Cells were lysed in a total volume of 50 µl cell processing mix in accordance to manufacturer's protocol with the following adaptations: (1) prolonged incubation (10 min) of the processing mix and (2) additional incubation of the lysates at 75 °C prior RT-qPCR (5 min). The RT-qPCR assays were performed with the QuantiTect SYBR Green RT-PCR Kit (Qiagen) in 384 well format. We used 3 µl of the cell processing mix (total of 50 µl) for amplification. Reactions were run in a Roche LightCycler 480 system. Primers were as follows: *LUC*, forward GAACATCACGTACGCGGAAT and reverse GCGCAA

CTGCAACTCCGATA. *LUC* mRNA expression was normalized to ubiquitin C (*UBC*) and glucuronidase beta (*GUSB*) housekeeping genes.

SNCA mRNA. For hit validation SH-SY5Y wildtype cells were treated at effective concentrations of 25 μ M (12.5 μ M for clomiphen-citrate) for 24 h in 24 well plate format and triplicates. Total RNA was extracted with the RNeasy Mini kit (Qiagen). RT-qPCR reactions were performed with the QuantiTect SYBR Green RT-PCR Kit (Qiagen) in a 96 well format and run in the Applied Biosystems HT7500 cyclor. We used 50 ng of total RNA for amplification. Primers were as follows: *SNCA*, accession number NM_000345, purchased from Qiagen (Hs_SNCA_1_SG QuantiTect Primer Assay (QT00035903)). *SNCA* mRNA expression was normalized to *UBC*, hypoxanthine phosphoribosyl-transferase 1 (*HPRT1*) and *GUSB* housekeeping genes.

Housekeeping primers were as follows: *HPRT1*, accession number NM_000194.3, forward TGACACTGG CAAAACAATGCA and reverse GGTCTTTTACCAGCAAGCT. *UBC*, accession number M26880, forward ATTTGGGTCGCGGTTCTTG and reverse TGCCTTGACATTCTCGATGGT³¹. *GUSB*, accession number XM_005250297.4, forward CCAGCGTGGAGCAAGACA and reverse CCATTGCCACGACTTTGTT. Relative mRNA levels were calculated using the $\Delta\Delta$ CT Method for multiple housekeeping genes from Pfaffl, published in “A–Z of quantitative PCR”³².

SDS PAGE and western blot analysis. For SDS-PAGE cells were harvested and lysed in RIPA buffer (50 mM TrisCl pH 7.5, 150 mM NaCl, 10 mM MgCl₂, 0.5% Triton X 100) supplemented with Halt Protease Inhibitor-Cocktail (1 \times final concentration) (Thermo Fisher Scientific) and 0.5 μ l/ml benzonase (Merck) for 30 min on ice. Lysates were mixed with 4 \times Laemmli loading buffer (200 mM TrisCl pH 6.8, 8% SDS, 6% β -mercapto-ethanol, 33% glycerol, spatula tip bromophenol blue) to a final concentration of 1 \times and boiled for 10 min at 95 $^{\circ}$ C. Samples were loaded onto 15% SDS-PAGE gels.

Nuclear extraction for histone Western blots. Nuclear extraction was performed according to Schreiber et al.³³ with the following adaptations: Buffer C was supplemented with 0.1% SDS. Buffer A and C were supplemented with Halt Protease Inhibitor-Cocktail 1 \times final concentration (Thermo Fisher Scientific). We used 200 μ l of buffer A and 60 μ l of buffer C (12-well plate format). Nuclei were sonicated for three seconds and three intervals at 50% power (Bandelin Sonopuls, HD2070, SH70G, type MS72), incubated on ice for 30 min and clarified by centrifugation. Supernatants were transferred to fresh tubes and stored at –80 $^{\circ}$ C. All centrifugation steps were carried out for 10 min at 16,000 rcf and 4 $^{\circ}$ C.

Western blot. Proteins were blotted onto methanol activated polyvinylidene difluoride (PVDF) membrane (GE Healthcare, Amersham Hybond), blocked with 5% milk-powder (Roth) in 1 \times PBS-TWEEN 20 0.1% (PBST 0.1%) for 1 h and incubated with SNCA 2F12 (1:2000, MABN1817, Sigma-Aldrich) and beta actin (1:10,000, A5441, Sigma-Aldrich) primary antibodies overnight at 4 $^{\circ}$ C. Secondary HRP conjugated anti mouse antibody (1:4000, P0447, Dako) was applied for 1 h at room temperature. For histone H3 and H4 global acetylation (# 06-599 and # 06-598, Millipore) and H3K4 tri-methylation (C42D8, Cell Signaling Technology) were used. For normalization of nuclear extracts, we used the Lamin B1 antibody (D4Q4Z, Cell Signaling Technology). Secondary HRP conjugated anti rabbit antibody (1:4000, 7074 V, Cell Signaling Technology) was applied.

Membranes were washed three times with PBST 0.1% (1 \times TBS-TWEEN 20 0.1% for histone Western blots) and imaged with enhanced chemiluminescence (ECL) in the ChemoCam imager (Intas). Signals were quantified with the ImageJ software³⁴.

For SNCA and beta actin the secondary IRDye 800CW Donkey anti-Mouse IgG antibody (1:4000, LI-COR) was applied for 1 h at room temperature (in the dark). Membranes were imaged with the LI-COR Odysseys Clx (Model 9140; S/N CLX-0554) and signals were quantified using the Image Studio software 4.0.21. Treated cells were normalized to actin and DMSO control, respectively.

In-Cell Western. For In-Cell Western (ICW) experiments, cells were plated in 96 well plates (black/clear, Falcon) at a density of 8×10^4 cells/well. Cells were treated at the next day. After treatment, media were discarded and cells were fixed with 100 μ l ice cold 100% methanol (–20 $^{\circ}$ C) for 15 min at RT on an orbital shaker. Methanol was discarded, permeabilized cells were washed with 100 μ l 1 \times PBS and blocked with 0.5% casein blocking solution (Casein diluted in 1 \times PBS) for 30 min at RT. After blocking, cells were incubated with 50 μ l of alpha synuclein 2F12 primary antibody dilution (diluted 1:2000 in 0.5% casein PBS + 0.1% blocking solution (PBST)) at 4 $^{\circ}$ C on an orbital shaker overnight. On the next day, cells were washed 3 \times with 100 μ l 1 \times PBST and incubated with 50 μ l of CellTag 700 Stain (1:1000 from LI-COR) and secondary IRDye 800CW Donkey anti-Mouse IgG antibody (1:1000, from LI-COR) in 0.5% casein PBST blocking solution for 1 h at RT on an orbital shaker. Plates were protected from light. Cells were washed 3 \times with 100 μ l PBST and 1 \times with PBS and imaged with the LI-COR Odyssey Clx (Model 9140; S/N CLX-0554) and signals were quantified using the Image Studio software 4.0.21.

For analysis the Image Studio 4.0 software (provided from LI-COR) was used and signals were normalized to CellTag700 and DMSO, respectively. As a background control, cells were incubated with secondary antibody and CellTag700 alone.

LUC assay. Bioactive compound collections (Selleckchem) were randomly spotted—initially at a concentration of 10 μ M in three independent experiments. We used valproic acid (VPA), a known modulator of α -syn expression, as a positive control (Fig. 2A).

The screening process was fully automated. For the luciferase assay 2×10^4 cells/well in a volume of 30 μ l were seeded into nunc white 384 well plates (Thermo Fisher Scientific). Cells attached and grew for approx. 18 h at 37 °C before treatment. The pre-spotted 384 well compound plates (100 nl/well) were diluted with 25 μ l medium/well and shaken for 5 min with 1200 rpm at RT. Subsequently, 10 μ l of the compound dilution were applied to 384 well cell plates, resulting in a final concentration of 10 μ M and incubated for 24 h at 37 °C. Controls were distributed on the assay plate in a fixed layout for all three independent experiments. The tested drugs were randomly distributed for the three experiments to avoid well location dependent effects (Fig. 2A). Cells were lysed by adding 40 μ l of ONE Glo (Lysis Buffer and Luciferase Substrate, Promega) to each well (on top of medium), incubated for 5 min while shaking at 1200 rpm and luciferase signal was measured with the Paradigm Reader at 1200 ms integration time.

For hit definition the luciferase signal of treated cells was normalized to untreated controls per plate. Compounds showing an increased (activators) or decreased (inhibitors) luciferase signal of more than the four-fold standard deviation of the mean (SD) of untreated controls were considered as effective modulators (Fig. 2B).

Repeated experiments were conducted in Nunc white 96 well plates and measured with the Centro LB 960 (Berthold Technologies) at 1200 ms integration time.

Cell viability tests. To screen for potentially cytotoxic effects we performed a combination of a homogenous resazurin test and an image-based high content screen (HCS) on single cell level in a dose range of 0.25–40 μ M, respectively. The resazurin assay was performed according to manufacturer's protocol. For the HCS, the nuclei of treated cells were stained with the fluorescent DNA probe DRAQ5. After imaging, living and dead cells were counted per well and total cell viability were calculated for each well and applied compound concentration.

Statistics. We used one-way ANOVA ($\alpha=0.05$) followed by the recommended Dunnett's multiple comparison test to check for statistical significance. All statistical analyses were performed in GraphPad Prism 7.02.

Received: 20 May 2021; Accepted: 8 September 2021

Published online: 06 October 2021

References

- Singleton, A. B. *et al.* alpha-Synuclein locus triplication causes Parkinson's disease. *Science* **302**, 841. <https://doi.org/10.1126/science.1090278> (2003).
- Hollerhage, M., Bickel, M. & Hoglinger, G. U. Unbiased screens for modifiers of alpha-synuclein toxicity. *Curr. Neurol. Neurosci. Rep.* **19**, 8. <https://doi.org/10.1007/s11910-019-0925-z> (2019).
- Mittal, S. *et al.* beta2-Adrenoreceptor is a regulator of the alpha-synuclein gene driving risk of Parkinson's disease. *Science* **357**, 891–898. <https://doi.org/10.1126/science.aaf3934> (2017).
- Jowaed, A., Schmitt, I., Kaut, O. & Wullner, U. Methylation regulates alpha-synuclein expression and is decreased in Parkinson's disease patients' brains. *J. Neurosci.* **30**, 6355–6359. <https://doi.org/10.1523/JNEUROSCI.6119-09.2010> (2010).
- Auld, D. S. &INGLESE, J. In *Assay Guidance Manual* (eds Markossian, S. *et al.*) (Eli Lilly, 2004).
- Auld, D. S., Thorne, N., Nguyen, D. T. &INGLESE, J. A specific mechanism for nonspecific activation in reporter-gene assays. *ACS Chem. Biol.* **3**, 463–470. <https://doi.org/10.1021/cb8000793> (2008).
- Thul, P. J. *et al.* A subcellular map of the human proteome. *Science* <https://doi.org/10.1126/science.aal3321> (2017).
- Xicoy, H., Wieringa, B. & Martens, G. J. The SH-SY5Y cell line in Parkinson's disease research: A systematic review. *Mol. Neurodegener.* **12**, 10. <https://doi.org/10.1186/s13024-017-0149-0> (2017).
- Wishart, D. S. *et al.* DrugBank 5.0: A major update to the DrugBank database for 2018. *Nucleic Acids Res.* **46**, D1074–D1082. <https://doi.org/10.1093/nar/gkx1037> (2018).
- Matsuda, H., Shimoda, H., Morikawa, T. & Yoshikawa, M. Phytoestrogens from the roots of *Polygonum cuspidatum* (Polygonaceae): Structure-requirement of hydroxyanthraquinones for estrogenic activity. *Bioorg. Med. Chem. Lett.* **11**, 1839–1842. [https://doi.org/10.1016/s0960-894x\(01\)00318-3](https://doi.org/10.1016/s0960-894x(01)00318-3) (2001).
- Wullner, U., Kaut, O., deBoni, L., Piston, D. & Schmitt, I. DNA methylation in Parkinson's disease. *J. Neurochem.* **139**(Suppl 1), 108–120. <https://doi.org/10.1111/jnc.13646> (2016).
- Marshall, L. L. *et al.* Epigenomic analysis of Parkinson's disease neurons identifies Tet2 loss as neuroprotective. *Nat. Neurosci.* **23**, 1203–1214. <https://doi.org/10.1038/s41593-020-0690-y> (2020).
- Leng, Y. & Chuang, D. M. Endogenous alpha-synuclein is induced by valproic acid through histone deacetylase inhibition and participates in neuroprotection against glutamate-induced excitotoxicity. *J. Neurosci.* **26**, 7502–7512. <https://doi.org/10.1523/JNEUROSCI.0096-06.2006> (2006).
- Dansithong, W., Paul, S., Scoles, D. R., Pulst, S. M. & Huynh, D. P. Generation of SNCA Cell models using zinc finger nuclease (ZFN) technology for efficient high-throughput drug screening. *PLoS One* **10**, e0136930. <https://doi.org/10.1371/journal.pone.0136930> (2015).
- Guhathakurta, S. *et al.* Targeted attenuation of elevated histone marks at SNCA alleviates alpha-synuclein in Parkinson's disease. *EMBO Mol. Med.* **13**, e12188. <https://doi.org/10.15252/emmm.202012188> (2021).
- Toker, L., Tran, T. G., Sundaresan, J., Tysnes, B. O., Alves, G., Haugarvoll, K., Nido, S. G., Dölle, C., Tzoulis, C. . Genome-wide dysregulation of histone acetylation in the Parkinson's disease brain. Preprint at <https://www.biorxiv.org/content/10.1101/785550v3> (2020).
- Godoy, L. D., Lucas, J. E., Bender, A. J., Romanick, S. S. & Ferguson, B. S. Targeting the epigenome: Screening bioactive compounds that regulate histone deacetylase activity. *Mol. Nutr. Food Res.* <https://doi.org/10.1002/mnfr.201600744> (2017).
- Evans, L. W. *et al.* Emodin and emodin-rich rhubarb inhibits histone deacetylase (HDAC) activity and cardiac myocyte hypertrophy. *J. Nutr. Biochem.* **79**, 108339. <https://doi.org/10.1016/j.jnutbio.2019.108339> (2020).
- Polymenopoulos, M. H. *et al.* Mutation in the alpha-synuclein gene identified in families with Parkinson's disease. *Science* **276**, 2045–2047. <https://doi.org/10.1126/science.276.5321.2045> (1997).
- Kruger, R. *et al.* Ala30Pro mutation in the gene encoding alpha-synuclein in Parkinson's disease. *Nat. Genet.* **18**, 106–108. <https://doi.org/10.1038/ng0298-106> (1998).

21. Chartier-Harlin, M. C. *et al.* Alpha-synuclein locus duplication as a cause of familial Parkinson's disease. *Lancet* **364**, 1167–1169. [https://doi.org/10.1016/S0140-6736\(04\)17103-1](https://doi.org/10.1016/S0140-6736(04)17103-1) (2004).
22. Su, X. *et al.* Alpha-synuclein mRNA is not increased in sporadic PD and alpha-synuclein accumulation does not block GDNF signaling in Parkinson's disease and disease models. *Mol. Ther.* **25**, 2231–2235. <https://doi.org/10.1016/j.ymthe.2017.04.018> (2017).
23. Tan, E. K. *et al.* Alpha-synuclein mRNA expression in sporadic Parkinson's disease. *Mov. Disord.* **20**, 620–623. <https://doi.org/10.1002/mds.20391> (2005).
24. Kingsbury, A. E. *et al.* Alteration in alpha-synuclein mRNA expression in Parkinson's disease. *Mov. Disord.* **19**, 162–170. <https://doi.org/10.1002/mds.10683> (2004).
25. Grundemann, J., Schlaudraff, F., Haackel, O. & Liss, B. Elevated alpha-synuclein mRNA levels in individual UV-laser-microdissected dopaminergic substantia nigra neurons in idiopathic Parkinson's disease. *Nucleic Acids Res.* **36**, e38. <https://doi.org/10.1093/nar/gkn084> (2008).
26. Chiba-Falek, O., Lopez, G. J. & Nussbaum, R. L. Levels of alpha-synuclein mRNA in sporadic Parkinson disease patients. *Mov. Disord.* **21**, 1703–1708. <https://doi.org/10.1002/mds.21007> (2006).
27. Liu, W. *et al.* Emodin inhibits zinc-induced neurotoxicity in neuroblastoma SH-SY5Y cells. *Biosci. Rep.* <https://doi.org/10.1042/BSR20182378> (2019).
28. Mahmoud, F. & Tampi, R. R. Valproic acid-induced parkinsonism in the elderly: A comprehensive review of the literature. *Am. J. Geriatr. Pharmacother.* **9**, 405–412. <https://doi.org/10.1016/j.amjopharm.2011.09.002> (2011).
29. Montague, T. G., Cruz, J. M., Gagnon, J. A., Church, G. M. & Valen, E. CHOPCHOP: A CRISPR/Cas9 and TALEN web tool for genome editing. *Nucleic Acids Res.* **42**, W401–W407. <https://doi.org/10.1093/nar/gku410> (2014).
30. Labun, K. *et al.* CHOPCHOP v3: Expanding the CRISPR web toolbox beyond genome editing. *Nucleic Acids Res.* **47**, W171–W174. <https://doi.org/10.1093/nar/gkz365> (2019).
31. Vandesompele, J. *et al.* Accurate normalization of real-time quantitative RT-PCR data by geometric averaging of multiple internal control genes. *Genome Biol.* <https://doi.org/10.1186/gb-2002-3-7-research0034> (2002).
32. Bustin, S. A. *A-Z of Quantitative PCR* (International University Line, 2004).
33. Schreiber, E., Matthias, P., Muller, M. M. & Schaffner, W. Rapid detection of octamer binding proteins with “mini-extracts”, prepared from a small number of cells. *Nucleic Acids Res.* **17**, 6419. <https://doi.org/10.1093/nar/17.15.6419> (1989).
34. Schneider, C. A., Rasband, W. S. & Eliceiri, K. W. NIH Image to ImageJ: 25 years of image analysis. *Nat. Methods* **9**, 671–675. <https://doi.org/10.1038/nmeth.2089> (2012).

Acknowledgements

We thank Birgit Kurkowsky and H. Khazneh for excellent technical assistance. This work was supported by an I2A grant of the DZNE.

Author contributions

P.B.: idea and study design, proof of principle, validation of appropriate luciferase substrate, writing of the manuscript; U.W.: data interpretation and writing of the manuscript; I.S.: cloning of CRISPR/Cas9 plasmid and HR-Vector; D.P.: transfection and screening of A1 cell line and validation of luciferase substrate; P.D.: screening automation, cell viability assays, dose response and data validation and interpretation, writing of the manuscript; L.B.: implementation of in-cell Western protocol and data analysis; B.O.E.: screening of the A6 cell line, data interpretation and writing of the manuscript; F.S.: RT-qPCR screening, protein assays, data analysis and interpretation, writing of the manuscript.

Funding

Open Access funding enabled and organized by Projekt DEAL. Laura de Boni was funded by the Thiemann foundation.

Competing interests

The authors declare no competing interests.

Additional information

Supplementary Information The online version contains supplementary material available at <https://doi.org/10.1038/s41598-021-98841-9>.

Correspondence and requests for materials should be addressed to P.B. or U.W.

Reprints and permissions information is available at www.nature.com/reprints.

Publisher's note Springer Nature remains neutral with regard to jurisdictional claims in published maps and institutional affiliations.



Open Access This article is licensed under a Creative Commons Attribution 4.0 International License, which permits use, sharing, adaptation, distribution and reproduction in any medium or format, as long as you give appropriate credit to the original author(s) and the source, provide a link to the Creative Commons licence, and indicate if changes were made. The images or other third party material in this article are included in the article's Creative Commons licence, unless indicated otherwise in a credit line to the material. If material is not included in the article's Creative Commons licence and your intended use is not permitted by statutory regulation or exceeds the permitted use, you will need to obtain permission directly from the copyright holder. To view a copy of this licence, visit <http://creativecommons.org/licenses/by/4.0/>.

© The Author(s) 2021



OPEN High throughput compound screening in neuronal cells identifies statins as activators of ataxin 3 expression

Fabian Stahl^{1,2}, Ina Schmitt², Philip Denner¹, Laura de Boni^{2,3}, Ullrich Wüllner^{1,2,4}✉ & Peter Breuer^{1,2,4}✉

The spinocerebellar ataxias (SCA) comprise a group of inherited neurodegenerative diseases. SCA3 is the most common form, caused by the expansion of CAG repeats within the ataxin 3 (*ATXN3*) gene. The mutation results in the expression of an abnormal protein, containing long polyglutamine (polyQ) stretches. The polyQ stretch confers a toxic gain of function and leads to misfolding and aggregation of *ATXN3* in neurons. Thus, modulators of *ATXN3* expression could potentially ameliorate the pathology in SCA3 patients. Therefore, we generated a CRISPR/Cas9 modified *ATXN3*-Exon4-Luciferase (*ATXN3*-LUC) genomic fusion- and control cell lines to perform a reporter cell line-based high-throughput screen comprising 2640 bioactive compounds, including the FDA approved drugs. We found no unequivocal inhibitors of, but identified statins as activators of the LUC signal in the *ATXN3*-LUC screening cell line. We further confirmed that Simvastatin treatment of wild type SK-N-SH cells increases *ATXN3* mRNA and protein levels which likely results from direct binding of the activated sterol regulatory element binding protein 1 (SREBP1) to the *ATXN3* promotor. Finally, we observed an increase of normal and expanded *ATXN3* protein levels in a patient-derived cell line upon Simvastatin treatment, underscoring the potential medical relevance of our findings.

Machado Joseph Disease (MJD) or Spinocerebellar Ataxia 3 (SCA3) is a neurodegenerative disorder caused by an abnormal expansion of the polyglutamine (polyQ) tract of the ataxin-3 gene (*ATXN3*)^{1,2}.

ATXN3 is a deubiquitinating enzyme (DUB), involved in protein homeostasis via the ubiquitin proteasome system (UPS) and endoplasmic reticulum associated degradation (ERAD) by interaction with VCP/p97³. In SCA3, the expanded polyQ tract within *ATXN3*, leads to misfolding, aggregation and accumulation of mutated (and the normal) *ATXN3* protein in nuclear inclusions in neurons. The pathological accumulation of *ATXN3* in turn impairs protein homeostasis within neurons^{3,4}.

As a result of the neurodegenerative process, SCA3 patients are severely disabled and die prematurely. Thus, reducing the amount of the disease-causing *ATXN3* protein constitutes a promising target for treatment approaches. In the past, several screens with different paradigms for *ATXN3* modulation have been performed in the quest for novel targets for SCA3. Druggable genome-wide- and drug library screenings mainly concentrated on the reduction of stably overexpressed *ATXN3*(PolyQ)protein and improvement of the resultant toxicity^{5–9}.

The antipsychotic drug Aripiprazole was identified as a potential *ATXN3*(PolyQ) reducing drug in a primary cell-based *ATXN3* overexpression model. Treatment of transgenic *ATXN3* *Drosophila* flies and mice confirmed the beneficial effects by increasing longevity in the flies and decreasing aggregated *ATXN3* protein in both SCA3 animal models⁸. More recently, Fardghassemi and colleagues found five neuroprotective drugs for *ATXN3*PolyQ induced toxicity in a compound screening assay performed in *C. elegans*. Thereby, they discovered that the transcription factor TFEB/HLH-30 was related to *ATXN3* toxicity⁹. However, these approaches considering transgenic overexpression models of toxic *ATXN3* alone missed modulators of endogenous *ATXN3* regulation.

Here, we performed a reporter cell line-based high-throughput compound screening (HTS) assay to identify modulators of endogenous *ATXN3*. To our knowledge, this is the first study seeking for compounds to alter

¹German Center for Neurodegenerative Diseases, DZNE, Venusberg-Campus 1, 53127 Bonn, NRW, Germany. ²Department of Neurology, University Hospital Bonn, Venusberg-Campus 1, 53127 Bonn, NRW, Germany. ³Institute of Aerospace Medicine, German Aerospace Center, Cologne, Germany. ⁴These authors jointly supervised this work: Ullrich Wüllner and Peter Breuer. ✉email: ullrich.wuellner@dzne.de; peter.breuer@ukbonn.de; peter.breuer@dzne.de

endogenous *ATXN3* expression levels. In our screening approach, we found no unequivocal inhibitors, but identified four statins i.e. Mevastatin, Atorvastatin, Fluvastatin and Simvastatin to increase LUC signal in the *ATXN3*-LUC screening cell line and further confirmed Simvastatin as an activator of *ATXN3* expression in SK-N-SH wild type cells. Statins are potent inhibitors of 3-hydroxy-3-methylglutaryl coenzyme A reductase (HMGCR). HMGCR is the rate-limiting enzyme in the mevalonate/cholesterol pathway. Inhibition of the enzyme results in cellular cholesterol reduction and in turn activates the sterol regulatory element binding proteins (SREBPs) which are key transcription factors for regulation of genes involved in cholesterol and lipid pathways. Three SREBPs are known and transcribed from two genes *SREBP1* and *SREBP2*. The *SREBP1* gene encodes for two *SREBP1* isoforms (1a and 1c)^{10,11}. In this study, we found that Simvastatin treatment increased *ATXN3* levels by direct binding of the activated SREBP1 transcription factor to the *ATXN3* promotor in wild type SK-N-SH cells.

Results

Simvastatin leads to increased *ATXN3* mRNA and protein levels by direct binding of activated SREBP1 transcription factor to the *ATXN3* promotor. We employed a similar HTS approach as published recently¹². We used the CRISPR/Cas9 based gene editing to modify the endogenous *ATXN3* gene in a SK-N-SH wild type cell line by insertion of a GFP-T2A-LUC cassette (*ATXN3*-LUC) (Fig. 1A, Supplementary Fig. S1). A second SK-N-SH cell line with a random integration of the reporter cassette (Rand-LUC) served as a control for unspecific modulators and toxicity.

We found no inhibitors of *ATXN3*, but identified statins as activators of LUC signal in the *ATXN3*-LUC screening cell line (Fig. 1B,C, Supplementary Fig. S2–3). The compound library contained eight statins and two other HMGCR inhibiting drugs. Interestingly, only four statins i.e. Mevastatin, Atorvastatin, Fluvastatin and Simvastatin increased the LUC signal in the *ATXN3* SK-N-SH model, while Lovastatin, Pitavastatin, Pravastatin and Rosuvastatin showed no signal change compared to controls. Simvastatin showed the most consistent effect in the primary HTS and was thus chosen for further validation in non-modified SK-N-SH cells. The non-statin HMGCR inhibiting drugs, Clonofibrate and SR12813, were not effective in our screening assay.

We performed time-course experiments in SK-N-SH wild type cells and Simvastatin was applied for 2, 4, and 8 h (h). The treatment showed a significant increase of *ATXN3* mRNA (1.4 fold after 2 h) and *ATXN3* protein levels (1.3 fold after 4 h), compared to DMSO-treated control cells (Fig. 2A,C,E). Additionally, we observed increased levels of the activated sterol responsive element binding proteins (SREBP1) transcription factor and HMGCR (Fig. 2C,D,F). To corroborate the hypothesis that *ATXN3* mRNA and protein increase was due to direct binding of activated SREBP1 (mSREBP1) to the *ATXN3* promotor, chromatin immunoprecipitation (ChIP)—qPCR experiments for SREBP1 were performed and revealed an average *ATXN3* promotor enrichment of 2.9-fold after 1 h Simvastatin treatment, compared to DMSO-treated control cells (Fig. 2B) in wild type SK-N-SH.

Time-controlled overexpression of active human SREBP1a in murine N2a cells increases endogenous *ATXN3* protein levels. To assess, which SREBP1 isoform increases levels of *ATXN3*, we

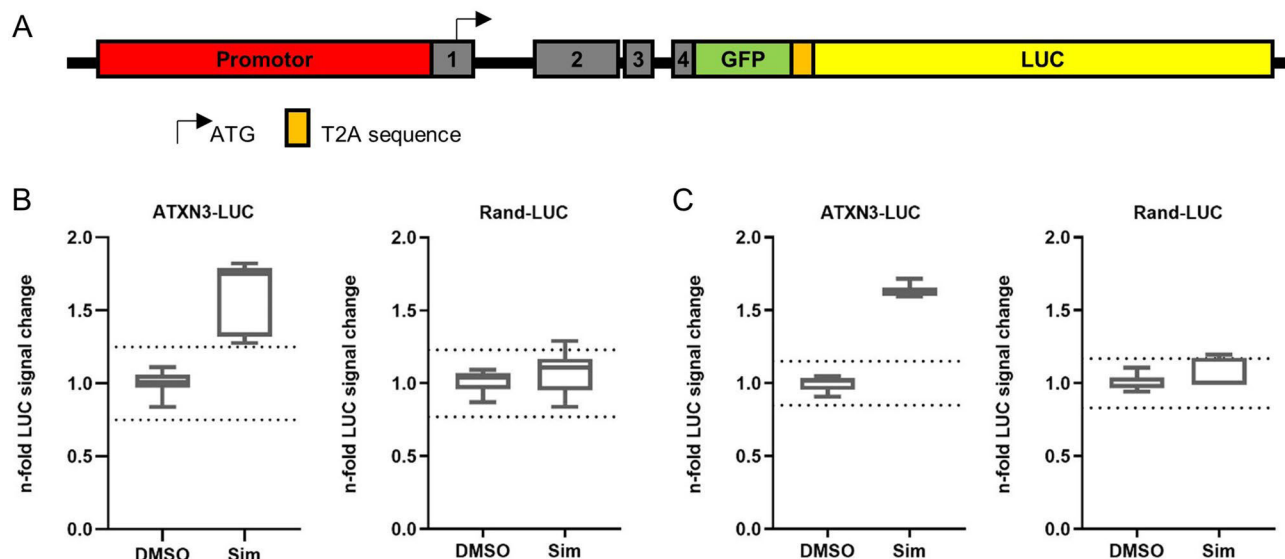


Figure 1. *ATXN3*-GFP-Luciferase (*ATXN3*-LUC) reporter cell line-based high throughput screening of 2,640 bioactive compounds, including FDA approved drugs identifies statins as modulators of *ATXN3* expression. (A) Schematic overview of CRISPR/Cas9 generated, genomic *ATXN3*-LUC fusion under control of the endogenous *ATXN3* promotor. (B,C) Simvastatin (Sim) treatment increased LUC signal in *ATXN3*-LUC screening cell line but not in the control cell line, bearing a randomly integrated LUC cassette (Rand-LUC) after 8 h (B) and 24 h (C). Maximal n-fold change was observed after 8 h. Boxplot diagrams represents 5–95 percentile and dotted line in depicts the three-fold standard deviation (SD) from the mean of DMSO controls, (B) $n=7$ and (C) $n=6$ biological replicates. Sim treatment was applied at a final concentration of 10 μ M. Additional information for *ATXN3*-LUC fusion see Supplementary Fig. S1.

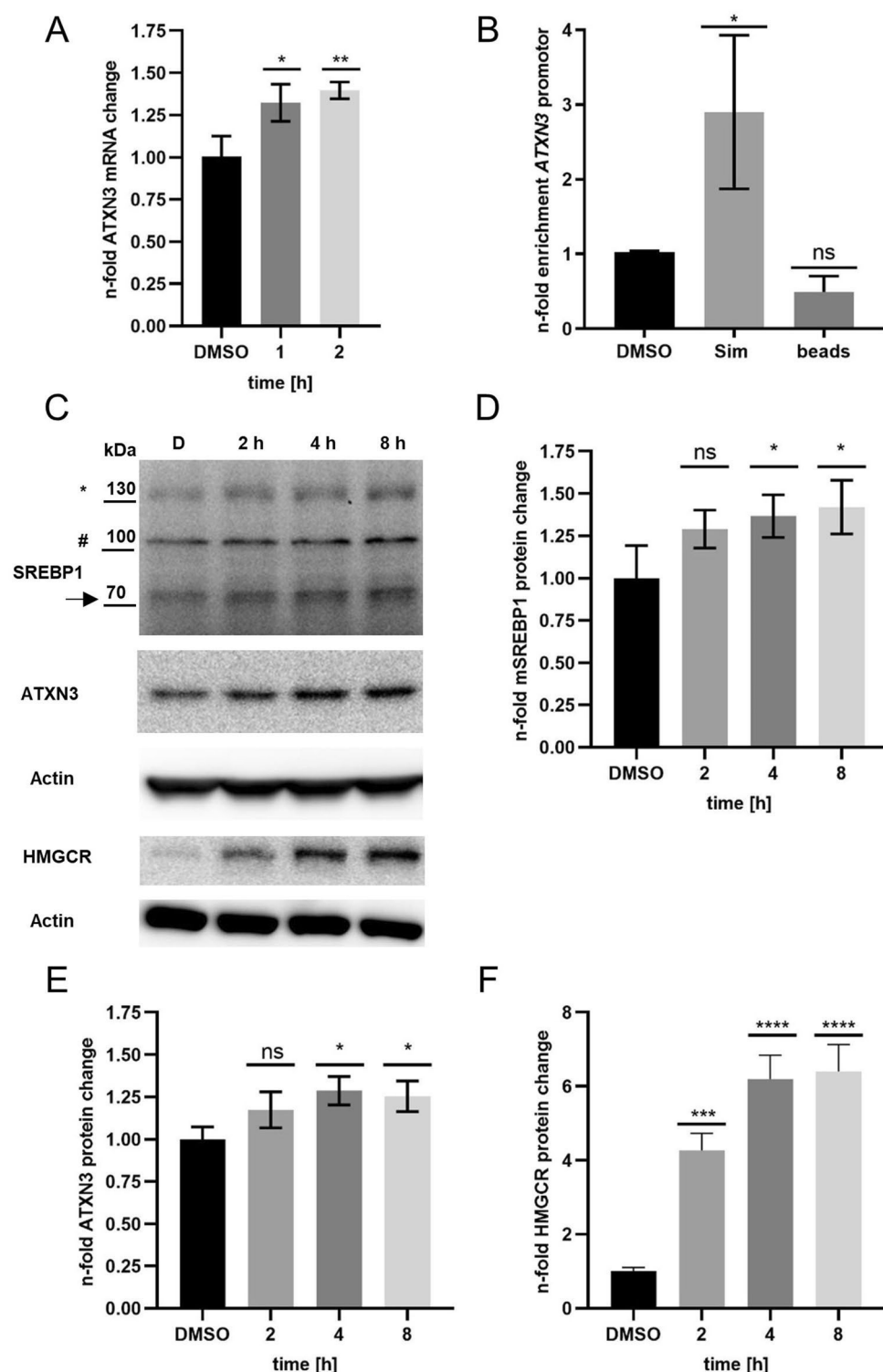


Figure 2. Simvastatin treatment increases *ATXN3* mRNA and protein levels, induces HMGCR protein level and activates the SREBP1 transcription factor and leads to binding of activated SREBP1 to the *ATXN3* promoter. **(A)** qRT-PCR of Simvastatin treated SK-N-SH wild type cells for 1–2 h. Data were normalized to three house-keeping genes and DMSO controls. **(B)** Relative n-fold enrichment of *ATXN3* promoter of three independent ChIP-qPCR experiments with the SREBP1 antibody (Proteintech 14088-1-AP) after 1 h Simvastatin (Sim) treatment. **(C)** Representative Western Blot (WB) of Sim treatment for 2–8 h. **(D)** Relative n-fold change of protein levels for mSREBP1, **(E)** *ATXN3* and **(F)** HMGCR. Asterisk and arrow indicate transcriptionally inactive- and mSREBP1, respectively. Hash: unspecific band. qRT-PCR Data were analysed using the $\Delta\Delta C_T$ method by Pfaffl. ChIP-qPCR data were normalized to input and DMSO controls and represent the mean of three technical replicates for each experiment, respectively. WB data were normalized to actin and the mean of DMSO controls. Error bars indicate SD of three biological repetitions. For all experiments, a final concentration of 10 μ M Sim was applied. Adjusted *p* values: **p* < 0.05; ***p* = 0.005; ****p* = 0.0002; *****p* < 0.0001.

used a tetracycline-controlled trans-activator (tTA) containing (pTet-Off)- and doxycycline (Dox)-responsive murine N2a cell line. This system allows the transient and time-controlled overexpression of the constitutively active human SREBP1a- and 1c isoforms, which were previously cloned into pTREhyg plasmids. While human SREBP1 expression was completely restricted by overnight incubation with Dox, removal for 1–3 h enabled the expression of human SREBP1a- and 1c proteins. We observed significantly increased endogenous ATXN3 protein levels after two (1.5-fold) and three (1.7-fold) hours for human SREBP1a overexpression (Fig. 3A,B) while SREBP1c was inactive (Fig. 3D,E). To confirm SREBP1a binding to the human ATXN3 promoter, we used the same expression system and co-transfected a LUC-reporter plasmid (pGL4 2.3) containing the promoter region of human ATXN3 together with the human SREBP1a (pTREhyg)- and the *Renilla* luciferase plasmid for normalization. Cells were incubated overnight with Dox and removal for 2–8 h lead to significant increased LUC signal after 8 h (Fig. 3C).

Simvastatin leads to increased ATXN3 and HMGCR protein levels in SCA3 patient-derived, induced pluripotent stem cell (iPSC)-derived long-term self-renewing neuroepithelial-like stem cells (MJD1 It-NES cells). To find out whether Simvastatin treatment effects ATXN3 levels in a human model, we analysed SCA3 patient-derived MJD1 It-NES cells. Simvastatin treatment led to similar and significantly increased levels of ATXN3 polyQ (L) (~1.75-fold)- and the normal allele (S) (~1.5-fold) which were quantified separately and summarized (T) (~1.6-fold), respectively (Fig. 4A–D). We also observed significantly increased HMGCR levels (~3.3-fold) (Fig. 4A,E).

Discussion

Using a LUC reporter cell line-based HTS screening assay of 2640 bioactive substances, including FDA approved drugs we identified statins as activators of ATXN3 expression, while no inhibitors of ATXN3 expression were found in this compound library.

The library contained eight different statins of which Mevastatin, Atovarstatin, Fluvastatin and Simvastatin were effective (Supplementary Fig. S3). Non-effective statins like Pravastatin and Rosuvastatin are considered

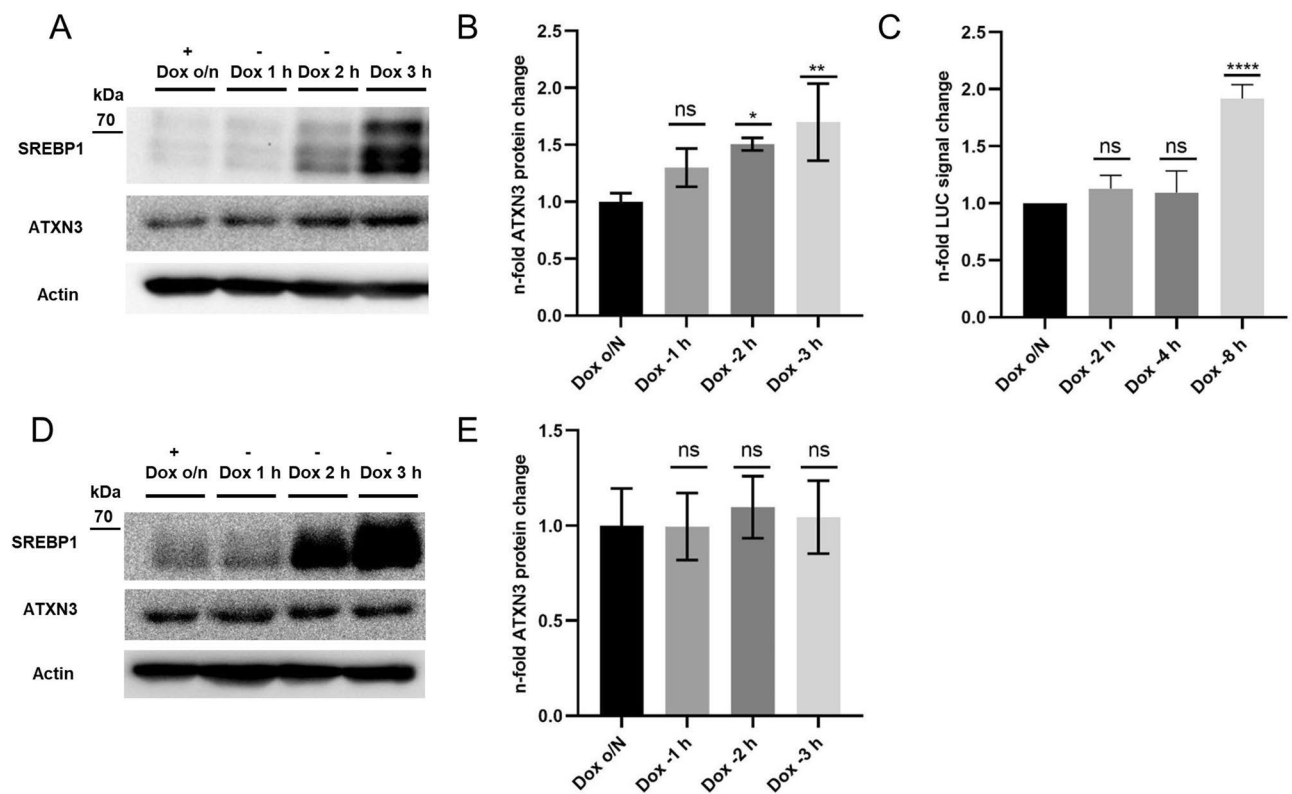


Figure 3. Overexpression of active human SREBP1a in murine N2a cells increases endogenous ATXN3 protein levels and the LUC signal of human ATXN3 promoter containing LUC-reporter plasmid. Tet-Off murine N2a cells were transfected with pTREhyg-SREBP1a/c plasmids, respectively. Dox containing media were applied (ratio 1:1) to the transfection reaction after 4 h and incubated overnight. On the next day, protein expression was induced by Dox removal for 1–3 h (Dox -1 to -3 h) (A,B,D,E). Endogenous ATXN3 protein levels were normalized to actin and the mean of + Dox o/n. Three biological repetitions were performed. For the LUC-reporter assay, Dox was removed for 2–8 h and LUC signal was normalized to signal of co-transfected *Renilla* luciferase and Dox o/N. Three independent experiments were performed and were measured in technical triplicates. Data represent the mean of each triplicate. Error bars indicate the SD. Adjusted p values: * $p < 0.05$; ** $p < 0.01$; **** $p < 0.0001$.

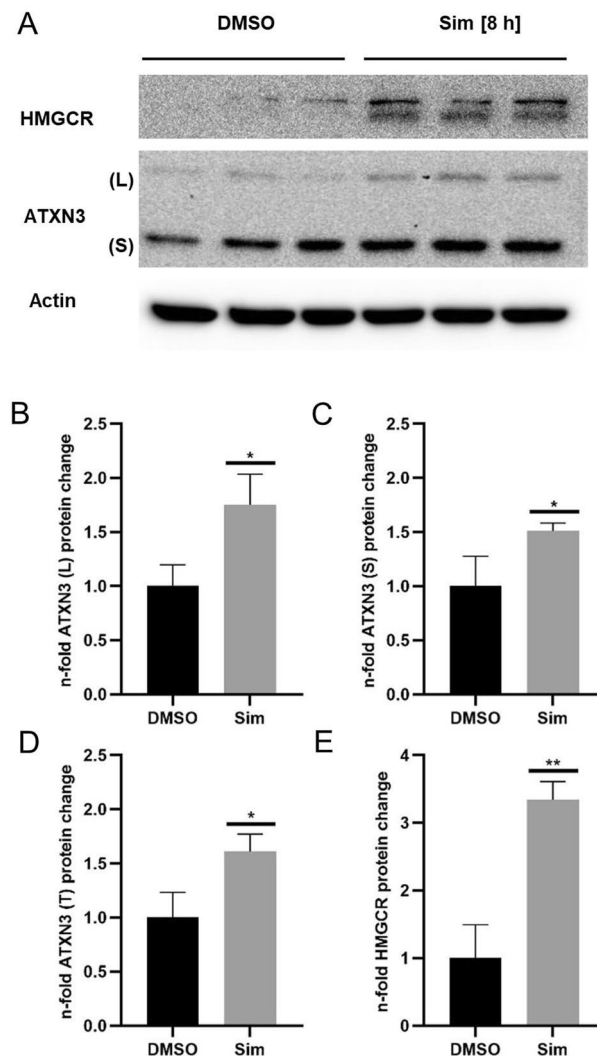


Figure 4. Simvastatin treatment increases ATXN3 and HMGCR protein levels in MJD1 It-NES cells. **(A)** WB of Simvastatin (Sim) treated MJD1 It-NES-cells. **(B), (C)** Quantification of the mutated ATXN3 polyQ allele (L) and the normal allele (S). **(D)** Summarized quantification of the L and S alleles. **(E)** Quantification of HMGCR. Data represent biological triplicates and were normalized to actin and the mean of DMSO controls. Sim was applied for 8 h at a final concentration of 10 μ M Sim. Adjusted p values: * $p < 0.05$; ** $p < 0.01$. Several exposure images for Actin WB see Supplementary Fig. S6).

as hydrophilic and may not easily pass cell membranes via diffusion. Thus, they may only reach low intracellular concentrations¹⁶. The other two statins, Lovastatin and Pitavastatin are lipophilic and should pass the cellular membranes but (also Prava- and Rosuvastatin) have also been shown to be less active in the reduction of total cholesterol levels in neuronal SK-N-MC cells compared to the four effective statins in our HTS. Furthermore, Simvastatin showed the highest reduction of total cholesterol in this assay, followed by Fluvastatin, Mevastatin and Atorvastatin¹⁷.

Simvastatin showed the most consistent effect in the primary HTS and led to increased ATXN3 mRNA and protein levels in wild-type SK-N-SH cells (Fig. 2A,C,E). Mechanistically, this induction likely occurs by direct binding of the activated human SREBP1 to the ATXN3 promotor as shown in ChIP-qPCR analyses in SK-N-SH wild type cells (Fig. 2B,C,D). In line with others, we observed increased protein levels of HMGCR after Simvastatin treatment in the SK-N-SH cells (Fig. 2F)¹⁵.

The human and murine ATXN3 promoters contain putative SREBP1 binding motifs^{18–22} (Supplementary Figs. S4 and S5) and time-controlled overexpression of the active human SREBP1a in murine Neuro 2a (N2a) cells increased protein levels of ATXN3 (Fig. 3A,B). The same model system was used to confirm SREBP1a binding to the human ATXN3 promotor by co-transfection of SREBP1a and a LUC-reporter plasmid containing the promotor sequence of human ATXN3 (Fig. 3C), suggesting a similar SREBP1 dependent regulation of murine- and human ATXN3 levels.

To investigate whether Simvastatin modifies levels of ATXN3 polyQ protein in a human neuronal disease model, patient-derived MJD1 It-NES cells were treated. As previously observed in the SK-N-SH cells, Simvastatin treatment led to increased levels of mutant and normal ATXN3-, and HMGCR protein (Fig. 4).

Statins are specific inhibitors of HMGCR, the rate-limiting enzyme in the mevalonate/cholesterol pathway¹⁰. Inhibition of HMGCR leads to reduced sterol levels in the cell, which in turn activates SREBPs to restore lipid and fatty acid homeostasis. SREBPs belong to the classic basic helix-loop-helix leucine zipper (bHLH zip) transcription factor family and consist of three proteins, SREBP1a, 1c and SREBP2 which are transcribed from two genes. SREBP1a and 1c differ in the length of their N-terminal transactivation domain and are involved in cholesterol- (SREBP1a) and fatty acid (SREBP1a/1c) homeostatic pathways. SREBP2 is encoded by the *SREBP2* gene and mainly involved in the cholesterol pathway^{11,23}.

Cholesterol levels are sensed by the endoplasmic reticulum (ER) transmembrane-SREBP cleavage activating protein (SCAP) which is directly bound to SREBP. At low cholesterol levels, the SCAP-SREBP complex is transported to the Golgi via COPII vesicles and subsequent processing of SREBP by site 1 and 2 proteases leads to activation and nuclear translocation of the mature N-terminal (mSREBP) transcription factor. At high/normal cholesterol levels the SCAP-SREBP complex is retained in the ER membrane by direct interaction of SCAP with the insulin induced genes, INSIG1 and 2¹³.

The ability of statins to pass cellular membranes or the blood brain barrier (BBB) are determined by their physico-chemical properties. Highly lipophilic statins like Simvastatin and Lovastatin may easily cross via passive diffusion whereas less lipophilic statins including Fluvastatin and Pravastatin are discussed to be actively transported via organic anion transporter polypeptide 2 (OATP2) or monocarboxylic acid transporter (MCT)^{24,25}. As a response to statin treatment, differential gene expression and slightly reduced cholesterol levels were observed in the brain, indicating potential regulatory properties in this tissue²⁶. Thelen and colleagues²⁷ found that short-term and high dose Simvastatin treatment in mice affected cholesterol synthesis and increased HMGCR mRNA levels in the brain, in contrast to pravastatin. In 2019, Fracassi and colleagues performed a broad meta study about the effect of statins in the brain e.g. mental disorders and neurodegenerative diseases like Alzheimer's disease, Parkinson's disease, and Huntington's disease. They concluded, that more research is required as studies failed to confirm beneficial effects of statin treatment initially observed in neurodegenerative disease models²⁵. Dependent on the pathophysiological condition of cholesterol levels in the respective neurodegenerative disease, in our opinion statin treatment requires careful consideration.

Little is known about altered cholesterol homeostasis in SCA3. Transcriptional changes of genes related to the cholesterol biosynthesis pathway in the brain of SCA3 transgenic mice have been reported²⁸. Nobrega and Colleagues (2019) recently found that cholesterol 24-hydroxylase (CYP46A1) is decreased in cerebellar extracts of SCA3 patients and SCA3 mice. CYP46A1 is the key enzyme allowing efflux of brain cholesterol via BBB into circulation and activating brain cholesterol turnover. Restoring CYP46A1 levels in SCA3 mice led to reduced ATXN3PolyQ accumulation and neuroprotection by alleviation of motor impairments. Vice versa, knocking-down of CYP46A1 in mice brain impairs cholesterol metabolism and resulted in severe neurodegeneration. The authors showed that CYP46A1 expression improved the endosomal-lysosomal pathway and increased the autophagy rate in general, linking a role of brain cholesterol pathway to mechanisms mediating clearance of aggregated proteins²⁹.

Although the above-mentioned studies observed dysregulation of genes within the cholesterol synthesis pathway or cholesterol turnover in SCA3 models, no data have yet described a distinct role of wild type or pathogenic ATXN3 in cholesterol homeostasis. We observed that Simvastatin treatment of patient-derived MJD1 It-NES cells led to increased levels of mutant ATXN3 protein pointing to a possible implication of statin treatment in SCA3 patients (Fig. 4). Based on our work, we postulate a putative new role of ATXN3 in cholesterol homeostasis by functioning as a DUB enzyme acting in concert with the known interaction partner VCP/p97^{30,31} to stabilize or target key proteins of the cholesterol homeostasis for ERAD (Fig. 5)^{13–15}, opening a novel door for future SCA3 research.

Methods

Cultivation and cell treatments of human neuroblastoma and N2A cell lines. The wild type human SK-N-SH neuroblastoma cell line was purchased from the European Collection of Authenticated Cell Cultures (ECACC) and used for the generation of our screening cell lines.

The wild type mouse Neuro 2A (N2a) was purchased from American Type Culture Collection (ATCC). All cell lines were cultivated in DMEM Glutamax (Gibco) supplemented with 1% penicillin/streptomycin (Gibco) and 10% inactivated FBS (Sigma-Aldrich), respectively. For detachment, cells were treated with 0.05% Trypsin-EDTA 1x (Gibco) for 10 min at 37 °C. All compounds were purchased from Selleckchem.

Cultivation of SCA3 patient-derived, induced pluripotent stem cell (iPSC)-derived long-term self-renewing neuroepithelial-like stem cells (MJD1 It-NES cells)³². Cells were plated on poly-L-ornithine/laminin (both Sigma) coated tissue culture plates and cultivated in a stock media (DMEMF12 Glutamax (Gibco) supplemented with 1% penicillin/streptomycin (Gibco), 1:100 N2 supplement (Gibco), 0.8 g D-glucose) with alternating concentrations of growth factors. On day one, cells were plated in stock media supplemented with 10 ng/ml EGF (Gibco) and 10 ng/ml FGF (Gibco). On the second day media was changed by stock media containing 40 ng/ml EGF and 40 ng/ml FGF. For further cultivation of MJD1 It-NES cells, media was changed every day with alternating concentrations of growth factors (low: 10 ng/ml and high: 40 ng/ml). Accutase (Sigma) was diluted 1:3 with PBS and used for cell detachment (10 min room temperature). Treatments were performed in media with low growth factor concentration.

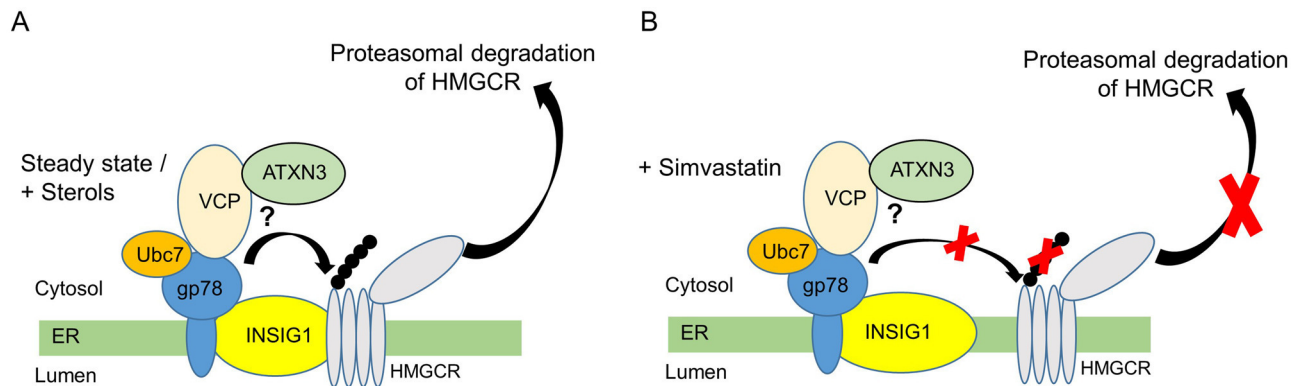


Figure 5. Putative role of ATXN3 in cholesterol homeostasis. Cholesterol homeostasis is tightly controlled at different levels within the cell. **(A)** Under normal (steady state) or under high sterol (+sterol) levels in a non-statin condition, ATXN3 may be involved in the sterol-induced and INSIG dependent, regulatory feedback degradation of HMGCR. **(B)** Statin treatment increases HMGCR levels by two mechanisms: First, it activates the SREBP pathway to upregulate genes involved in cholesterol homeostasis (including HMGCR, ATXN3). Second, statins strongly increase HMGCR protein levels by abolishing INSIG dependent ubiquitination and subsequent proteasomal degradation of the reductase. Modified from^{13–15}. ER endoplasmic reticulum, VCP valosin-containing protein, Ubc7 ubiquitin-conjugating enzyme E2 7, gp78 glycoprotein78 E3 ubiquitin ligase, INSIG1 insulin-induced gene 1, HMGCR 3-hydroxy-3-methylglutaryl coenzyme A reductase.

Generation of ATXN3-GFP-LUC reporter- and control cell line via CRISPR/Cas9 gene editing and homologous recombination. CRISPR target sites for ATXN3 exon 4 were selected from the web tool chopchop (<https://chopchop.cbu.uib.no/>)³³ using the genomic sequence of ATXN3 Exon4 (EU009923.1) and cloned into GeneArt CRISPR Nuclease Vector Kit (Thermo Fisher Scientific) according to manufacturer's protocol. Primers for ATXN3_CRISPR target site 7 (TS7) Exon 4 were as follows: forward GATACTCTGGAC TGTGAACGTTTT, reverse GTTCAACAGTCCAGAGTATCCGGTG.

For cloning of the homologous recombination (HR) vector HR150PA-1 (PrecisionX HR Targeting Vectors, System Bioscience), primers for the HR arms were tagged with 5' palindromic sequences for respective restriction enzymes (bold). Amplification of HR arms were performed with Hercules II Fusion DNA Polymerase (Agilent) from genomic DNA (gDNA) of SK-N-SH. Primers were as follows: left HR arms upstream GFP-LUC cassette (HR150PA-1), forward **GAATTCAAGCGGCAAGCCCATGACC** and reverse **GAATTCAGGATTAGT TCTAAACCCCAAACTTTC**, *EcoRI*; for right HR arm downstream GFP-LUC cassette (HR150PA-1), forward **GGATCC AACAGTCCAGAGTATCAGAGGCTCAG** and reverse **GTCGAC GACAGGACCTCCCTTTGT TGCCC**, *BamHI* and *Sall*, respectively. Total length of HR arms was as follows: left HR arm 816 bp and right HR arm 702 bp. PCR products were sub-cloned into pJET1.2 (CloneJET PCR Cloning Kit, Thermo Fisher Scientific) and finally inserted into the HR150PA-1. Vector integrity was confirmed by sequencing. All restriction enzymes were fast digest enzymes and purchased from Fermentas, Thermo Fisher Scientific.

Transfection, selection and screening of the ATXN3-GFP-LUC knock-in cell line. Performed as described in Stahl et al.¹².

Generation of stable tetracycline-controlled trans-activator (tTA) containing (pTet-Off)-N2a cell line. Wild type N2a cells were transfected with the pTet-Off regulatory plasmid according to manufacturer's protocol (ClontechTet-Off Gene Expression System). Selection pressure was applied after 24 h and maintained for 1–2 weeks. Single colonies were picked and transferred into 96 well plates. To check for the best responding cell line, the single colonies were expanded in 24 well plates and transfected with the pTRE2hyg-LUC plasmid to measure luciferase activity in plus doxycycline (1:1000)—and minus doxycycline conditions. Doxycycline was purchased from Sigma.

Cloning of SREBP constructs into pTRE2hyg plasmid. We purchased the pcDNA3.1-2xFLAG-SREBP1a, and 1c plasmids (#26801 and #26802) from addgene and cloned the coding sequence into pTRE-2hyg vectors. pcDNA3.1 was linearized with XbaI and blunted. The SREBP sequences were finally excised with BamHI and cloned into BamHI and EcoRV digested pTRE2hyg plasmid (ClontechTet-Off Gene Expression System). pcDNA3.1-2xFLAG-SREBP1a, and 1c plasmids were a gift from Timothy Osborne (#26801 and #26802)³⁴.

Cloning of human ATXN3 promotor into pGL 4 2.3 plasmid. For cloning of the ATXN3 promotor into pGL 4 2.3 (Promega) plasmid, genomic DNA from SK-N-SH was amplified with forward CTCGAG ccttaacctctcgtgcc and reverse AAGCTTaccgagaccaatcaccc primer flanking the ATXN3 promotor (promotor sequence see Supplementary Fig. S4) and sub-cloned in TOPO TA-vector (Thermofisher). The PCR product was excised with *Xho* and *HindIII* and cloned into *Xho*, *HindIII* opened pGL 4 2.3. Vector integrity was confirmed by sequencing.

Transfection of pTRE2Hyg plasmids into pTet-Off containing N2a cells. Transfection of N2A cells was performed with the Roti-Fect PLUS (Roth) transfection reagent according to manufacturer's protocol. Cells were seeded in 12 well plates 4 h prior transfection. A total of 1 µg plasmid DNA was transfected to each well. The DNA to Roti-Fect ratio was 1:3 (1 µg and 3 µl). After 4 h, doxycycline-containing media (1.2×10^5) was added to the transfection reaction (ratio 1:1) and incubated overnight. On the next day, doxycycline containing media was changed and protein expression was induced by doxycycline removal for 1–3 h.

Isolation of nucleic acids. *Genomic DNA (gDNA).* Performed as described in Stahl et al.¹².

PCR

Standard PCR and gel-electrophoreses. For the generation of the homologous recombination arms 100–200 ng DNA was amplified in a total volume of 20 µl. Mastermix was prepared at final concentrations of 1 × reaction buffer (BioTherm, Genecraft), 250 µM dNTPs (Thermo Fisher Scientific), 0.2 µM of each primer, 1 unit Taq DNA polymerase (BioTherm, Genecraft) and filled up to 20 µl with H₂O. After initial denaturation at 94 °C for 3 min PCR were run for 30 cycles (denaturation 94 °C for 30 s, annealing for 30 s at respective temperature, extension 68 °C for 1 min). PCR products were amplified in the Biometra TADvanced thermocycler and separated in 1% TBE agarose gel containing 2.5 × GelRed Nucleic Acid Gel Stain (Biotium) for visualization. For the validation of *ATXN3-GFP-LUC*-fusion, mRNA was converted into cDNA (QuantiTect Reverse Transcription Kit, Qiagen) and amplified by using hMJD-27 CGTGGGGGCCGTTGGCTCCAGACAAA and HR150GFP reverse TGTCACGATCAAAGGACTCTGG primer.

Miniprep/Maxipreparation. Performed as described in Stahl et al.¹².

RT-qPCR assays

ATXN3 mRNA. For hit validation SK-N-SH wildtype cells were treated at effective concentrations of 10 µM for 2 h in 24 well plate format and triplicates. Total RNA was extracted with the RNeasy Mini kit (Qiagen). RT-qPCR reactions were performed with the QuantiTect SYBR Green RT-PCR Kit (Qiagen) in a 96 well format and run in the Applied Biosystems HT7500 cyclor. We used 75 ng of total RNA for amplification. Primers were as follows: *ATXN3*, forward CACGAGAAACAAGAAGGCTCAC and reverse CTCCTTCTGCCATTCTCATCC.

ATXN3 mRNA expression were normalized to ubiquitin C (*UBC*), glucuronidase beta (*GUSB*) and hypoxanthine phosphoribosyl-transferase 1 (*HPRT1*) housekeeping genes as described in Stahl et al.¹².

Relative mRNA levels were calculated using the $\Delta\Delta CT$ Method for multiple housekeeping genes from Pfaffl, published in “A–Z of quantitative PCR”³⁵.

ChIP-qPCR. ChIP-qPCR was performed with Sigma Jumpstart SYBR Green Mastermix in a total volume of 25 µl. We used 3 µl of ChIP-DNA as a template. Primer were designed according to SREBP binding site annotation in UCSC human genome browser^{20,21}. Primers as follows: *ATXN3* Promotor SREBP binding site FW CCAGGTGAGCGGTCCAGAC and RV GCAGACCAATCACCCGTGA. IP data were normalized to input and DMSO control according to Pfaffl. As a negative control we used empty controls (chromatin incubated with beads without antibodies).

LUC assay. Bioactive compound collections L1700 (Selleckchem) were randomly spotted at a concentration of 10 µM in three independent experiments.

The screening process was fully automated and performed at the Laboratory Automation Technologies (LAT), DZNE Bonn. For the luciferase assay 1.5×10^4 cells/well in a volume of 30 µl were seeded into nunc white 384 well plates (Thermo Fisher Scientific). Cells attached and grew for approx. 18 h at 37 °C before treatment. The pre-spotted 384 well compound plates (100 nl/well) were diluted with 25 µl medium/well and shaken for 5 min with 1200 rpm at RT. Subsequently, 10 µl of the compound dilution were applied to 384 well cell plates, resulting in a final concentration of 10 µM and incubated for 24 h at 37 °C. Controls were distributed on the assay plate in a fixed layout for all three independent experiments. The tested drugs were randomly distributed for the three experiments to avoid well location dependent effects. Cells were lysed by adding 40 µl of ONE Glo (Lysis Buffer and Luciferase Substrate, Promega) to each well (on top of medium), incubated for 5 min while shaking at 1200 rpm and luciferase signal was measured with the Paradigm Reader at 1200 ms integration time.

For hit definition the LUC signal of treated cells was normalized to untreated controls per plate. Compounds showing an increased (activators) or decreased (inhibitors) LUC signal of more than the three-fold standard deviation (SD) of the median of untreated controls were considered as effective modulators. Repeated experiments were conducted in Nuncwhite 96 well plates and measured with the Centro LB 960 (Berthold Technologies) at 1200 ms integration time.

Luciferase reporter gene assay of pGL4 2.3 Luciferase vector containing the human *ATXN3* promotor sequence and pTRE2HYG-SREBP1a co-transfection. For the reporter assay N2A cells were seeded in 12 well plates. Cells were transfected 4 h later with Roti-Fect PLUS transfection reagent according to manufacturer's protocol with 500 ng DNA of the LUC reporter plasmid (pGL4 2.3, Promega) and the pTRE2Hyg-SREBP1a. The co-reporter *Renilla* Luciferase (pRL-CMV, Promega) was co-transfected at a concentration of 50 ng and was used for normalization. After 4 h, doxycycline-containing media (1.2×10^5) was added to the transfection reaction (ratio 1:1) and incubated overnight. On the next day, doxycycline containing media was changed and SREBP1a expression was induced by doxycycline removal for 2–8 h. Cells were lysed with 400 µl

1 × passive lysis buffer (Promega). For the luciferase and *Renilla* luciferase assays 40 µl of the cell lysates were transferred to 96 well Nuncwhite plates. The same amount of luciferase- or *Renilla* luciferase substrate (substrate composition upon request) was added respectively, and measured with the Centro LB 960 (Berthold Technologies) at 1200 ms integration time.

SDS PAGE and western blot analysis. For SDS-PAGE cells were harvested and lysed in RIPA buffer (50 mM TrisCl pH 7.5, 150 mM NaCl, 10 mM MgCl₂, 0.5% Triton X 100, 1% SDS) supplemented with Halt Protease Inhibitor-Cocktail (1 × final concentration) (Thermo Fisher Scientific) and 0.5 µl/ml benzonase (Merck) for 30 min on ice. Lysates were mixed with 4 × Laemmli loading buffer (200 mM TrisCl pH 6.8, 8% SDS, 6% β-mercapto-ethanol, 33% glycerol, spatula tip bromophenol blue) to a final concentration of 1 × and boiled for 10 min at 95 °C. Samples were loaded onto 10% SDS-PAGE gels.

Western blot. Proteins were blotted onto methanol activated polyvinylidene difluoride (PVDF) membrane (GE Healthcare, Amersham Hybond), blocked with 0.5% casein PBS (Roth) for 1 h and incubated with respective antibodies ATXN3 (1:1,000, #986) SREBP1 (1:1000, Proteintech 14088-1-AP), beta actin (1:10,000, A5441, Sigma-Aldrich) and HMGCR (1:4000, ABS229, Millipore) primary antibodies overnight at 4 °C. Secondary HRP conjugated anti mouse antibody (1:4000, P0447, Dako) was applied for 1 h at room temperature. Secondary HRP conjugated anti rabbit antibody (1:4000, 7074 V, Cell Signaling Technology) was applied.

Membranes were washed three times with 1 × PBS-TWEEN 20 0.1% (PBST 0.1%) and imaged with enhanced chemiluminescence (ECL) in the ChemoCam imager (Intas). Signals were quantified with the ImageJ software³⁶. Treated cells were normalized to actin and DMSO controls, respectively.

Chromatin immunoprecipitation (ChIP). For ChIP assays, cells were plated in 10 cm dishes and treated the next day with DMSO or 10 µM Simvastatin in a total volume of 10 ml for 1 h. Cells were crosslinked with a final concentration of 0.85% formaldehyde (37% Stock, Sigma). The reaction was stopped after 8 min by adding glycine to a final concentration of 0.125 M. Cells were washed twice with ice cold PBS, scraped from plates and transferred to 15 ml falcon tubes. After centrifugation, the supernatant was removed and 1 ml of cell lysis buffer (10 mM Tris Cl pH 8, 10 mM NaCl, 0.2% NP40 and freshly added protease inhibitor) was added. Cells were lysed on ice for 10 min and centrifuged. Centrifugations were performed at 4 °C for 10 min at 1200 rcf. Supernatant was removed and 0.5 ml nuclei lysis buffer (50 mM Tris Cl pH 8, 10 mM EDTA, 1% SDS and freshly added protease inhibitor) was applied and incubated for 10 min at 4 °C. Samples were diluted with 0.5 ml RIPA buffer (without benzonase and SDS) and sonicated for 10 s in 10 intervals at cycle 2 and 40% power for three rounds with the Bandelin Sonopuls, HD2070, SH70G, type MS72. Chromatin was cleared by centrifugation at 4 °C for 10 min at 13,000 rcf and supernatant was transferred to fresh reaction tubes. To check fragment size, 50 µl of the samples were incubated with 5 µl of 5 M NaCl, 10 mg/ml RNase (1 h, 37 °C) and 20 mg/ml proteinase K (3 h—o/N, 65 °C). Subsequently, agarose gel electrophoresis was performed to check chromatin size which is best between 200 and 700 bp length.

For ChIP assays, 400 µl of chromatin was diluted with 1 ml RIPA buffer (without benzonase and SDS). We used 2% of the chromatin as input control and added 7 µl (5.25 µg) of SREBP 1 antibody (Proteintech, 14,088-1-AP) for overnight incubation.

The next day, 20 µl Magna ChIP Protein A + G Magnetic Beads (Merck Millipore) were used for the pulldowns or empty controls (beads only) for 1.5 h at 4 °C. Samples were washed with 500 µl of low salt- (0.1% SDS, 1% Triton X-100, 2 mM EDTA, 20 mM Tris HCl pH 8, 150 mM NaCl), high salt- (equal to low salt, except 500 mM NaCl), lithium salt buffer (0.25 M LiCl, 1% NP40, 1% Sodium Deoxycholate, 1 mM EDTA, 10 mM Tris HCl pH 8) and PBS, respectively. Antibody-antigen complexes were eluted by incubation with 200 µl freshly prepared elution buffer (100 mM NaHCO₃ and 1% SDS) for 15 min. Input samples were also incubated with 200 µl elution buffer. All samples were incubated with 10 µl 5 M NaCl, 10 mg/ml RNase (1 h, 37 °C) and 20 mg/ml proteinase K (3 h—o/N, 65 °C) and purified with ChIP-DNA purification kit from Zymo.

Statistics. We used one-way ANOVA ($\alpha=0.05$) followed by the recommended Dunnett's multiple comparison test to check for statistical significance. Significance in Fig. 4B–E, was checked by the recommended unpaired- and two-tailed t-test. All statistical analyses were performed in GraphPad Prism 8.3.0.

Data availability

The datasets used and analysed during the current study are available from the corresponding author on reasonable request.

Received: 20 June 2023; Accepted: 23 August 2023

Published online: 09 September 2023

References

1. Coutinho, P. & Andrade, C. Autosomal dominant system degeneration in Portuguese families of the Azores Islands. A new genetic disorder involving cerebellar, pyramidal, extrapyramidal and spinal cord motor functions. *Neurology* **28**, 703–709. <https://doi.org/10.1212/wnl.28.7.703> (1978).
2. Kawaguchi, Y. *et al.* CAG expansions in a novel gene for Machado–Joseph disease at chromosome 14q32.1. *Nat. Genet.* **8**, 221–228. <https://doi.org/10.1038/ng1194-221> (1994).
3. Costa Mdo, C. & Paulson, H. L. Toward understanding Machado–Joseph disease. *Prog. Neurobiol.* **97**, 239–257. <https://doi.org/10.1016/j.pneurobio.2011.11.006> (2012).

4. Paulson, H. L. *et al.* Intracellular inclusions of expanded polyglutamine protein in spinocerebellar ataxia type 3. *Neuron* **19**, 333–344. [https://doi.org/10.1016/S0896-6273\(00\)80943-5](https://doi.org/10.1016/S0896-6273(00)80943-5) (1997).
5. Bilen, J. & Bonini, N. M. Genome-wide screen for modifiers of ataxin-3 neurodegeneration in *Drosophila*. *PLoS Genet.* **3**, 1950–1964. <https://doi.org/10.1371/journal.pgen.0030177> (2007).
6. Vo, S. H. *et al.* Large-scale screen for modifiers of ataxin-3-derived polyglutamine-induced toxicity in *Drosophila*. *PLoS ONE* **7**, e47452. <https://doi.org/10.1371/journal.pone.0047452> (2012).
7. Ashraf, N. S. *et al.* Druggable genome screen identifies new regulators of the abundance and toxicity of ATXN3, the Spinocerebellar Ataxia type 3 disease protein. *Neurobiol. Dis.* **137**, 104697. <https://doi.org/10.1016/j.nbd.2019.104697> (2020).
8. Costa, M. D. C. *et al.* Unbiased screen identifies aripiprazole as a modulator of abundance of the polyglutamine disease protein, ataxin-3. *Brain* **139**, 2891–2908. <https://doi.org/10.1093/brain/aww228> (2016).
9. Fardghassemi, Y., Maios, C. & Parker, J. A. Small molecule rescue of ATXN3 toxicity in *C. elegans* via TFEB/HLH-30. *Neurotherapeutics* **18**, 1151–1165. <https://doi.org/10.1007/s13311-020-00993-5> (2021).
10. Endo, A., Kuroda, M. & Tanzawa, K. Competitive inhibition of 3-hydroxy-3-methylglutaryl coenzyme A reductase by ML-236A and ML-236B fungal metabolites, having hypocholesterolemic activity. *FEBS Lett.* **72**, 323–326. [https://doi.org/10.1016/0014-5793\(76\)80996-9](https://doi.org/10.1016/0014-5793(76)80996-9) (1976).
11. Brown, M. S. & Goldstein, J. L. The SREBP pathway: Regulation of cholesterol metabolism by proteolysis of a membrane-bound transcription factor. *Cell* **89**, 331–340. [https://doi.org/10.1016/S0092-8674\(00\)80213-5](https://doi.org/10.1016/S0092-8674(00)80213-5) (1997).
12. Stahl, F. *et al.* Activators of alpha synuclein expression identified by reporter cell line-based high throughput drug screen. *Sci. Rep.* **11**, 19857. <https://doi.org/10.1038/s41598-021-98841-9> (2021).
13. Espenshade, P. J. & Hughes, A. L. Regulation of sterol synthesis in eukaryotes. *Annu. Rev. Genet.* **41**, 401–427. <https://doi.org/10.1146/annurev.genet.41.110306.130315> (2007).
14. DeBose-Boyd, R. A. Feedback regulation of cholesterol synthesis: Sterol-accelerated ubiquitination and degradation of HMG CoA reductase. *Cell Res.* **18**, 609–621. <https://doi.org/10.1038/cr.2008.61> (2008).
15. Jiang, S. Y. *et al.* Discovery of a potent HMG-CoA reductase degrader that eliminates statin-induced reductase accumulation and lowers cholesterol. *Nat. Commun.* **9**, 5138. <https://doi.org/10.1038/s41467-018-07590-3> (2018).
16. Climent, E., Benaiges, D. & Pedro-Botet, J. Hydrophilic or lipophilic statins? *Front. Cardiovasc. Med.* **8**, 687585. <https://doi.org/10.3389/fcvm.2021.687585> (2021).
17. Sierra, S. *et al.* Statins as neuroprotectants: A comparative in vitro study of lipophilicity, blood-brain-barrier penetration, lowering of brain cholesterol, and decrease of neuron cell death. *J. Alzheimers Dis.* **23**, 307–318. <https://doi.org/10.3233/JAD-2010-101179> (2011).
18. Schmitt, I., Evert, B. O., Khazneh, H., Klockgether, T. & Wuellner, U. The human MJD gene: Genomic structure and functional characterization of the promoter region. *Gene* **314**, 81–88. [https://doi.org/10.1016/S0378-1119\(03\)00706-6](https://doi.org/10.1016/S0378-1119(03)00706-6) (2003).
19. Xie, X., Rigor, P. & Baldi, P. MotifMap: A human genome-wide map of candidate regulatory motif sites. *Bioinformatics* **25**, 167–174. <https://doi.org/10.1093/bioinformatics/btn605> (2009).
20. Kent, W. J. *et al.* The human genome browser at UCSC. *Genome Res* **12**, 996–1006. <https://doi.org/10.1101/gr.229102> (2002).
21. Rosenbloom, K. R. *et al.* ENCODE data in the UCSC genome browser: Year 5 update. *Nucleic Acids Res.* **41**, D56–63. <https://doi.org/10.1093/nar/gks1172> (2013).
22. Mathelier, A. *et al.* JASPAR 2014: An extensively expanded and updated open-access database of transcription factor binding profiles. *Nucleic Acids Res.* **42**, D142–147. <https://doi.org/10.1093/nar/gkt997> (2014).
23. Horton, J. D. *et al.* Combined analysis of oligonucleotide microarray data from transgenic and knockout mice identifies direct SREBP target genes. *Proc. Natl. Acad. Sci. U S A* **100**, 12027–12032. <https://doi.org/10.1073/pnas.1534923100> (2003).
24. Hamelin, B. A. & Turgeon, J. Hydrophilicity/lipophilicity: Relevance for the pharmacology and clinical effects of HMG-CoA reductase inhibitors. *Trends Pharmacol. Sci.* **19**, 26–37. [https://doi.org/10.1016/S0165-6147\(97\)01147-4](https://doi.org/10.1016/S0165-6147(97)01147-4) (1998).
25. Fracassi, A. *et al.* Statins and the brain: More than lipid lowering agents? *Curr. Neuropharmacol.* **17**, 59–83. <https://doi.org/10.2174/1570159X15666170703101816> (2019).
26. Johnson-Anuna, L. N. *et al.* Chronic administration of statins alters multiple gene expression patterns in mouse cerebral cortex. *J. Pharmacol. Exp. Ther.* **312**, 786–793. <https://doi.org/10.1124/jpet.104.075028> (2005).
27. Thelen, K. M. *et al.* Brain cholesterol synthesis in mice is affected by high dose of simvastatin but not of pravastatin. *J. Pharmacol. Exp. Ther.* **316**, 1146–1152. <https://doi.org/10.1124/jpet.105.094136> (2006).
28. Toonen, L. J. A. *et al.* Transcriptional profiling and biomarker identification reveal tissue specific effects of expanded ataxin-3 in a spinocerebellar ataxia type 3 mouse model. *Mol. Neurodegener.* **13**, 31. <https://doi.org/10.1186/s13024-018-0261-9> (2018).
29. Nobrega, C. *et al.* Restoring brain cholesterol turnover improves autophagy and has therapeutic potential in mouse models of spinocerebellar ataxia. *Acta Neuropathol.* **138**, 837–858. <https://doi.org/10.1007/s00401-019-02019-7> (2019).
30. Boeddrich, A. *et al.* An arginine/lysine-rich motif is crucial for VCP/p97-mediated modulation of ataxin-3 fibrillogenesis. *EMBO J.* **25**, 1547–1558. <https://doi.org/10.1038/sj.emboj.7601043> (2006).
31. Zhong, X. & Pittman, R. N. Ataxin-3 binds VCP/p97 and regulates retrotranslocation of ERAD substrates. *Hum. Mol. Genet.* **15**, 2409–2420. <https://doi.org/10.1093/hmg/ddl164> (2006).
32. Koch, P. *et al.* Excitation-induced ataxin-3 aggregation in neurons from patients with Machado-Joseph disease. *Nature* **480**, 543–546. <https://doi.org/10.1038/nature10671> (2011).
33. Labun, K. *et al.* CHOPCHOP v3: Expanding the CRISPR web toolbox beyond genome editing. *Nucleic Acids Res.* **47**, W171–W174. <https://doi.org/10.1093/nar/gkz365> (2019).
34. Toth, J. I., Datta, S., Athanikar, J. N., Freedman, L. P. & Osborne, T. F. Selective coactivator interactions in gene activation by SREBP-1a and -1c. *Mol. Cell. Biol.* **24**, 8288–8300. <https://doi.org/10.1128/MCB.24.18.8288-8300.2004> (2004).
35. Bustin, S. A. *A-Z of Quantitative PCR* (International University Line, 2004).
36. Schneider, C. A., Rasband, W. S. & Eliceiri, K. W. NIH Image to ImageJ: 25 years of image analysis. *Nat Methods* **9**, 671–675. <https://doi.org/10.1038/nmeth.2089> (2012).

Acknowledgements

We thank Bernd Evert for helpful scientific discussion and H. Khazneh for excellent technical assistance.

Author contributions

Conceptualization: P.B., U.W., F.S.; Methodology: P.B., I.S., F.S.; Software: P.D., F.S. Validation: F.S., Formal Analysis: P.D., F.S., Investigation: P.B., F.S., Resources: P.B., U.W., L.d.B., P.D., I.S., Writing: Original Draft, P.B., U.W., L.d.B., F.S., Visualization: F.S., Supervision: P.B., U.W., Project Administration, L.d.B., Funding Acquisition: P.B., U.W., L.d.B.

Funding

Open Access funding enabled and organized by Projekt DEAL. The study was funded by Novartis Stiftung für therapeutische Forschung and the DZNE.

Competing interests

The authors declare no competing interests.

Additional information

Supplementary Information The online version contains supplementary material available at <https://doi.org/10.1038/s41598-023-41192-4>.

Correspondence and requests for materials should be addressed to U.W. or P.B.

Reprints and permissions information is available at www.nature.com/reprints.

Publisher's note Springer Nature remains neutral with regard to jurisdictional claims in published maps and institutional affiliations.



Open Access This article is licensed under a Creative Commons Attribution 4.0 International License, which permits use, sharing, adaptation, distribution and reproduction in any medium or format, as long as you give appropriate credit to the original author(s) and the source, provide a link to the Creative Commons licence, and indicate if changes were made. The images or other third party material in this article are included in the article's Creative Commons licence, unless indicated otherwise in a credit line to the material. If material is not included in the article's Creative Commons licence and your intended use is not permitted by statutory regulation or exceeds the permitted use, you will need to obtain permission directly from the copyright holder. To view a copy of this licence, visit <http://creativecommons.org/licenses/by/4.0/>.

© The Author(s) 2023